Engineering Complex Co-culture Models to Mimic Endochondral Ossification *In Vitro*

Encheng Ji

ISBN: 978-94-6522-427-5

Printing: Ridderprint, the Netherlands

The printing of this thesis was financially supported by:

- Erasmus University Rotterdam, Rotterdam
- Netherlands society for Biomaterials and Tissue Engineering (NBTE)

Engineering Complex Co-culture Models to Mimic Endochondral Ossification *In Vitro*

Het ontwikkelen van complexe co-kweek modellen voor endochondrale botvorming *in vitro*

Thesis

to obtain the degree of Doctor from the
Erasmus University Rotterdam
by command of the
rector magnificus

Prof. dr. ir. A.J. Schuit

and in accordance with the decision of the Doctorate Board.
The public defence shall be held on

Wednesday 27 August 2025 at 13.00 hrs

by

Encheng Ji

born in Zhejiang, People's Republic of China.

Erasmus University Rotterdam

Doctoral Committee:

Promotors:	Prof. dr. E.J. Farrell Prof. dr. G.J.V.M. van Osch
Other members:	Prof. dr. M.P.M. de Maat Dr. ing. B.C.J. van der Eerden Dr. ir. J. Rouwkema
Co-promotors:	Dr. A. Lolli

TABLE OF CONTENTS

CHAPTER 1

Introduction

CONTRIBUTION STATEMENT

Encheng Ji drafted and revised the chapter and drew the figures.

INTRODUCTION

1. Bone formation via endochondral ossification

Endochondral ossification is a critical biological process that shapes our skeletal system, involving the gradual replacement of transient cartilage with bone tissue. During endochondral ossification, most bones develop from a cartilaginous template, transforming soft tissue into the stiff framework of mature bone that supports our bodies [1].

Endochondral ossification begins during embryonic development and continues into early adulthood to allow the growth of most of bones. It is composed of several stages, presented in Fig. 1. First, human mesenchymal stromal cells (hMSCs) differentiate into chondrocytes, producing a cartilaginous extracellular matrix (ECM). The chondrocytes in the center of the cartilage template undergo hypertrophy. Hypertrophic chondrocytes trigger mineralisation by precipitating calcium and phosphate, thus mineralising the cartilage matrix. This mineralised matrix serves as the scaffold for bone formation. Blood vessels are formed and recruited due to the angiogenic factors released by the hypertrophic chondrocytes [2]. At this time, in endochondral bone formation of primary ossification the transverse partitions of the hypertrophic zone are incompletely mineralised, consequently permitting vascular invasion, while the longitudinal intercolumnar septa are well-mineralised and serve as scaffolds for primary trabeculae spicules [3]. Blood vessels invade this primary ossification center through the cartilage matrix. Blood-derived monocytes can differentiate into osteoclasts to resorb the mineralised or unmineralised cartilage matrix, which is necessary for cartilage matrix removal [4]. Hypertrophic chondrocytes mainly undergo apoptosis, but some are also described to transdifferentiate into osteoblasts and osteocytes [5]. Osteoblasts differentiated from osteoprogenitors migrating into the remodelling cartilage eventually lay down new bone matrix on the mineralised cartilage remnants, gradually replacing it with spongy bone tissue. The spaces within this spongy bone form the initial bone marrow cavity [1]. As the marrow cavity expands, various niche cell types including endothelial cells (ECs), stromal cells including CXCL12-abundant reticular (CAR) cells and osteoblasts home near the bony surface, creating distinct microenvironments or niches for hematopoietic stem cells (HSCs) [6]. In this way, mature bone containing bone marrow is eventually formed. Primary ossification occurs in the centre of the diaphysis leading to the formation of the primary ossification center during fetal life. After birth, secondary ossification will occur in the epiphyses of long bones [3]. In the case of secondary ossification the sequence of events is partially different, as vessels can invade cartilage which has not yet undergone hypertrophy or mineralisation [7]. This form of bone growth will continue until puberty to allow for bone elongation.

Cartilage mineralisation and remodelling during endochondral ossification

In the early stages of endochondral ossification, chondrocytes generate the cartilage matrix consisting of various components that play essential roles in bone formation. The matrix components include glycosaminoglycans/proteoglycans, aggrecan, hyaluronic acid and collagens [8]. Unlike most connective tissues, cartilage is avascular, meaning it lacks blood vessels for nutrient supply and waste removal, relying on diffusion through the matrix for these functions [9]. In the growth plate, the

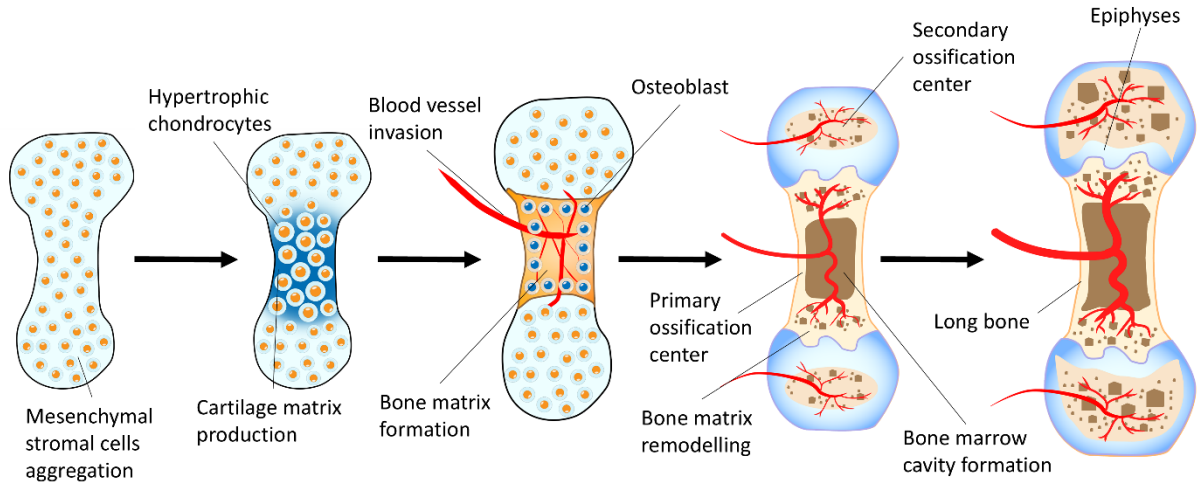

Fig. 1. The process of endochondral ossification.

area of new bone growth, proliferation and hypertrophy of chondrocytes occur in a sequential manner within specific zones of the developing cartilage: a resting zone, where chondrocytes are quiescent; a proliferative zone, where chondrocytes are actively dividing; this is followed by a prehypertrophic zone, where cells begin to enlarge; finally, a hypertrophic zone which consists of enlarged chondrocytes. The hypertrophic differentiation stage is regulated by several signalling molecules, including indian hedgehog (IHH), parathyroid hormone-related protein (PTHrP), and bone morphogenetic proteins (BMPs) [10]. The start of the mineralisation process involves the formation of matrix vesicles (MVs) by hypertrophic chondrocytes [11], through mechanisms which have not been fully clarified [12]. The hypertrophic chondrocytes thus contribute to the calcification of the surrounding cartilage matrix. The mineralisation process creates a barrier that prevents nutrients from reaching the chondrocytes, leading to their apoptosis. This makes the cartilage matrix less continuous, creating spaces or cavities which allow migrated or transdifferentiated osteoblasts to form mature bone matrix on top of the mineralised cartilage template [13].

In endochondral ossification, cartilage and bone resorption and remodelling occur along with mineralisation. Unmineralised cartilage, mineralised cartilage and bone formed by osteoblasts can all be degraded and resorbed by monocyte-derived chondroclasts/osteoclasts [14]. In the early stages of endochondral ossification, monocytes migrate to the cartilage template with the invading vessels. After differentiating into multinucleated clasts, they secrete enzymes including cathepsin K and collagenase that break down the organic components of the cartilage extracellular matrix. They also dissolve the mineral component of the cartilage through the release of hydrogen ions [15].

Vascularisation of the cartilage template

Vascularisation is a critical process in endochondral ossification which provides the nutrients required for bone formation and growth. Vessels not only constitute mature bone structures, but also support the bone forming process. The invasion of blood vessels allows the recruitment of osteoprogenitor cells, monocytes as osteoclast

precursors, immune cells and HSCs, which all contribute to cartilage remodelling and new bone formation with the establishment of a marrow niche [16].

Vascularisation during endochondral ossification is comprised of several stages. The initial attraction of ECs or endothelial progenitors is mediated by several cell types including hypertrophic chondrocytes, osteoclasts and septoclasts. Septoclasts are specialised perivascular cells that play a crucial role in bone growth by breaking down the terminal transverse septum of cartilage in the growth plate, facilitating the invasion of capillaries necessary for bone elongation [17]. Angiogenesis is initiated by the secreted pro-angiogenic factors, including vascular endothelial growth factor (VEGF), epidermal growth factor (EGF) and platelet-derived growth factor (PDGF) [18]. These pro-angiogenic factors are important mediators that regulate blood vessel invasion (neovascularisation) into hypertrophic cartilage [16]. Hypoxic conditions in the cartilage template also stimulate the production of VEGF by chondrocytes. At the same time, chondrocytes and clastic cells produce catabolic enzymes which mediate ECM proteolysis and pave the way for vessel infiltration [19]. The ECs themselves secrete matrix metalloproteinases (MMPs), such as MMP9 and MMP14, to facilitate vessel ingrowth [20].

Other than forming vessels, ECs actively and directly participate in the regulation of cartilage remodelling and bone formation. Vessels invade and grow into the forming bone thanks to matrix remodelling, and the central portion of the cartilage template is digested to make space for the formation of bone marrow [21]. Two types of vessels, called H type vessels and L type vessels, constitute the hematopoietic niche of the bone marrow. The ECs of H type vessels exhibit higher levels of the adhesion molecule CD31 and the transmembrane glycoprotein endomucin compared to L type vessels [22]. The studies focused on ECs in type H vessels indicated their unique function in affecting different types of cells. Type H vessels can promote bone formation by secreting various factors, including transforming growth factor β1 (TGF-β1) and TGF-β3, that stimulate proliferation and differentiation of osteoprogenitors in the bone marrow [23; 24]. Type H vascular ECs exhibit high expression of Noggin protein under the influence of Notch signalling [25]. Noggin is an antagonist of BMP signalling pathway and regulates chondrocyte maturation and osteogenesis [26]. The ECs in type H vessels also exhibit increased proteolytic activity by secreting MMPs, which in turn facilitates osteoclast activity and angiogenesis [22]. In contrast to the type H vessels, the ECs in type L vessels do not directly contribute to bone formation. Although direct proof is still necessary, type L vessels are thought to secrete stem cell factor (SCF), CXCL12, and angiopoietin-1 (ANG1), which interact with HSCs in the regulation of haematopoiesis [24; 27]. The paracrine crosstalk between ECs and bone cells is thus essential for bone formation to occur effectively.

Tissue engineering bone via endochondral ossification

A model widely employed by several groups including ours for studying endochondral bone formation is the hMSC pellet culture system. In this model, hMSCs are centrifuged to form a three-dimensional (3D) pellet, which recapitulates the condensation process that occurs during embryonic skeletal development. The hMSC 3D-pellets are then cultured in chondrogenic medium containing growth factors like TGF-βs and BMPs to induce chondrogenesis. During this chondrogenic priming phase, typically lasting 2-4 weeks, hMSCs differentiate towards the chondrocyte lineage and

produce a cartilage-like extracellular matrix rich in glycosaminoglycans and type II collagen. hMSC-derived chondrocytes generally exhibit hypertrophic features, with increased expression of *COL10A1*, *RUNX2* and *MMP13*. The cartilage template generated *in vitro* provides the initial shape and structure for bone formation. At this stage, pellets need to be transplanted into animals, usually via subcutaneous implantation in nude mice [28-30], to induce cartilage mineralisation, remodelling, vascularisation and new bone formation. Bone marrow, vessels, osteoclasts and cancellous bone can be normally observed after 8-12 weeks *in vivo* [31]. This strategy thus models the natural *in vivo* process of bone formation, generating fully mature bone with similar structure to the native tissue.

2. Towards modelling endochondral ossification *in vitro* using tissue engineering

Due to the complexity of bone formation and the number of cell types involved, it is still impossible to completely recapitulate this process *in vitro*. This severely limits the options for *in vitro* disease modelling in the bone field. Developing *in vitro* models of endochondral ossification could provide us with new tools to study pathological cartilage resorption during growth or repair, which can lead to skeletal deformities, short stature, and disrupted fracture healing [32]. Such *in vitro* models would enable us to investigate the (dys)regulation of the crosstalk between hypertrophic cartilage/chondrocytes, endothelial cells and osteoclasts, and evaluate tools to rescue physiological interactions [33]. In the field of bone regeneration, *in vitro* modelling could help us better understanding and utilising the mechanisms which enhance bone repair, such as effective vascularisation [34]. Among other bone-related diseases which could particularly benefit from *in vitro* modelling is cancer metastasis to the bone. Bone is one of the most frequent metastatic sites, and bone metastasis remains an incurable condition and a leading cause of death worldwide [35]. This is partly due to the lack of understanding of the molecular basis of the metastatic process. There remains an urgent need to identify effective drug targets that could inhibit the migration of cancer cells to the bone and disrupt their crosstalks with bone cells.

In vitro bone models: towards the replacement of animal models

Bone research relies on a variety of models to investigate bone formation, regeneration, and disease processes. This spectrum of models ranges from *in vivo* animal studies to increasingly complex *in vitro* systems. Each type of model offers unique advantages and limitations in our quest to understand bone biology and develop new therapeutic strategies. Animal models allow systematic evaluation of bone formation processes, making it possible to study bone degeneration and healing in the context of specific diseases, or tissue engineering approaches to promote bone repair. These *in vivo* models include calvarial defects, long bone segmental defects, partial cortical defects and cancellous bone defects [36; 37]. Furthermore, subcutaneous or intramuscular implantation models are commonly used as ectopic bone formation systems [38]. Animal models have however important limitations in relation to the bone formation process. Ectopic bone models lack the physiological microenvironment and are thus significantly influenced by the site of implantation [38]. Orthotopic bone defect models may not accurately reflect the human bone physiology, anatomic properties of the defect site and biomechanical conditions. For instance, the

use of an intramedullary pin for fixation limits the volume of material that can be tested and affects the stability of the model, leading to challenges in reproducing rotational and axial stability that would be present in human cases [39]. There are also concerns about the regulation of biological processes. For example, the role of angiogenic factors and their interactions with bone cells may not be fully recapitulated due to species-specific differences in signalling pathways and vascular responses [40]. Finally, *in vivo* imaging and quantitative analysis on vascularised bone can be extremely challenging in animal models, especially in small rodents, due to technical limitations and the small size of the vasculature. Similar problems also occur with animal models to study bone metastasis, with the complex interactions between cancer cells and the bone cells taking place in a not fully humanised microenvironment [41].

In view of these limitations, developing suitable *in vitro* models could provide several advantages. They can be potentially fully humanised, better controlled, more reproducible, and eventually reduce the need for animal testing. *In vitro* models can be used to study the fundamental processes of bone formation, maturation and bone remodelling, enabling researchers to dissect and investigate the roles of different cell types, signalling pathways and mechanical stimuli that regulate bone homeostasis [42]. *In vitro* systems can more accurately reflect aspects of human bone physiology and allow for precise manipulation of specific anatomical and biomechanical conditions. Additionally, *in vitro* bone models can be adapted to study bone-related diseases, such as growth diseases and metastatic cancers, as well as to test the reliability and safety of new treatments and biomaterials for bone regeneration [43]. These models can overcome some of the scale issues present in small rodent studies and allow for more detailed examination of human-specific biological processes and responses. Nevertheless, *in vitro* bone models currently lack sufficient biological complexity to replace the *in vivo* setting. By advancing *in vitro* bone modelling, researchers can obtain deeper insights into bone biology, accelerate the development of novel therapies, and reduce the reliance on animal experiments, finally leading to improved patient status.

Strategies and directions of in vitro bone modelling

There are multiple strategies available for designing *in vitro* bone models, as summarised in Fig. 2. 2D models represent a minority of the work, although they may still be applicable to answer some of the basic questions or to gain knowledge towards the development of more complex structures. Current strategies to model bone formation *in vitro* mainly involve developing 3D co-culture systems that strive to mimic aspects of the native bone environment, matrix formation and remodelling process. These differ in terms of supportive scaffolds, choice of cell type(s), presence of a vascularisation component, and incorporation of biological factors. The co-culture setup enables the incorporation of multiple relevant cell types including osteoprogenitors, osteoblasts, osteoclasts and ECs, allowing better recapitulation of the native bone microenvironment and cellular crosstalks [44]. Microfluidic systems have been developed to create dynamic environments that allow for continuous nutrient flow and waste removal, which are crucial for maintaining cell viability and functionality over extended culture periods [45]. Furthermore, spheroid/pellet

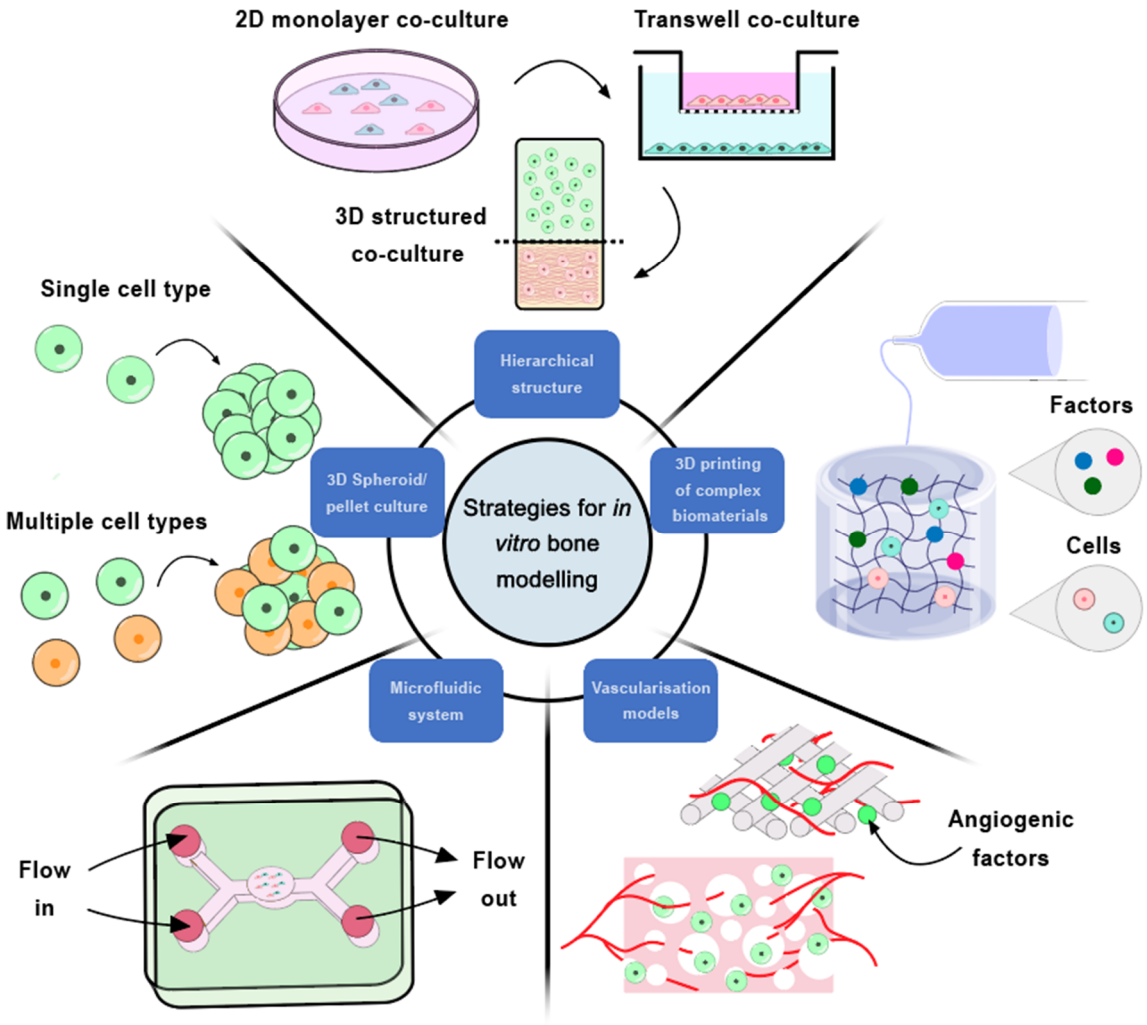

Fig. 2. The main strategies for in vitro bone modelling

(co)culture systems have shown the potential to produce bone-like organoids via self-assembly procedures that do not require exogenous biomaterials [46; 47]. Several strategies have also been developed to include a vascular component, such as loading angiogenic factors [48], 3D-printed scaffolds with vascular channels [49] and self-assembly of microvasculature [50]. Compared to animal models, 3D co-culture systems integrating vasculature and multiple bone cells may present advantages for studying molecular mechanisms, drug effects, screening treatments and overall serving as preclinical models [51].

Despite the variety of experimental systems, there are still several limitations concerning all the current *in vitro* bone models. This mainly relates to the difficulty of mimicking the complexity of the bone tissue, in terms of architecture, number of cell types and vascular supply [40]. There is still the challenge to support the co-culture of multiple cell types (osteoblasts, osteoclasts, and endothelial cells) over extended periods to study their interplay [52] and their involvement in multiple stages including vascularisation, remodelling, and new bone formation.

The achievements and challenges of in vitro vascularisation of tissue-engineered bone models

The cellular interplay between ECs and other bone cells is of critical relevance for the control of skeletal remodelling and bone formation. In mature bone or during the processes of endochondral ossification, ECs form the lining of blood vessels and interact closely with other cell types, including stromal cells, osteoblasts, osteoclasts, and chondrocytes. Recapitulation of interactions between ECs and bone cells can improve the physiological relevance of *in vitro* models and improve the functionality of different bone cell types *in vitro*. For example, in the co-culture system with human microvascular endothelial cells (HMECs) and adipose-derived stromal cells (ASCs), osteogenic markers (*BMP-2* and osteopontin (*OPN*)) and the mineralised tissue volume were increased compared with monoculture conditions [53]. The study also indicated that endothelial progenitor cells can promote the survival, migration, and osteoclastogenic differentiation of monocytes in co-culture [54]. More complex models were established via tri-cultures that used ECs as vascularisation component, and incorporated osteoblasts and osteoclasts for mimicking the bone microenvironment *in vitro* [55]. In this model, the presence of osteoblasts and osteoclasts improved human umbilical vein endothelial cell (HUVEC) survival. Chondrocytes have also been employed to support vascularisation. In a study by Freeman *et al.*, hMSC-derived chondrocytes were co-cultured with HUVECs to mimic angiogenesis during endochondral ossification [56]. In this circumstance, osteogenesis with the formation of rudimentary vessels was detected in the 3D tissue-engineered constructs *in vitro*, without the addition of osteogenic supplements. Thus, recapitulating the natural crosstalk between ECs and chondrocytes can be advantageous to stimulate vessel formation as well as cell differentiation and activity *in vitro*.

To date, researchers have applied several approaches for vascularising *in vitro* bone models:

1) 3D bioprinting/manufacturing to generate 3D vascular network-like structures. This includes the use of multi-material bioprinting and the integration of vascular channels within the printed constructs [57].

2) Conjugation of angiogenic factors to scaffolds to stimulate vessel formation. For instance, a 3D biodegradable porous calcium phosphate (CaP) scaffold combined with BMP2, WNT and VEGF promoted angiogenesis as well as osteogenic differentiation *in vitro* [58].

3) Direct introduction of the stromal vascular fraction derived from adipose tissue, ASCs or hMSCs, which can facilitate endothelial cell assembly. When co-cultured with HUVECs, ASCs derived from non-expanded stromal vascular fraction could support capillary structure formation [59]. Similar results were obtained using hMSCs as pericyte-like cells [60]. hMSCs can also promote vessel formation in *in vitro* models through secreted angiogenic factors, including VEGF and HGF [61; 62].

4) Dynamic fluid flow to induce the maturation of vessel structures. Vessel-like structures were significantly more developed under dynamic fluid flow conditions in comparison to static controls [63].

Despite these significant achievements, there are still several challenges regarding vascularisation in *in vitro* bone models. The first one is to recapitulate the complex biological structure of vessels in bone. The vessel structure of bone is

hierarchical, and involves multiple cell types including ECs, pericytes, and smooth muscle cells. The ECM providing the proper conditions for vessel development is also indispensable. All the characteristics of ECM, including the mechanical properties, the binding of growth factors, proteins and ligands, and the remodelling process, can affect the behaviour of ECs and the vascularisation process [64; 65]. Controlling the manner of administrating factors is also a challenge since the angiogenic factors supporting vessel formation might negatively influence the behaviour of other cultured cell types [33]. Thus, vascular structures of native bone tissue are extremely difficult to establish *in vitro*. The specific signals required to induce suitable vessel generation, maturation, and their integration with the mineralisation/osteogenic components are still not fully understood. Overcoming these challenges is critical to developing more physiologically relevant *in vitro* bone models with functional vascular networks, which will eventually improve our understanding of skeletal biology and facilitate the development of novel therapeutic strategies.

In vitro modelling of bone formation via endochondral ossification

Existing *in vitro* models primarily mimic direct osteogenesis, which limits their ability to fully recapitulate the natural process of long bone formation [66]. A promising alternative is to emulate endochondral ossification, starting with the formation of a cartilage template. Several research groups including ours previously succeeded in recapitulating endochondral ossification in a tissue engineering setting via subcutaneous implantation of chondrogenically-differentiated hMSCs in mice [31; 67; 68]. We hypothesise that reconstructing such events “in a dish” with a step-by-step approach that gradually increases in complexity could lead us to ultimately develop fully *in vitro* endochondral bone. To date, several groups have successfully generated cartilage templates and achieved *in vitro* mineralisation [31; 69-71]. However, most aspects of endochondral ossification remain challenging to replicate *in vitro.* The complex interplay between mineralisation, angiogenesis and tissue remodelling has not been sufficiently investigated in the tissue engineering context and the effective incorporation of vessels in a mineralised cartilage construct is still an open challenge [69]. Overall, progressing beyond the stage of mineralised cartilage remains challenging without implantation, highlighting the need for further advancements in *in vitro* models to mimic the endochondral bone formation process.

AIM AND THESIS OUTLINE

In vitro bone models provide us with precious tools for the study of bone biology, bone-related diseases, and drug development. They could help overcoming the problems associated with the limitations of animal models, i.e. ethical concerns and the high costs. The development of reliable *in vitro* bone models would be particularly instrumental for a better understanding of bone formation or loss in the context of disease, and for developing new treatments for incurable conditions such as bone metastasis. Developing such models represents however a serious challenge, due to the complexity of the process and the multiple cell types and interactions involved. To date, this challenge is still far from being overcome.

In the work of this thesis, we take inspiration from endochondral ossification, the developmental process through which most bones are formed via vascularised cartilage, to develop *in vitro* models that recapitulate specific aspects of bone formation. We aim to gradually construct a tissue-engineered model of endochondral ossification that encompasses essential elements present *in vivo*, namely the mineralised cartilage matrix, a vascular network and tissue-remodelling osteoclasts. We focus on multiple challenges that stand before us. Firstly, the need to better understand and mimic cellular and tissue changes during endochondral ossification, starting with the chondrogenic differentiation of human mesenchymal/marrow stromal cells (hMSCs) and their interaction with relevant cell types, such as endothelial cells and osteoclasts. Secondly, the creation of a polarised three-dimensional vascular network in contact with the bone-forming construct. Finally, we applied an *in vitro* model of endochondral ossification to investigate cellular mechanisms involved in bone metastasis, a process for which relevant *in vitro* models are still severely lacking.

To mimic a process *in vitro* appropriately, we first need to characterise how it normally occurs *in vivo*. In **Chapter 2**, as a starting point for our work, we characterise the process of hMSC-based endochondral ossification in the tissue engineering setting, using an established animal model. Chondrogenically differentiated cells instruct bone formation, but the dynamics of the process and the effect of the duration of chondrogenic priming have not been comprehensively described. Thus, we characterise the sequence of events induced by chondrogenic priming that leads to bone formation *in vivo*. Furthermore, we perform RNA sequencing studies and identify critical gene regulatory networks in chondrocytes that lead them to instruct tissue remodelling and vascularisation during bone formation. This can provide us with crucial knowledge to recapitulate these processes *in vitro*.

Since *in vivo* implanted cartilage undergoes mineralisation and vascularisation, we next investigate how to recapitulate these processes in the *in vitro* setting. The pro-angiogenic ability of tissue-engineered cartilage is already well known, but we still need to understand how it changes in time when the mineralisation process starts. In **Chapter 3** we investigate how mineralisation of tissue-engineered cartilage affects its pro-angiogenic potential. We induce *in vitro* cartilage mineralisation by the addition of β-glycerophosphate and evaluate the effect on endothelial cell migration, proliferation and tube formation. By this mean, the relationship between *in vitro* mineralisation and the pro-angiogenic effect of hMSC tissue-engineered cartilage can be revealed.

During endochondral ossification, cartilage remodelling is highly dependent on the catabolic activity of monocyte-derived osteoclasts and endothelial cells. In

Chapter 4, we aim to establish an *in vitro* model incorporating hMSC-derived mineralised cartilage, vasculature and osteoclasts. We first separately co-culture chondrogenic pellets undergoing mineralisation with vessels or with osteoclasts, and characterise these co-cultures. Eventually, we combine (mineralised) hMSC-derived cartilage, tissue-engineered vessels and osteoclasts *in vitro*, with the aim to recapitulate *in situ* osteoclastogenesis and vascular network formation during cartilage mineralisation.

Finally, we aim to demonstrate that *in vitro* models of endochondral ossification can be applied to study bone-related pathological conditions, such as bone metastasis. In **Chapter 5**, we evaluate an *in vitro* system including a tissue engineered model of endochondral ossification and fluid-flow to recapitulate the migration of metastatic breast and melanoma cancer cells to the bone. We further investigate how *in vitro* mineralised pellets can affect the proliferation and migratory behaviour of metastatic cancer cells.

In **Chapter 6**, the findings of this thesis are placed in a broader context, with a thorough examination of the challenges and perspectives related to the *in vitro* modelling of bone formation. Finally, there is an English summary in **Chapter 7**.

REFERENCES

[1] R. Nishimura, K. Hata, K. Ono, R. Takashima, M. Yoshida, and T. Yoneda, Regulation of endochondral ossification by transcription factors. Journal of Oral Biosciences 54 (2012) 180-183.
[2] H.-P. Gerber, T.H. Vu, A.M. Ryan, J. Kowalski, Z. Werb, and N. Ferrara, VEGF couples hypertrophic cartilage remodeling, ossification and angiogenesis during endochondral bone formation. Nature Medicine 5 (1999) 623-628.
[3] N. Ortega, D.J. Behonick, and Z. Werb, Matrix remodeling during endochondral ossification. Trends Cell Biol 14 (2004) 86-93.
[4] E.J. Mackie, Y.A. Ahmed, L. Tatarczuch, K.S. Chen, and M. Mirams, Endochondral ossification: How cartilage is converted into bone in the developing skeleton. The International Journal of Biochemistry & Cell Biology 40 (2008) 46-62.
[5] G. Yang, L. Zhu, N. Hou, Y. Lan, X.-M. Wu, B. Zhou, Y. Teng, and X. Yang, Osteogenic fate of hypertrophic chondrocytes. Cell Research 24 (2014) 1266-1269.
[6] T. Sugiyama, and T. Nagasawa, Bone marrow niches for hematopoietic stem cells and immune cells. Inflamm Allergy Drug Targets 11 (2012) 201-6.
[7] K. Hashimoto, T. Hasegawa, T. Yamamoto, H. Hongo, Y. Imin, M. Abe, A. Nasoori, K. Nakanishi, H. Maruoka, and Y. Morimoto, Histological observation on the initial stage of vascular invasion into the secondary ossification of murine femoral epiphyseal cartilage. Biomedical Research 42 (2021) 139-151.
[8] V.H. Pomin, and B. Mulloy, Glycosaminoglycans and proteoglycans, MDPI, 2018, pp. 27.
[9] M. Huber, S. Trattnig, and F. Lintner, Anatomy, biochemistry, and physiology of articular cartilage. Investigative radiology 35 (2000) 573-580.
[10] E. Minina, H.M. Wenzel, C. Kreschel, S. Karp, W. Gaffield, A.P. McMahon, and A. Vortkamp, BMP and Ihh/PTHrP signaling interact to coordinate chondrocyte proliferation and differentiation. (2001).
[11] H.C. Anderson, Matrix vesicles and calcification. Current rheumatology reports 5 (2003) 222-226.
[12] L. Zazzeroni, G. Faggioli, and G. Pasquinelli, Mechanisms of arterial calcification: the role of matrix vesicles. European Journal of Vascular and Endovascular Surgery 55 (2018) 425-432.
[13] S.F. Gilbert, Developmental Biology, Spektrum Akademischer Verlag, 1988.
[14] H. Knowles, L. Moskovsky, M. Thompson, J. Grunhen, X. Cheng, T. Kashima, and N. Athanasou, Chondroclasts are mature osteoclasts which are capable of cartilage matrix resorption. Virchows Archiv 461 (2012) 205-210.
[15] H.C. Blair, How the osteoclast degrades bone. Bioessays 20 (1998) 837-846.
[16] Y.Q. Yang, Y.Y. Tan, R. Wong, A. Wenden, L.K. Zhang, and A.B. Rabie, The role of vascular endothelial growth factor in ossification. Int J Oral Sci 4 (2012) 64-8.
[17] A. Gartland, A. Mason-Savas, M. Yang, C.A. MacKay, M.J. Birnbaum, and P.R. Odgren, Septoclast deficiency accompanies postnatal growth plate chondrodysplasia in the toothless (tl) osteopetrotic, colony-stimulating factor-1 (CSF-1)-deficient rat and is partially responsive to CSF-1 injections. Am J Pathol 175 (2009) 2668-75.
[18] K. Hu, and B.R. Olsen, The roles of vascular endothelial growth factor in bone repair and regeneration. Bone 91 (2016) 30-38.

[19] C. Maes, and G. Carmeliet, Vascular and Nonvascular Roles of VEGF in Bone Development. in: C. Ruhrberg, (Ed.), VEGF in Development, Springer New York, New York, NY, 2008, pp. 79-90.
[20] S.G. Romeo, K.M. Alawi, J. Rodrigues, A. Singh, A.P. Kusumbe, and S.K. Ramasamy, Endothelial proteolytic activity and interaction with non-resorbing osteoclasts mediate bone elongation. Nature cell biology 21 (2019) 430-441.
[21] C.I. Colnot, and J.A. Helms, A molecular analysis of matrix remodeling and angiogenesis during long bone development. Mechanisms of development 100 (2001) 245-250.
[22] Y. Peng, S. Wu, Y. Li, and J.L. Crane, Type H blood vessels in bone modeling and remodeling. Theranostics 10 (2020) 426-436.
[23] S.K. Ramasamy, A.P. Kusumbe, L. Wang, and R.H. Adams, Endothelial Notch activity promotes angiogenesis and osteogenesis in bone. Nature 507 (2014) 376-380.
[24] A.P. Kusumbe, S.K. Ramasamy, and R.H. Adams, Coupling of angiogenesis and osteogenesis by a specific vessel subtype in bone. Nature 507 (2014) 323-328.
[25] J. Zhang, J. Pan, and W. Jing, Motivating role of type H vessels in bone regeneration. Cell Prolif 53 (2020) e12874.
[26] I.T. Ling, L. Rochard, and E.C. Liao, Distinct requirements of wls, wnt9a, wnt5b and gpc4 in regulating chondrocyte maturation and timing of endochondral ossification. Developmental biology 421 (2017) 219-232.
[27] M. Chen, Y. Li, X. Huang, Y. Gu, S. Li, P. Yin, L. Zhang, and P. Tang, Skeleton-vasculature chain reaction: a novel insight into the mystery of homeostasis. Bone Research 9 (2021) 21.
[28] C.A. Knuth, J. Witte-Bouma, Y. Ridwan, E. Wolvius, and E. Farrell, Mesenchymal stem cell-mediated endochondral ossification utilising micropellets and brief chondrogenic priming. European Cells & Materials 34 (2017) 142-161.
[29] V. Palomares Cabeza, N. Fahy, C.H. Kiernan, A. Lolli, J. Witte-Bouma, S. Fahmy Garcia, A. Merino, N. Kops, Y. Ridwan, E.B. Wolvius, P.A.J. Brama, M.J. Hoogduijn, and E. Farrell, Bone formation by human paediatric marrow stromal cells in a functional allogeneic immune system. Biomaterials 306 (2024) 122471.
[30] K. Pelttari, A. Winter, E. Steck, K. Goetzke, T. Hennig, B.G. Ochs, T. Aigner, and W. Richter, Premature induction of hypertrophy during in vitro chondrogenesis of human mesenchymal stem cells correlates with calcification and vascular invasion after ectopic transplantation in SCID mice. Arthritis & Rheumatism 54 (2006) 3254-3266.
[31] C. Knuth, J. Witte-Bouma, Y. Ridwan, E. Wolvius, and E. Farrell, Mesenchymal stem cell-mediated endochondral ossification utilising micropellets and brief chondrogenic priming. European Cells & Materials 34 (2017) 142-161.
[32] J.-I. Sasaki, T. Matsumoto, H. Egusa, M. Matsusaki, A. Nishiguchi, T. Nakano, M. Akashi, S. Imazato, and H. Yatani, In vitro reproduction of endochondral ossification using a 3D mesenchymal stem cell construct. Integrative Biology 4 (2012) 1207-1214.
[33] S. Ehnert, H. Rinderknecht, R.H. Aspera-Werz, V. Häussling, and A.K. Nussler, Use of in vitro bone models to screen for altered bone metabolism, osteopathies, and fracture healing: challenges of complex models. Archives of Toxicology 94 (2020) 3937-3958.
[34] F.E. Freeman, M.Á. Brennan, D.C. Browe, A. Renaud, J. De Lima, D.J. Kelly, L.M. McNamara, and P. Layrolle, A developmental engineering-based approach to bone repair: endochondral priming enhances vascularization and new bone

formation in a critical size defect. Frontiers in bioengineering and biotechnology 8 (2020) 230.
[35] M.G. Cecchini, A. Wetterwald, G.v.d. Pluijm, and G.N. Thalmann, Molecular and Biological Mechanisms of Bone Metastasis. EAU Update Series 3 (2005) 214-226.
[36] J.A. McGovern, M. Griffin, and D.W. Hutmacher, Animal models for bone tissue engineering and modelling disease. Disease models & mechanisms 11 (2018) dmm033084.
[37] H. Gao, J. Huang, Q. Wei, and C. He, Advances in animal models for studying bone fracture healing. Bioengineering 10 (2023) 201.
[38] M.A. Scott, B. Levi, A. Askarinam, A. Nguyen, T. Rackohn, K. Ting, C. Soo, and A.W. James, Brief review of models of ectopic bone formation. Stem cells and development 21 (2012) 655-667.
[39] M. Manassero, A. Decambron, B.T. Huu Thong, V. Viateau, M. Bensidhoum, and H. Petite, Establishment of a Segmental Femoral Critical-size Defect Model in Mice Stabilized by Plate Osteosynthesis. J Vis Exp (2016).
[40] M. Stein, F. Elefteriou, B. Busse, I.A. Fiedler, R.Y. Kwon, E. Farrell, M. Ahmad, A. Ignatius, L. Grover, and L. Geris, Why animal experiments are still indispensable in bone research: A statement by the European Calcified Tissue Society. Journal of Bone and Mineral Research 38 (2023) 1045-1061.
[41] T.J. Rosol, S.H. Tannehill-Gregg, S. Corn, A. Schneider, and L.K. McCauley, Animal models of bone metastasis. Cancer Treat Res 118 (2004) 47-81.
[42] S. Ansari, B.W. de Wildt, M.A. Vis, C.E. de Korte, K. Ito, S. Hofmann, and Y. Yuana, Matrix vesicles: role in bone mineralization and potential use as therapeutics. Pharmaceuticals 14 (2021) 289.
[43] R. Owen, and G.C. Reilly, In vitro models of bone remodelling and associated disorders. Frontiers in bioengineering and biotechnology 6 (2018) 134.
[44] I.L. Tsiklin, A.V. Shabunin, A.V. Kolsanov, and L.T. Volova, In Vivo Bone Tissue Engineering Strategies: Advances and Prospects. Polymers (Basel) 14 (2022).
[45] M.A.M. Vis, F. Zhao, E.S.R. Bodelier, C.M. Bood, J. Bulsink, M. van Doeselaar, H.E. Amirabadi, K. Ito, and S. Hofmann, Osteogenesis and osteoclastogenesis on a chip: Engineering a self-assembling 3D coculture. Bone 173 (2023) 116812.
[46] S. Wrublewsky, J. Schultz, T. Ammo, C. Bickelmann, W. Metzger, T. Später, T. Pohlemann, M.D. Menger, and M.W. Laschke, Biofabrication of prevascularized spheroids for bone tissue engineering by fusion of microvascular fragments with osteoblasts. Frontiers in Bioengineering and Biotechnology 12 (2024).
[47] B. Gurumurthy, P.C. Bierdeman, and A.V. Janorkar, Spheroid model for functional osteogenic evaluation of human adipose derived stem cells. J Biomed Mater Res A 105 (2017) 1230-1236.
[48] N.P. Omorphos, C. Gao, S.S. Tan, and M.S. Sangha, Understanding angiogenesis and the role of angiogenic growth factors in the vascularisation of engineered tissues. Molecular Biology Reports 48 (2021) 941-950.
[49] P. Laowpanitchakorn, J. Zeng, M. Piantino, K. Uchida, M. Katsuyama, and M. Matsusaki, Biofabrication of engineered blood vessels for biomedical applications. Sci Technol Adv Mater 25 (2024) 2330339.
[50] M. Nie, and S. Takeuchi, Bottom-up biofabrication using microfluidic techniques. Biofabrication 10 (2018) 044103.

[51] A. Pirosa, R. Gottardi, P.G. Alexander, and R.S. Tuan, Engineering in-vitro stem cell-based vascularized bone models for drug screening and predictive toxicology. Stem cell research & therapy 9 (2018) 1-23.
[52] G. Bouet, D. Marchat, M. Cruel, L. Malaval, and L. Vico, In Vitro Three-Dimensional Bone Tissue Models: From Cells to Controlled and Dynamic Environment. Tissue Engineering Part B: Reviews 21 (2015) 133-156.
[53] T. Genova, S. Petrillo, E. Zicola, I. Roato, R. Ferracini, E. Tolosano, F. Altruda, S. Carossa, F. Mussano, and L. Munaron, The Crosstalk Between Osteodifferentiating Stem Cells and Endothelial Cells Promotes Angiogenesis and Bone Formation. Frontiers in Physiology 10 (2019).
[54] H. Pang, X.-H. Wu, S.-L. Fu, F. Luo, Z.-H. Zhang, T.-Y. Hou, Z.-Q. Li, Z.-Q. Chang, B. Yu, and J.-Z. Xu, Co-culture with endothelial progenitor cells promotes survival, migration, and differentiation of osteoclast precursors. Biochemical and Biophysical Research Communications 430 (2013) 729-734.
[55] S. Pagani, P. Torricelli, F. Veronesi, F. Salamanna, S. Cepollaro, and M. Fini, An advanced tri-culture model to evaluate the dynamic interplay among osteoblasts, osteoclasts, and endothelial cells. Journal of Cellular Physiology 233 (2018) 291-301.
[56] F.E. Freeman, H.Y. Stevens, P. Owens, R.E. Guldberg, and L.M. McNamara, Osteogenic Differentiation of Mesenchymal Stem Cells by Mimicking the Cellular Niche of the Endochondral Template. Tissue Eng Part A 22 (2016) 1176-1190.
[57] P.N. Nwokoye, and O.J. Abilez, Bioengineering methods for vascularizing organoids. Cell Reports Methods (2024).
[58] X. Sun, Y. Kang, J. Bao, Y. Zhang, Y. Yang, and X. Zhou, Modeling vascularized bone regeneration within a porous biodegradable CaP scaffold loaded with growth factors. Biomaterials 34 (2013) 4971-4981.
[59] H. Bi, H. Li, C. Zhang, Y. Mao, F. Nie, Y. Xing, W. Sha, X. Wang, D.M. Irwin, and H. Tan, Stromal vascular fraction promotes migration of fibroblasts and angiogenesis through regulation of extracellular matrix in the skin wound healing process. Stem Cell Res Ther 10 (2019) 302.
[60] C. Correia, W.L. Grayson, M. Park, D. Hutton, B. Zhou, X.E. Guo, L. Niklason, R.A. Sousa, R.L. Reis, and G. Vunjak-Novakovic, In vitro model of vascularized bone: synergizing vascular development and osteogenesis. PLoS One 6 (2011) e28352.
[61] J.-I. Sasaki, M. Hashimoto, S. Yamaguchi, Y. Itoh, I. Yoshimoto, T. Matsumoto, and S. Imazato, Fabrication of Biomimetic Bone Tissue Using Mesenchymal Stem Cell-Derived Three-Dimensional Constructs Incorporating Endothelial Cells. PLOS ONE 10 (2015) e0129266.
[62] Y.-W. Chen, Y.-F. Shen, C.-C. Ho, J. Yu, Y.-H.A. Wu, K. Wang, C.-T. Shih, and M.-Y. Shie, Osteogenic and angiogenic potentials of the cell-laden hydrogel/mussel-inspired calcium silicate complex hierarchical porous scaffold fabricated by 3D bioprinting. Materials Science and Engineering: C 91 (2018) 679-687.
[63] C. Quintard, E. Tubbs, G. Jonsson, J. Jiao, J. Wang, N. Werschler, C. Laporte, A. Pitaval, T.-S. Bah, G. Pomeranz, C. Bissardon, J. Kaal, A. Leopoldi, D.A. Long, P. Blandin, J.-L. Achard, C. Battail, A. Hagelkruys, F. Navarro, Y. Fouillet, J.M. Penninger, and X. Gidrol, A microfluidic platform integrating functional vascularized organoids-on-chip. Nature Communications 15 (2024) 1452.

[64] X. Lin, S. Patil, Y.-G. Gao, and A. Qian, The bone extracellular matrix in bone formation and regeneration. Frontiers in pharmacology 11 (2020) 757.
[65] F. Simunovic, and G. Finkenzeller, Vascularization Strategies in Bone Tissue Engineering. Cells 10 (2021).
[66] A. Iordachescu, H.D. Amin, S.M. Rankin, R.L. Williams, C. Yapp, A. Bannerman, A. Pacureanu, O. Addison, P.A. Hulley, and L.M. Grover, An In Vitro Model for the Development of Mature Bone Containing an Osteocyte Network. Advanced Biosystems 2 (2018) 1700156.
[67] J. van der Stok, M. Koolen, H. Jahr, N. Kops, J. Waarsing, H. Weinans, and O. van der Jagt, Chondrogenically differentiated mesenchymal stromal cell pellets stimulate endochondral bone regeneration in critical-sized bone defects. European cells & materials 2014 (2014) 137-148.
[68] E. Farrell, S.K. Both, K.I. Odörfer, W. Koevoet, N. Kops, F.J. O'Brien, R.J.B. de Jong, J.A. Verhaar, V. Cuijpers, J. Jansen, R.G. Erben, and G.J.V.M. van Osch, In-vivo generation of bone via endochondral ossification by in-vitro chondrogenic priming of adult human and rat mesenchymal stem cells. BMC Musculoskeletal Disorders 12 (2011) 31.
[69] E. Ji, L. Leijsten, J. Witte-Bouma, A. Rouchon, N. Di Maggio, A. Banfi, G.J. van Osch, E. Farrell, and A. Lolli, In Vitro Mineralisation of Tissue-Engineered Cartilage Reduces Endothelial Cell Migration, Proliferation and Tube Formation. Cells 12 (2023) 1202.
[70] H. Agten, I. Van Hoven, J. Van Hoorick, S. Van Vlierberghe, F.P. Luyten, and V. Bloemen, In vitro and in vivo evaluation of periosteum-derived cells and iPSC-derived chondrocytes encapsulated in GelMA for osteochondral tissue engineering. Frontiers in Bioengineering and Biotechnology 12 (2024).
[71] S. Herberg, D. Varghai, D.S. Alt, P.N. Dang, H. Park, Y. Cheng, J.-Y. Shin, A.D. Dikina, J.D. Boerckel, M.W. Rolle, and E. Alsberg, Scaffold-free human mesenchymal stem cell construct geometry regulates long bone regeneration. Communications Biology 4 (2021) 89.

CHAPTER 2 (EMBARGO)

Making a long story short: tissue engineering bone with stromal cells subjected to brief chondrogenic priming

Andrea Lolli, Encheng Ji, Janneke Witte-Bouma, Remco M. Hoogenboezem, Eric M.J. Bindels, Marc H.G.P. Raaijmakers, Gerjo J.V.M. van Osch, Niamh Fahy, Eric Farrell

Manuscript submitted.

CONTRIBUTION STATEMENT

Encheng Ji performed sample analysis, data processing and visualisation, assisted in performing *in vivo* experiments and partly drafted the manuscript.

CHAPTER 3

In vitro mineralisation of tissue-engineered cartilage reduces endothelial cell migration, proliferation and tube formation

Encheng Ji, Lieke Leijsten, Janneke Witte-Bouma, Adelin Rouchon, Nunzia Di Maggio, Andrea Banfi, Gerjo J. V. M. van Osch, Eric Farrell, Andrea Lolli

2023, *Cells, 12(8), 1202.*

CONTRIBUTION STATEMENT

Encheng Ji performed the experiments, data analysis and visualisation, and drafted and revised the manuscript.

ABSTRACT

Tissue engineering bone via endochondral ossification requires the generation of a cartilage template which undergoes vascularisation and remodelling. While this is a promising route for bone repair, achieving effective cartilage vascularisation remains a challenge. Here, we investigated how mineralisation of tissue-engineered cartilage affects its pro-angiogenic potential. To generate *in vitro* mineralised cartilage, human mesenchymal stromal cell (hMSC)-derived chondrogenic pellets were treated with β-glycerophosphate (BGP). After optimising this approach, we characterised the changes in matrix components and pro-angiogenic factors by gene expression analysis, histology and ELISA. Human umbilical vein endothelial cells (HUVECs) were exposed to pellet-derived conditioned media, and migration, proliferation and tube formation were assessed. We established a reliable strategy to induce *in vitro* cartilage mineralisation, whereby hMSC pellets are chondrogenically primed with TGF-β for 2 weeks and BGP is added from week 2 of culture. Cartilage mineralisation determines loss of glycosaminoglycans, reduced expression but not protein abundance of collagen II and X, and decreased VEGFA production. Finally, the conditioned medium from mineralised pellets showed a reduced ability to stimulate endothelial cell migration, proliferation and tube formation. The pro-angiogenic potential of transient cartilage is thus stage-dependent, and this aspect must be carefully considered in the design of bone tissue engineering strategies.

INTRODUCTION

Endochondral ossification is the most common process of bone formation and long bone elongation. It involves the condensation of mesenchymal cells which form a cartilaginous template of the future bone. Over time, these cells become enlarged (hypertrophy), and the cartilage matrix is mineralised and remodelled. Pro-angiogenic factors secreted by hypertrophic chondrocytes lead to blood vessel invasion, which allows the homing of remodelling osteoclasts and bone-forming osteoblasts [1-3]. The endochondral ossification process has been reproduced in the tissue engineering setting by several research groups around the world as a promising strategy to (re)generate bone [4-8]. This involves priming cells chondrogenically *in vitro*, followed by implantation in rodents to allow mineralisation, remodelling, vascularisation and formation of the true bone organ to occur. To date, this approach has not yet been translated to the patient, partly due to the effort required to expand and prime the cells *in vitro*, as well as the long time necessary to achieve complete remodelling of the implanted cartilage into mature bone following implantation. Improving these aspects remains a significant challenge, particularly since our understanding of the kinetics of cartilage vascularisation and remodelling in the tissue engineering setting is still limited. *In vitro* models of the early stages of endochondral ossification are lacking, further limiting our ability to study how hypertrophic cartilage is remodelled and to elucidate the underlying crosstalk between the several cell types that take part in the process.

The most commonly used cell type for bone tissue engineering is the marrow stromal cell (MSC), which is differentiated chondrogenically for as little as 7 days [9] to as many as 42 days [10]. After implantation of MSC-derived cartilage in an animal, rapid mineralisation occurs (within 7 days, unpublished data). In our previous study, we proposed that an adequate chondrogenic matrix and hypertrophic chondrocytes are the requirements for successful mineralisation and consequent bone formation [9]. However, vascularisation of the (mineralised) cartilage, which allows the homing of the cell types that can drive cartilage remodelling, is observed only much later (4 to 8 weeks post-implantation), likely due to slow invasion of a dense and compact matrix. Achieving sufficient and rapid implant vascularisation is a general concern in the bone tissue engineering field, and various strategies have been proposed to improve vascularisation dynamics, such as incorporating angiogenic growth factors [11; 12] and including hollow channels in the constructs [13-15]. Alternatively, several studies have investigated the use of pre-vascularisation strategies [16-18], whereby a rudimentary microvasculature pre-formed *in vitro* undergoes anastomosis with host blood vessels after implantation. A better understanding of the interactions between vessel-forming (endothelial) cells and bone-forming constructs is required for improved strategies to (pre-)vascularise tissue-engineered implants *in vitro* or *in vivo* [19; 20]. Particularly in the field of endochondral tissue engineering, research is needed to identify and harness the optimal cues that could drive the rapid vascularisation of chondrogenic implants.

Angiogenesis, the formation of new blood vessels from pre-existing vessel structures, provides the nutrients required for bone formation and growth, and for cells involved in bone formation such as osteoblasts and monocytes/osteoclasts. During endochondral ossification, several cell types including hypertrophic chondrocytes [21], osteoclasts [22] and septoclasts [23] produce catabolic enzymes which mediate extracellular matrix (ECM) proteolysis [24] and pave the way for vessel infiltration [25;

26]. The endothelial cells themselves secrete matrix metalloproteinases (MMPs), such as MMP2 and MMP9, to facilitate vessel ingrowth [27]. Much research into the function of angiogenesis and its modulators in endochondral ossification has been conducted, but mainly in connection to the production of pro-angiogenic and anti-angiogenic factors by hypertrophic cartilage [28-30]. Previous work from our group and others has demonstrated that both human patient-derived cartilage and tissue-engineered cartilage (chondrogenic hMSC pellets) are pro-angiogenic [31-34]. Nevertheless, how cartilage mineralisation may impact the pro-angiogenic potential of cartilage has not been broadly investigated. Increased concentrations of calcium and phosphate have been shown to increase oxidative stress [35] and apoptosis [36] in endothelial cells. Therefore, we hypothesise that the mineralisation of MSC-derived cartilage could impact its ability to attract endothelial cells and stimulate the formation a vascular network. Importantly, this may strongly affect the vascularisation of chondrogenic implants, which undergo rapid mineralisation after implantation and prior to or during vascular infiltration. Furthermore, understanding the interactions between mineralised cartilage and endothelial cells will be crucial for tissue engineering strategies which aim to induce cartilage mineralisation prior to implantation to accelerate *in vivo* bone formation.

In this work, we aimed to investigate how *in vitro* mineralisation of MSC-derived cartilage affects its ability to stimulate endothelial cell migration, proliferation and tube formation. First, we aimed to setup an optimised strategy to induce the *in vitro* mineralisation of chondrogenically primed hMSC pellets. We then characterised the response of the pellets to mineralisation in terms of matrix changes and expression of angiogenic markers. Finally, we examined how cartilage mineralisation affected endothelial cell behaviour and the formation of microvascular networks *in vitro*.

RESULTS

Establishment of the Culture Protocol to Induce *In vitro* Mineralisation of Chondrogenic Pellets

In order to establish an effective culture scheme to induce *in vitro* mineralisation of hMSC-derived chondrogenic pellets, we tested several combinations of TGF-β and BGP addition over 28 days of culture (Fig. 1a). For all experimental groups, TGF-β was added from day 0 of pellet culture to induce chondrogenesis. In the case of group 1 (TGF (4w) + BGP (2w)), we added BGP to the chondrogenic medium from day 14, according to a protocol that was previously used by our group for pellet mineralisation [8]. Since we generally observed that with this strategy the onset of mineralisation does not always occur within 28 days (Fig. 1b, c; donor 2), we hypothesised that a briefer chondrogenic priming whereby TGF-β is removed on day 14 could facilitate BGP-induced mineralisation. Hence, for groups 2, 3 and 4, TGF-β administrations were reduced to 2 weeks and BGP was added for 2, 3 or 4 weeks, respectively (TGF (2w) + BGP (2w/3w/4w)). The media from the pellets were collected at different time points to monitor the drop in extracellular calcium concentration, which is indicative of calcium uptake during mineralisation (Fig. 1b). Group 1 showed a decline in extracellular calcium levels during week 3 in the case of donor 1, but no sign of calcium uptake was observed in the case of donor 2 within 28 days. Interestingly, groups 2–4 all showed a decline in calcium levels, suggesting an increase in the uptake of calcium

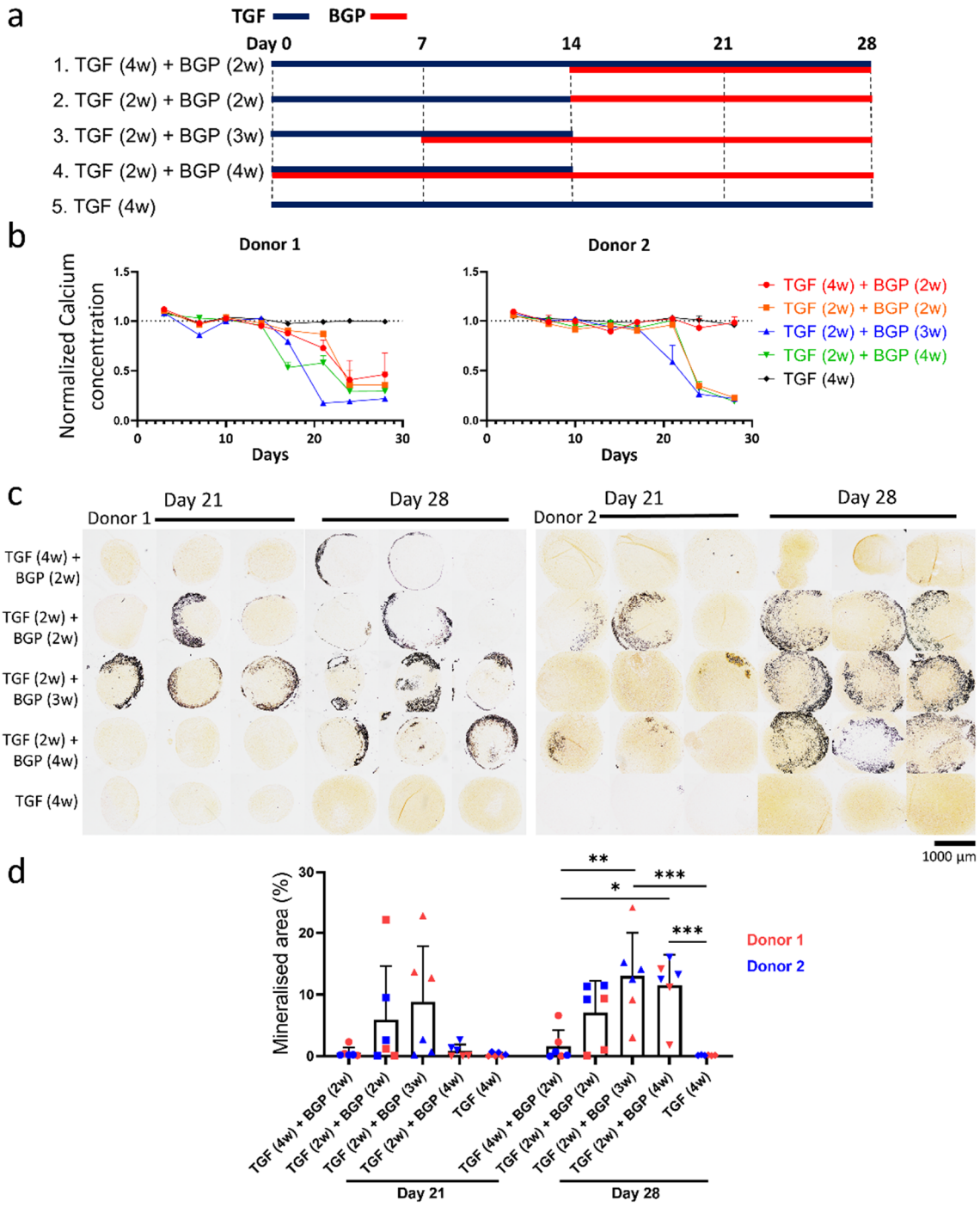

Fig. 1. Sequential exposure to TGF-β and BGP leads to in vitro mineralisation of chondrogenic pellets. ***(a)*** *Culture scheme of the different approaches to stimulate in vitro pellet mineralisation over 28 days. N = 2 hMSC donors in triplicate samples per time-point.* ***(b)*** *Longitudinal measurements of extracellular calcium levels in the culture medium to assess calcium uptake by the pellets over 28 days. Data were normalised vs. medium only and shown as average ± SD. Error bars denote standard deviation.* ***(c)*** *Von Kossa-stained histological sections of the pellets subjected to the different mineralisation protocols (3 pellets/condition from 2 hMSC donors on day 21 and 28 of culture).* ***(d)*** *Quantification of the mineralised area using Von Kossa-stained histological sections. Data are presented as average ± SD (N = 2 hMSC donors). * 0.01< p < 0.05, ** 0.01< p < 0.001, *** p < 0.001.*

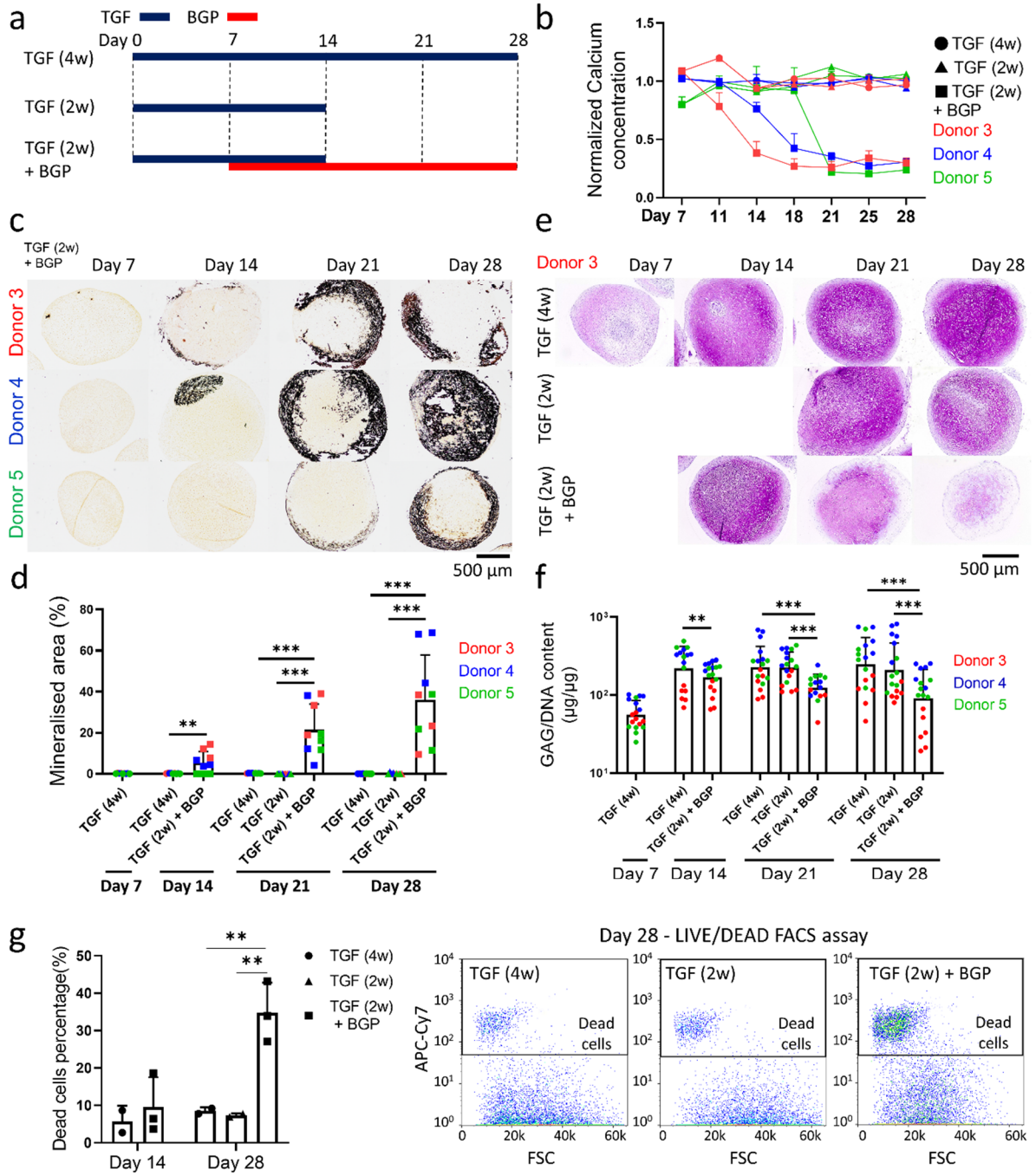

Fig. 2. Effect of BGP-induced mineralisation on GAG production and cell viability. ***(a)*** *Culture scheme of chondrogenic (TGF-β (4w)) and mineralised pellets (TGF-β (2w) + BGP). A third group whereby TGF-β is withdrawn on day 14 but BGP is not added was included to account for potential effects caused by TGF-β withdrawal and unrelated to BGP.* ***(b)*** *Longitudinal measurements of extracellular calcium levels in the culture medium to assess calcium uptake by the pellets over 28 days. Data are normalised vs. medium only and shown as average ± SD.* ***(c)*** *Von Kossa-stained histological sections of the pellets of the BGP-treated group. Groups treated with TGF-β only did not exhibit any staining (Fig. S2).* ***(d)*** *Quantification of the mineralised area using Von Kossa-stained histological sections. Data are shown as average ± SD (N = 3 hMSC donors).* ***(e)*** *Representative images of the thionine staining of the pellets for the different experimental groups for donor 3.* ***(f)*** *Quantification of GAG content in pellet lysates by DMB assay. Data are shown as average ± SD (N = 3 hMSC donors).*

*(**g**) Flow cytometry-based live/dead assay of the pellets on day 14 and day 28 of culture. Data in the bar graph indicate the % of dead cells in the pellets and are shown as average ± SD (2–3 replicates per group per time point). Representative FACS plots are reported on the right. ** 0.01< p < 0.001, *** p < 0.001.*

by the pellets, within 4 weeks of culture for both donors. Of note, group 3 showed more consistency overall in terms of early onset of mineralisation among the two donors. Von Kossa staining of the pellets at day 21 and 28 indicated very limited (donor 1) to no mineralisation (donor 2) for the TGF (4w) +BGP (2w) group within 28 days (Fig 1c, d). Groups 2–4 showed an overall larger mineralised region, mainly in the peripheral area of the pellets. In agreement with the calcium uptake results, we found slightly accelerated or more intense deposition of minerals in the case of the group 3. Thus, the culture scheme of group 3 (TGF (2w) + BGP (3w)) was selected for all subsequent experiments.

BGP-Driven Mineralisation Induces Cell Death and Matrix Changes in Chondrogenic Pellets

We next investigated how mineralisation of chondrogenic pellets affects cell viability and matrix components. Importantly, these aspects may significantly impact the pro-angiogenic potential of cartilage. To answer these questions, we subjected pellets from 3 hMSC donors to the optimised mineralisation protocol and performed von Kossa staining, thionine staining, DMB assay and Live/Dead FACS assay throughout differentiation. To discriminate the effect of BGP-induced mineralisation from the effect of TGF-β withdrawal, control pellets were cultured with TGF-β for 2 weeks, and the factor was then removed from the medium for the last 2 weeks without BGP addition (TGF (2w) condition) (Fig. 2a). As expected, calcium uptake measurements and von Kossa staining showed that BGP addition induced consistent pellet mineralisation (Fig. 2b–d; Fig. S2), starting of mineral deposits in the pellets was detected from day 14, and further progressed afterwards; donor 5 showed slower and more limited mineralisation (Fig 2c, d). H&E staining of the pellets further evidenced hypertrophic chondrocytes embedded in the calcified matrix of BGP-treated pellets (Fig. S3.). Thionine staining of the pellets and a DMB assay performed on the pellet lysates showed that glycosaminoglycans (GAGs) accumulated over time in the matrix of chondrogenic pellets from week 2–3 of culture for all donors. In the case of donors 3 and 4, the presence (TGF (4w)), and this was not significantly affected by the removal of TGF-β after 2 weeks of culture (TGF (2w)) (Fig 2e,f). In the case of mineralised pellets (TGF (2w) + BGP), the GAG content was significantly decreased at all time-points (Fig 2f). During endochondral ossification, most hypertrophic chondrocytes in mineralised cartilage undergo apoptosis. Hence, we next aimed to quantify the number of viable cells in mineralised pellets. The live/dead FACS assay showed that on day 14, chondrogenic and mineralised pellets exhibited a low % of dead cells (TGF (4w): 5.69 ± 4.21%; TGF (2w) + BGP: 9.58 ± 7.93%). On day 28, mineralised pellets exhibited an increased ratio of dead cells (TGF (2w) + BGP: 34.73 ± 8.08%) when compared to chondrogenic pellets (TGF (4w): 8.47 ± 1.00%; TGF (2w): 7.29 ± 0.58%) (Fig 2g, bar graph).

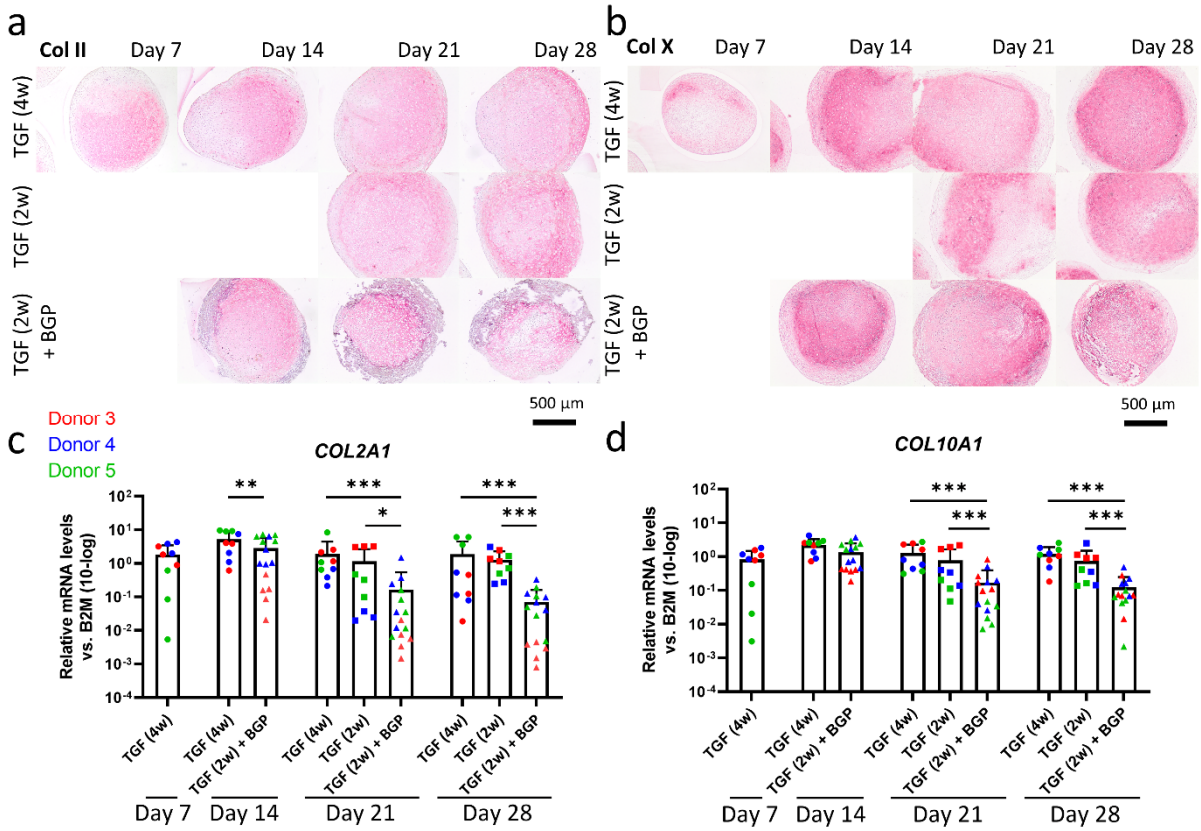

Fig. 3. Effect of in vitro mineralisation on collagen expression and accumulation in the pellets. ***(a)*** *Representative images of the collagen type II (Col II) immunohistochemical staining of the pellets.* ***(b)*** *Representative images of the collagen type X (Col X) immunohistochemical staining of the pellets.* ***(c)*** *COL2A1 mRNA expression determined by qRT-PCR.* ***(d)*** *COL10A1 mRNA expression determined by qRT-PCR. B2M was used as the housekeeper gene. Data are presented as average ± SD (N = 3 hMSC donors). * 0.01< p < 0.05, ** 0.01< p < 0.001, *** p < 0.001.*

To further investigate changes in the cartilage matrix, immunohistochemistry and gene expression analysis for collagen type II and X were performed. TGF-β induced abundant collagen type II and X production and accumulation during chondrogenesis, which was maintained in the last 2 weeks of culture regardless of the presence of TGF-β in the culture medium (Fig 3a, b). Mineralised pellets did not exhibit major qualitative differences in collagen type II or X staining when compared with the other conditions. Further gene expression analyses showed that the mRNA expression of *COL2A1* and *COL10A1* was significantly reduced upon BGP-induced mineralisation, particularly at day 21 and 28 of culture (Fig 3c, d). A similar trend was observed for the osteogenic markers *RUNX2* and *COL1A1* (Fig. S4).

In summary, our data show that BGP-induced mineralisation leads to specific changes in chondrogenic pellets, namely increased cell death, loss of GAGs and reduced expression but not protein abundance of collagen type II and X.

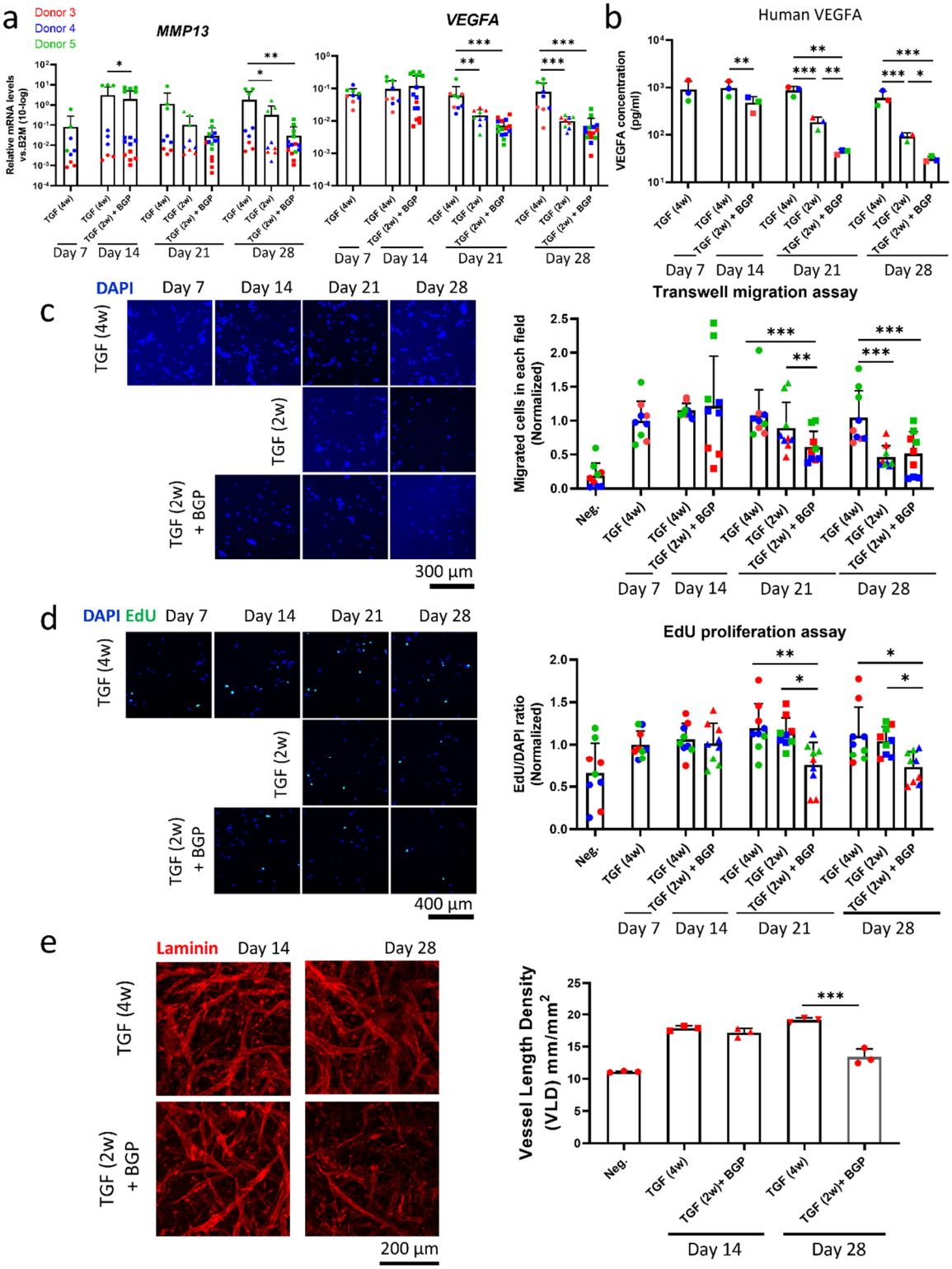

Fig. 4. Assessment of the angiogenic potential of in vitro mineralised pellets. (a) *MMP13 and VEGFA mRNA expression was determined by qRT-PCR. B2M was used as the housekeeper gene (N = 3 hMSC donors).* ***(b)*** *ELISA-based quantification of secreted VEGFA in the CM of chondrogenic and mineralised pellets over time (N = 3 hMSC donors).* ***(c)*** *Transwell migration assay performed with HUVECs exposed to the CM of the pellets. Representative images of migrated cells are shown. The graph displays the normalised number of migrated cells per field (vs. TGF (4w) day 7) (N = 3 hMSC donors).* ***(d)*** *dEdU proliferation assay performed with HUVECs exposed to*

the CM of the pellets. The graph displays the normalised EdU-positive cells per field (vs. TGF (4w) day 7 (N = 3 hMSC donors). ***(e)*** *3D tube formation assay in fibrin hydrogel performed using the CM from chondrogenic (TGF (4w)) and mineralised (TGF (2w) + BGP) groups from donor 3. Representative z-stack images obtained by confocal microscopy are shown. The graph displays the average VLD values per condition. All data are presented as average ± SD. * 0.01< p < 0.05, ** 0.001< p < 0.01, *** p < 0.001.*

In vitro Mineralisation Reduces the Pro-Angiogenic Potential of Chondrogenic Pellets

To gain insight into how cartilage mineralisation may potentially affect vessel attraction and invasion, we next performed multiple experiments to examine the angiogenic potential of in vitro mineralised pellets. First, we quantified MMP13 and VEGFA mRNA expression levels in hMSC-derived chondrocytes during in vitro mineralisation due to the relevance of these factors to matrix remodelling and angiogenesis during endochondral ossification. The TGF (2w) and TGF (2w) + BGP groups exhibited significantly lower VEGFA and MMP13 expression on day 21 (VEGFA) and 28 (VEGFA, MMP13) when compared to TGF (4w), suggesting that TGF-β supplementation is necessary to sustain their expression (Fig. 4a). While TGF-β withdrawal caused a significant decrease in VEGFA release in the medium, the effect was further anticipated and exacerbated by BGP-induced mineralisation (Fig. 4b). Next, endothelial cell migration and proliferation assays were performed to investigate how HUVEC behaviour was affected by the CM from the pellets. The withdrawal of TGF-β from chondrogenic pellets (TGF (2w) group) led to decreased HUVEC migration in comparison to (4w) group on day 28 (Fig. 4c). In the case of mineralised pellets (TGF (2w) + BGP group), an inhibitory effect on cell migration was already observed for CM derived from day 21 pellets. Regarding HUVEC proliferation, there was no effect due to the withdrawal of TGF-β, while BGP-induced mineralisation resulted in significantly decreased proliferation levels compared with the other groups on day 21 and 28 (Fig. 4d). Finally, to further validate the overall reduction in the pro-angiogenic potential of mineralised cartilage, we applied a model of 3D vascular network formation in fibrin hydrogels in the presence of CM. Here, we compared the effect of CM from TGF (4w) and TGF (2w) + BGP pellets at day 14 and day 28 on vessel length density (VLD) (Fig. 4e). In the case of day 14 CM, we observed similar VLDs for TGF (4w) and TGF (2w) + BGP groups (17.86 ± 0.38 and 17.52 ± 0.23 mm/mm2, respectively). However, hydrogels cultured with CM derived from day 28 mineralised pellets exhibited lower VLD when compared to the day 28 TGF (4w) group (19.12 ± 0.35 and 13.41 ± 1.23 mm/mm2, respectively) (Fig. 4e).

In conclusion, our data show that the ability of chondrogenic pellets to induce endothelial cell migration, proliferation and tube formation is strongly reduced upon prolonged cartilage mineralisation.

DISCUSSION

In this study, we investigated the changes in angiogenic potential that occur during the mineralisation of hMSC-derived cartilage. While the pro-angiogenic potential of tissue-engineered cartilage is well documented [4; 31; 32], the manner in which mineralisation specifically affects angiogenesis still requires investigation. Here, we optimised an *in vitro* strategy to induce the mineralisation of hMSC-derived chondrogenic pellets and characterised the cellular and matrix changes that occur overtime. Our data show that cartilage mineralisation leads to a strong reduction in the ability of tissue-engineered cartilage to stimulate migration, proliferation, and network formation by endothelial cells. These findings suggest that mineralisation itself is not one of the major factors in driving blood vessels to infiltrate cartilage during endochondral ossification, but may instead significantly delay vascularisation processes, at least *in vitro*.

We first focused on establishing a reliable culture method to introduce mineralisation in chondrogenic pellets. Previously published protocols for *in vitro* mineralisation often require the use of multiple culture media and/or prolonged culture periods (4–6 weeks) due to the induction of mineralisation after prolonged maturation of the chondrogenic template [4; 6; 8; 10; 37-39]. Since there is evidence that TGF-β can inhibit mineralisation [40-42], we here withdrew TGF-β from the pellets after 2 weeks of culture, and showed that this does not negatively affect the cartilage matrix or the expression of matrix-related genes.

Furthermore, previous studies from our group have shown that 7 days of chondrogenic priming are sufficient to achieve cartilage mineralisation and bone formation after subcutaneous implantation of the pellets [9]. Therefore, we started adding BGP from day 7 of chondrogenesis. We succeeded in inducing the mineralisation of hMSC pellets as early as day 14. Interestingly, the region of mineralisation normally originates from the edge of pellets in our studies. This is consistent with previous *in vitro* mineralisation studies and may to some extent mimic the formation of the bone collar on the border of the cartilage rudiment during endochondral ossification [43]. These cells produce ECM to form the osteoid structure and also aggregate calcium phosphate to form hydroxyapatite [44]. Previously, we have observed that normally the same peripheral area of chondrogenic pellets undergoes bone formation after *in vivo* transplantation, leading to the generation of a ring of bone tissue [45]. The reason for this spatial difference in the distribution of mineral deposits and bone formation is not fully understood. Some possible explanations are the gradient in the diffusion of nutrients, growth factors and oxygen, as well as intrinsic heterogeneity in cellular populations within the pellets. Application of spatial omics approaches to these experimental models may provide further insights into the cellular processes underlining cartilage mineralisation and bone formation during endochondral ossification.

In vitro cartilage mineralisation led to specific changes in matrix components. While collagen II and X protein expression was well maintained overall, the mRNA expression of collagens and RUNX2 was reduced after prolonged mineralisation. This is not surprising, since hypertrophic chondrocytes generally exhibit high expression of osteogenic markers, even in the absence of active mineralisation. The decrease in the expression of genes encoding for matrix and osteogenic factors may be due to an overall transition from an anabolic (chondrogenic) stage to a “remodelling” stage,

which is consistent with the fact that *in vivo* mineralised cartilage is infiltrated by blood vessels and gradually resorbed. At this stage, downregulation in the expression of these genes may occur. Alternatively, the downregulation of these factors may be related to the limitation of *in vitro* models, wherein only a limited number of cell types can be included and not all cellular crosstalk can be captured. BGP-induced mineralisation further led to a strong decrease in GAGs in the matrix from day 21 of culture. The fact that chondrogenic pellets from which TGF-β was withdrawn after 14 days did not show GAG loss indicates that this process was related to BGP-driven mineralisation. During the early stages of endochondral ossification, GAGs are abundantly present in the matrix around hypertrophic chondrocytes. It has previously been shown that negatively charged GAGs could inhibit hydroxyapatite formation [46-49], and the cartilage matrix thus needs to be degraded for endochondral ossification to proceed. With the expansion of the mineralisation border, the ECM containing collagen I will be calcified. Meanwhile, the protein components of the proteoglycans will be finally degraded by enzymes such as matrix metalloproteases (MMPs) and aggrecanases produced by the hypertrophic chondrocytes themselves [50]. Viable chondrocytes also play a direct role in maintaining GAGs [51] and the overall matrix integrity. In this study, we found that high levels of cell death occurred at the late time-point of *in vitro* mineralisation (day 28). While few hypertrophic chondrocytes can transdifferentiate into osteoblasts during endochondral ossification, most late hypertrophic chondrocytes will undergo apoptosis and be removed from the cartilage template [52]. The increased levels of Pi and Ca^{2+} at the mineralisation front could locally induce chondrocyte apoptosis. Mansfield et al. showed that this ion pair can induce chondrocyte death by causing an increase in reactive oxygen species (ROS), which can initiate the induction of apoptosis [53]. Accordingly, studies on rickets, a disorder associated with failure of endochondral ossification and impaired mineralisation, have shown that hypophosphatemia leads to enlarged late hypertrophic chondrocytes and diminished cell death due to reduced caspase activation in the presence of lower Pi levels [54; 55]. Whether and to what extent these or other mechanisms mediate chondrocyte death during *in vitro* mineralisation remains to be clarified.

Prolonged *in vitro* mineralisation strongly diminished the pro-angiogenic potential of hMSC-derived cartilage, as demonstrated by the proliferation and migration assay performed with HUVECs exposed to conditioned media from the pellets. The withdrawal of TGF-β itself led to a drop in the production of VEGFA by the pellets and a reduction in their ability to stimulate HUVEC migration. TGF-β has a variety of biophysical effects on MSCs [56; 57], and it was reported that angiogenic factors, such as hepatocyte growth factor (HGF), angiogenin (ANG) or VEGFA, can be released from MSCs exposed to TGF-β [31; 32; 45; 57]. BGP-driven mineralisation further exacerbated this loss of pro-angiogenic potential. It is likely that cell death occurring after prolonged mineralisation contributed to the reduction in VEGFA secretion. The reduction of VEGFA in (normalised) gene expression levels also indicate reduced VEGFA expression in each cell. Furthermore, TGF (2w) pellets did not show increased cell death, but exhibited decreased VEGF expression and secretion. In conclusion, it is likely that both cell death and cellular downregulation of angiocrine expression and secretion contributed to the reduced stimulatory effect of mineralised cartilage on endothelial cell migration and proliferation.

When we performed a 3D vascular network formation assay in fibrin hydrogel, no significant difference in vascular network formation was found in the case of the

conditioned medium from chondrogenic and mineralised pellets on day 14. Since the VEGFA level already dropped on day 14 in the presence of BGP, it is likely that additional secreted factors may still be able to support vessel network formation. Nevertheless, the pro-angiogenic effect was again lost after prolonged mineralisation. While our data clearly show a negative impact of mineralisation on endothelial cell migration, proliferation and tube formation, further research should aim to untangle the exact mechanisms by which secreted factors from (mineralised) cartilage regulate endothelial cell differentiation and tube formation. Furthermore, it is important to consider that the use of a conditioned medium can only recapitulate unidirectional cellular interactions mediated by secreted factors, and future studies will be necessary to explore the additional mechanisms by which mineralisation can impact angiogenesis. In this work, we focused our attention on the very initial stages of angiogenesis during endochondral ossification, whereby new vessels form and grow towards a mineralising cartilage template. The later infiltration of blood vessels into the cartilage template with the formation of a vascularised marrow niche is likely heavily dependent on local and direct cell contact [58; 59]. To completely address these phenomena, experimental models with direct contact between the matrix and forming vessels will be needed, so that the processes of matrix remodelling and vascular infiltration can be further studied.

Tissue-engineered grafts using MSCs hold a great deal of promise for bone regeneration, but achieving sufficient graft vascularisation is still a concern. While there is abundant evidence that such an issue can be overcome by inducing bone formation via the endochondral pathway, translating this approach to patients will require addressing the issues of prolonged *in vitro* handling and relatively slow *in vivo* bone formation. In recent years, extensive research efforts have been directed towards developing tools to minimise the time required for priming the cells and achieving graft vascularisation after implantation. Nevertheless, ideal strategies that can at the same time support rapid angiogenesis and MSC-mediated tissue production are still under investigation. The results of our study show that cartilage mineralisation in the tissue engineering setting may be a crucial process counteracting the pro-angiogenic potential of cartilage. Strategies attempting pre-mineralisation of the chondrogenic constructs (prior to implantation) should be handled with care. Whether it is possible to “engineer” the mineralisation process by providing further cues that can sustain angiogenesis is a relevant question for the future. In this regard, suitable *in vitro* models to answer this and other fundamental questions on the processes of endochondral bone formation are still lacking. Several co-culture systems with MSCs and endothelial cells or endothelial progenitor cells (EPCs) have been established [20], and these models can be applied to study how cellular interactions can affect specific osteogenic and angiogenic properties. However, further bone or vascular development of the tissue-engineered constructs still has to be achieved with *in vivo* transplantation [60-62], which poses challenges related to the controllability of the models. Particularly, to recapitulate the processes of cartilage remodelling, mineralisation and angiogenesis in a coordinated manner *in vitro*, more complicated models are needed. This not only relates to the process of blood vessel formation and physical interactions with the mineralised matrix, but also to the presence of additional cell types that may directly intervene in these processes, such as osteoclasts and macrophages. The outcomes of our study provide relevant knowledge for the development of such models, in particular concerning the coordination of cartilage formation, mineralisation and angiogenesis.

CONCLUSIONS

In conclusion, we established a reliable strategy to induce mineralisation of hMSC-derived cartilage *in vitro* and characterised tissue changes on both a cellular and histological level. We showed that mineralisation leads to a progressive decrease in the ability of tissue-engineered cartilage to stimulate endothelial cell migration, proliferation and tube formation. These data indicate that the pro-angiogenic potential of hypertrophic and mineralising cartilage may be strictly stage-dependent, and these features represent a crucial aspect to consider in the design of bone tissue-engineering strategies. Finally, our study can act as the basis for development of more sophisticated *in vitro* models to recapitulate and study the vascularisation of mineralised cartilage during endochondral ossification.

MATERIALS AND METHODS

Cell Culture

Human mesenchymal stromal cells (hMSCs) from human bone marrow were used to generate chondrogenic and mineralised pellets (N = 5 donors in total). Donors 1–2 were used to optimise the protocol of *in vitro* mineralisation. Donors 3–5 were subjected to a time-course analysis to study the effect of mineralisation on the ability of tissue-engineered cartilage to stimulate endothelial cell migration, proliferation and tube formation. The cells were isolated from leftover materials obtained from paediatric patients undergoing alveolar bone graft surgery (5 male patients, age 9–12 years). All samples were harvested after informed consent and with the approval of the Medical Ethics Review Committee at Erasmus MC University Medical Center Rotterdam, The Netherlands (MEC2014-106). Cells were plated in alpha minimum essential medium (αMEM, ThermoFisher, Waltham, USA) containing 10% *v*/*v* heat inactivated foetal bovine serum (FBS, Sigma-Aldrich, St. Louis, USA) and supplemented with 50 µg/mL gentamicin (ThermoFisher, Waltham, USA), 1.5 µg/mL Amphotericin B (ThermoFisher, Waltham, USA), 25 µg/mL ascorbic acid 2-phosphate (Sigma-Aldrich, St. Louis, USA), 1 ng/mL fibroblast growth factor-2 (Instruchemie B.V., Delfzijl, The Netherlands) and Amphotericin B/gentamicine (F/G, ThermoFisher, Waltham, USA), with a seeding density of 2300 cells/cm^2, in T175 flasks. After 24 h, flasks were washed to remove non-adherent cells and debris, and the medium was renewed. Cells were cultured in a humidified atmosphere at 37 °C and 5% carbon dioxide (CO_2), and the medium was changed twice a week. hMSCs were subcultured once 85–90% confluence was reached, using 0.05% *w*/*v* trypsin (ThermoFisher, Waltham, USA), and replated at a density of 2300 cells/cm^2. Cells were expanded until passage 2–3 for pellet formation.

Adipose-derived stromal/stem cells (ASCs) were co-cultured with endothelial cells for the generation of a 3D vascular network. The cells were isolated from human adipose tissue obtained from one healthy patient undergoing plastic surgery after informed consent and approval from the Ethical Committee of the Basel University Hospital (Ethikkommission beider Basel [EKKB], Ref. 78/07). The adipose tissue was minced and digested with 0.15% *w*/*v* collagenase (Worthington Biochemical Corporation, Lakewood, USA) in phosphate-buffered saline (PBS) at 37 °C under continuous shaking for 60 min. After centrifugation at 1500 rpm for 10 min, the lipid-rich layer was discarded and the cellular pellet was washed once with PBS. Released cells were strained through a 100-µm strainer to remove fibrous debris. Cells were plated in T175 flasks at the density of 10,000 cells/cm^2. High-glucose Dulbecco's modified Eagle's medium (ThermoFisher, Waltham, USA) with 10% *v*/*v* heat inactivated foetal bovine serum (Sigma-Aldrich, St. Louis, USA), 1% HEPES (ThermoFisher, Waltham, USA), 1% glutamine solutions, 1% penicillin/streptomycin (P/S, ThermoFisher, Waltham, USA) and 5 ng/mL fibroblast growth factor-2 (FGF-2, R&D System, Minneapolis, USA) were used for cell culture. Cells were expanded until passage 1 for experiments.

Human umbilical vein endothelial cells (HUVECs) were purchased from Promocell (C-12203; pooled donors) and expanded until passage 4 with a seeding density of nearly 3300 cells/cm^2. Endothelial cell growth medium-2 (EGM2, Promocell, Huissen, The Netherlands or Lonza, Basel, Switzerland) was used for HUVEC expansion. The medium was changed twice a week. Cells were subcultured when 85–90% confluence was reached, until passage 4 or 5.

Generation and *In vitro* Differentiation of hMSC Pellets

200,000 hMSCs were resuspended in 500 µL of complete chondrogenic medium [high-glucose Dulbecco's modified Eagle's medium (DMEM) supplemented with 50 µg/mL gentamicin (ThermoFisher, Waltham, USA), 1.5 µg/mL Amphotericin B (ThermoFisher, Waltham, USA), 1 mM sodium pyruvate (ThermoFisher, Waltham, USA), 40 µg/mL proline (Sigma-Aldrich, St. Louis, USA), 1:100 *v*/*v* insulin-transferrin-selenium (ITS+; BD Biosciences, Franklin Lakes, USA), 10 ng/mL transforming growth factor-β3 (TGF-β3, R&D System, Minneapolis, USA), 25 µg/mL L-ascorbic acid 2-phosphate (Sigma-Aldrich, St. Louis, USA) and 100 nM dexamethasone (Sigma-Aldrich, St. Louis, USA)] in 15 mL-polypropylene tubes and centrifuged for 8 min at 200× *g*. After 24 h of culture, the tubes were gently tapped to dislodge the pellets, which were further cultured in a humidified atmosphere at 37 °C in 5% CO_2 for up to 28 days. To induce mineralisation of chondrogenic pellets, 10 mM β-Glycerophosphate (BGP, Sigma-Aldrich, St. Louis, USA) was added to the culture medium, according to the different culture schemes reported in Fig. 1a.

Calcium Uptake Assay

The mineralisation of chondrogenic pellets was monitored during culture by determining the calcium uptake from the medium. To monitor calcium uptake by the pellets, 100 µL of supernatant was collected from 3 pellets for each condition twice a week, and the calcium concentration was calculated using a standard curve of 0–3.0 mM $CaCl_2$ (Sigma-Aldrich, St. Louis, USA) in calcium-free DMEM (ThermoFisher, Waltham, USA). In a 96-well plate, 100 µL of reagent [1:1 of reagent 1 (1M ethanolamine pH 10.5 (Sigma-Aldrich, St. Louis, USA)) and reagent 2 (0.35 mM o-cresolphthalein complexone (Sigma-Aldrich, St. Louis, USA), and 19.8 mM 8-hydroxyquinoline (Sigma-Aldrich, St. Louis, USA), 0.6 M hydrochloric acid)] were added to 10 µL medium or standard. The assay is based on the reaction between Ca^{2+} in the culture medium, and o-Cresophthalein complexone in an alkaline solution. This produces a purple-pink colour that was measured at 570 nm on a Versamax spectrophotometer. A standard curve generated with samples with known Ca^{2+} concentration (standards) was used to calculate the concentration of experimental samples by interpolation. Samples consisting of medium only (no pellets) were taken during culture and used as a blank for data normalisation.

Generation of Conditioned Medium from hMSC Pellets

At time points 7, 14, 21 and 28 days, the culture medium of pellets was renewed. Then, 24 h later, the pellets were washed with PBS three times and incubated with basal medium (high-glucose DMEM supplemented with 50 µg/mL gentamicin (Thermofisher, Waltham, USA), 1.5 µg/mL Amphotericin B (Thermofisher, Waltham, USA), 0.1% *w*/*v* bovine serum albumin (Sigma-Aldrich, St. Louis, USA), and 0.1 mM L-ascorbic acid 2-phosphate (Sigma-Aldrich, St. Louis, USA) for 24 h (37 °C and 5% CO_2). After 24 h, the conditioned medium (CM) of 16 pellets per condition was collected and pooled, and cell debris was removed by centrifugation at 700× *g* for 8 min at 4 °C. The same procedure was performed with basal medium without pellets to generate a non-conditioned medium (negative control). All the media were stored at −80 °C until use.

Live/Dead Flow Cytometry Assay

To evaluate cell viability, pellets were collected for live/dead fluorescence-activated cell sorting (FACS) assay. hMSC pellets were incubated with 3 mg/mL collagenase A (Sigma-Aldrich, St. Louis, USA) and 1.5 mg DNase I (Sigma-Aldrich, St. Louis, USA) in RPMI-1640 media (ThermoFisher, Waltham, USA) containing 5% FBS, at 37 °C for 90 min. After incubation, the cell suspension was filtered through a 100-µm cell strainer to remove the pellet debris, and centrifuged at 400× *g* for 5 min. One vial of fluorescent reactive dye (Component A) and 50 µL of anhydrous DMSO (Component B) from the LIVE/DEAD™ Fixable Dead Cell Stain Kit (ThermoFisher, Waltham, USA) were mixed. PBS was used to wash and resuspend cells, and cell numbers were adjusted to the density of 1×10^6 cells/mL by cell counting and PBS. 1 µL of the reconstituted fluorescent reactive dye was mixed with 1 mL of the cell suspension. After 30 min incubation in the dark, cells were analysed with a FACS Jazz cell sorter (Becton Dickinson, Franklin Lakes, USA), and the results were processed with FlowJo software version 10.0.7 (FlowJo LLC, Ashland, USA).

Histological Analysis

hMSC pellets were fixed overnight in 4% formalin prior to dehydration and paraffin-wax embedding. Sections 6 µm thick were cut from all samples. Slides were deparaffinised with xylene and then rehydrated with ethanol gradients. Cell morphology was assessed by haematoxylin and eosin (H&E) staining. To evaluate mineralisation, von Kossa staining was performed. Slides were washed with distilled water and immersed in a silver nitrate solution (Sigma-Aldrich, St. Louis, USA) for 10 min under a desk light (>60 W). Then, 5% sodium thiosulphate (Sigma-Aldrich, St. Louis, USA) was used to remove unreacted silver nitrate. Finally, the slides were mounted with mounting solution (VectaMount, Vector Laboratories, Newark, USA) and enclosed with coverslips. The staining was quantified by a computerised video camera-based image analysis system (NIH, USA ImageJ software, public domain available at: http://rsb.info.nih.gov/nih-image/) under brightfield microscopy and expressed as % of mineralised area (3 sections/pellet at different depths). For the evaluation of matrix glycosaminoglycan (GAG), thionine staining was performed. Deparaffinised slides were stained with 0.4% thionine (Sigma-Aldrich, St. Louis, USA) in 0.01 M aqueous sodium acetate (Sigma-Aldrich, St. Louis, USA), pH 4.5, for 5 min. Then, slides were immersed in 70% ethanol (10 s), 96% ethanol (30 s), 100% ethanol (1 min), and xylene (twice for 1 min) for differentiating the staining. Finally, the slides were mounted with mounting solution (VectaMount, Vector Laboratories, Newark, USA) and coverslips.

Immunocytochemistry for collagen type II and X was employed to evaluate collagens in the matrix of the pellets. For antigen retrieval, slides were treated with 0.1% pronase (Sigma-Aldrich, St. Louis, USA) at 37 °C for 30 min for collagen type II; for collagen type X, pepsin 1 mg/mL in 0.5 M acetic acid pH 2 for 2 h at 37 °C was used for this step. Afterwards, for both types of staining, 10 mg/mL hyaluronidase (Sigma-Aldrich, St. Louis, USA) in PBS was applied to improve antibody penetration, at 37 °C for 30 min. Then, samples were incubated with 10% normal goat serum (Southern Biotech, Birmingham, USA) in PBS with 1% BSA (ThermoFisher, Waltham, USA). Slides were subsequently incubated with either mouse monoclonal 1:100 1st antibody against collagen type II (DSHB, 0.4 µg/mL stock) or 1:100 collagen type X (5 µg/mL stock, ThermoFisher, Waltham, USA) overnight. The slides were then

incubated with a biotinylated 1:100 goat-anti-mouse antibody (Biogenex, Fremont, USA) for 30 min followed by an incubation with 1:50 streptavidin-AP (Biogenex, Fremont, USA). Staining was revealed by incubation with New Fuchsin substrates (Chroma, 1 g/25 mL with 2M HCl). Finally, the slides were mounted with mounting solution (VectaMount, Vector Laboratories, Newark, USA) and coverslips.

Glycosaminoglycan (GAG) Quantification

The pellets were digested using 1 mg/mL Proteinase K, 1 mM iodoacetamide, 10 µg/mL Pepstatin A in 50 mM Tris, 1 mM EDTA buffer (250 µL) (pH 7.6; all Sigma-Aldrich, St. Louis, USA) for 16 h at 56 °C, followed by Proteinase K inactivation at 100 °C for 10 min. To determine the amount of DNA, the cell lysates were treated with 0.415 IU/mL heparin and 1.25 µg/mL RNase for 30 min at 37 °C, followed by addition of 0.375 µL CYQUANT GR solution (ThermoFisher, Waltham, USA). The samples were analysed using a SpectraMax Gemini plate reader with an excitation of 480 nm and an emission of 520 nm. As a standard, DNA sodium salt from calf thymus (Sigma-Aldrich, St. Louis, USA) was used. To determine the amount of GAG, the cell lysates were diluted in PBS supplemented with 10 mM EDTA (pH 6.5) to a volume of 50µL and mixed with 200 µL of 32 mg/L 1,9-dimethylmethylene blue (DMB, Sigma-Aldrich, St. Louis, USA) in 0.04 M Glycin, 0.04 M NaCl pH 3.0. Then the absorbance was measured on a Versamax microplate reader at 590 nm and 530 nm. A 530:590 nm ratio was used to determine the glycosaminoglycan concentration. As a standard, chondroitin sulphate sodium salt from shark cartilage (Sigma-Aldrich, St. Louis, USA) was used.

Gene Expression Analysis

The pellets were manually homogenised with a pestle in 350 µL RNAstat (Tel-Test, Inc., Alvin, USA). Then, 70 µL chloroform (Sigma-Aldrich, St. Louis, USA) was added and thoroughly mixed. Following a 10 min incubation at room temperature and phase separation at 10,000× *g* for 15 min, the aqueous phase was collected, mixed with an equal volume of 70% *v*/*v* ethanol and loaded onto an RNeasy® micro kit column (Qiagen, Hilden, Germany). RNA was isolated and purified following manufacturer's instructions. cDNA was reverse transcribed as per the manufacturer's instructions, using the First Strand cDNA Synthesis Kit (Thermo Fisher, Waltham, USA). The expression of the genes of interest was quantified using qPCR with a Bio-Rad CFX96 Real-Time PCR detection system (Bio-Rad), with either TAQman (ThermoFisher, Waltham, USA) or SYBR-green-based chemistry (ThermoFisher, Waltham, USA). The target genes were *COL2A1* (forward: 5′-GGCAATAGCAGGTTCACGTACA-3′, reverse: 5′-CGATAACAGTCTT GCCCCACT T-3′, and FAM-TAMRA-*COL2A1*-probe: 5′-CCGGTATGTT TCGTGCAGCCATCCT-3′), *COL10A1* (forward: 5′-CAAGGCACCA TCTCCAGGAA-3′, reverse: 5′-AAAGGGTATTTGTGGCAGCATATT-3′, and FAM-TAMRA-*COL10A1*-probe: 5′-TCCAGCACGCAGAATCCATCT GA-3′), *MMP13* (forward: 5′-AAGGAGCATGGCGACTTCT-3′, reverse: 5′-TGGCCCAGGAGGAAAAG C-3′, and FAM-TAMRA-*MMP13* probe: 5′-CCCTCTGGCCTGCGGCTCA-3′), *VEGFA* (forward: 5′-CTTGCCTTGCTGCTCTACC-3′, reverse: 5′-CACACAGGATGGCTTGA AG-3′), *RUNX2* (forward: 5′-ACGTCCCCGTCCATCCA-3′, reverse: 5′-TGGCAGTG TCATCATCTGAAATG-3′, and FAM-TAMRA- *RUNX2*-probe: 5′- ACTGGGCTTC TTGCCATCACCGA-3′), and *COL1A1* (forward: 5′-CAGCCGCTTCACCTACAGC-3′,

reverse: 5′-TTTTGTATTCAATCACTGTCTTGCC-3′, and FAM-TAMRA-*COL1A1*-probe: 5′- CCGGTGTGACTCGTGCAGCC ATC-3′). *B2M* (forward: 5′-TGCTC GCGCTACTCTCTCTTT-3′, reverse: 5′-TCTGCTGGATGACGTGAGTAAAC-3′) was selected for normalisation after evaluation of 3 different housekeeping genes. The expression data were analysed by the $2^{-\Delta CT}$ method.

Cell Proliferation Analysis

To measure HUVEC proliferation, 2.5 × 10^3 cells/cm^2 were seeded in 48-well plates in 300 µL EGM2. After 24 h, the medium was replaced with a mix of 150 µL EBM and 150 µL pellet-derived CM (1:1). Non-conditioned medium + EBM was used as negative control. 10 mM dEdU (BaseClick GmbH, Munich, Germany) was added to label the DNA of replicating cells. After 24 h, the cells were washed three times with PBS and fixed with 4% formalin for 5 min. The EdU label was then revealed according the protocol provided by the manufacturer. The cells were counterstained with DAPI and imaged using fluorescence microscopy. Utilising the particle analysis macro in ImageJ, we determined the amount of positively stained cells for DAPI and EdU, and the percentage of EdU-positive cells was calculated. Three non-overlapping pictures/wells (1388×1040 μm^2 per field) were taken, with triplicate wells for each independent experiment (N = 3 hMSC donors).

Cell Migration Analysis

Migration assays were performed by seeding HUVEC (1.5 × 10^5 cells/cm^2) in 24-well Transwell inserts (8 um pore size, Corning Life Sciences, Tewksbury, USA) in 200 µL endothelial basal medium (EBM) containing 0.05% BSA (Sigma-Aldrich, St. Louis, USA). The CM from pellets was mixed with EBM at the ratio of 1:1 (total volume = 500 µL) and placed in the lower compartment of the wells. Non-conditioned medium + EBM was used as negative control. After 10 h of incubation at 37 °C 5% CO_2, the cells on the membrane were fixed with 4% formalin/PBS, and the non-migrated cells from the upper surface of the membrane were removed with a cotton swab. The migrated cells on the lower surface of the membrane were stained with DAPI and then quantified by fluorescence microscopy and image analysis through ImageJ (software version 1.53t). Five non-overlapping pictures/wells were taken, with triplicate wells for each independent experiment. (N = 3 hMSC donors).

VEGFA ELISA

To quantify the amount of the pro-angiogenic cytokine VEGFA released into the CM, an ELISA assay (R&D System, Minneapolis, USA) was performed. The capture antibody was diluted according to the manufacturer's instructions and added into a 96-well plate at room temperature overnight. Then, wells were washed with 300 µL wash buffer two times and subsequently incubated with 300 µL reagent diluent at RT for 1 h. After washing the wells with wash buffer, CM from the pellets was added and the plate was sealed and incubated for 2h at RT. Then, 100 µL of detection antibody, 100 µL of working dilution of Streptavidin-HRP, 100 µL of substrate solution and 50 µL of stop solution were added into each well and incubated for 2 h, 2 h, 20 min, and 20 min, respectively. Between incubations, wells were washed with wash buffer twice, and the plate was sealed with an adhesive strip without exposure to direct light. Finally, the

optical density of each well was measured at 450 nm and 570 nm (Versamax, Molecular Devices, San Jose, USA).

Vascular Network Formation Assay in Fibrin Hydrogel

For each hydrogel, 300,000 HUVECs and 300,000 ASCs were resuspended in 50 µL of 20 mg/mL fibrinogen in 0.9% *w*/*v* NaCl (plasminogen, vWF and fibronectin-depleted human fibrinogen, MILAN Analytica AG). Human thrombin (Sigma-Aldrich, St. Louis, USA) and Factor XIII (CSL Behring, King of Prussia, USA) were added at a concentration of 6 U/mL to 50 µL of 40 mM $CaCl_2$ solution. The cell suspension and enzyme solution were mixed to generate fibrin hydrogel with a total volume of 100 µL. 15–20 min was required for hydrogel crosslinking (37 °C). 270 µL of culture medium (1:1 mix of EGM2 and pellet CM from donor 1) was added to each hydrogel. Non-conditioned medium + EGM2 was used as negative control. The medium was renewed twice a week, and cultures were kept in a humidified atmosphere at 37 °C and 5% CO_2. The hydrogels were fixed on day 14 of culture for confocal imaging analysis of vessel formation.

To perform whole-mount staining, the fibrin hydrogels were fixed with 1% paraformaldehyde (PFA) overnight at 4 °C. Samples were placed on a shaker to improve hydrogel penetration during staining. The gels were washed three times with PBS, for 3 h at 4 °C. After washing, 3% BSA and 5% donkey serum (Sigma-Aldrich, St. Louis, USA) in PBS was used overnight to block non-specific binding. The gels were subsequently incubated with 1:100 anti-human laminin antibody (0.7 mg/mL stock, Abcam, Cambridge, UK) in PBS with 3% BSA and 5% donkey serum (Sigma-Aldrich, St. Louis, USA) overnight. The PBS washing step was repeated, and incubation with 1:200 Alexa fluor 647 secondary antibody (2 mg/mL stock, Thermo Fisher, Waltham, USA) at 4 °C was performed overnight with foil cover to avoid exposure to direct light. The hydrogels were imaged using a Leica Stellaris 5 low-incidence angle upright microscope, with an excitation wavelength of 638nm and a long-pass emission filter for laminin signal. The gels were optically scanned (distance between every scanned layer: 6 µm), and all the images were stacked through a Z-stack program in ImageJ for Vessel length density (VLD) analysis. Vessel lengths were measured by overlaying captured microscopic images with a square grid (field size = 200,000 μm^2). Squares were randomly chosen and the length of each vessel (if any) in the selected squares was measured and summed up. For each sample, 10 fields of the whole image for vessel length measurements were obtained, with triplicate samples for each experimental group. A schematic of the VLD measurement is reported in Fig. S1.

Statistical Analysis

Data representation was performed using GraphPad Prism (software version 8.0), and statistical analyses was performed with SPSS 24 (IBM). The normality of the data was first verified using the Kolmogorov–Smirnov test. Subsequently, for all multiple comparisons, a linear mixed model with Bonferroni correction was used; the different conditions were considered as a fixed parameter and the donor as a random factor. Statistical significance was evaluated between conditions within the same time-point and defined as $p < 0.05$. All results are presented as mean ± standard deviation (SD).

REFERENCES

[1] J.A. Gasser, and M. Kneissel, Bone Physiology and Biology, Bone Toxicology, 2017, pp. 27-94.
[2] C. Kiernan, C. Knuth, and E. Farrell, Endochondral Ossification, Developmental Biology and Musculoskeletal Tissue Engineering, Elsevier Science, Amsterdam, The Netherlands, 2018, pp. 125-148.
[3] E.M. Thompson, A. Matsiko, E. Farrell, D.J. Kelly, and F.J. O'Brien, Recapitulating endochondral ossification: a promising route to in vivo bone regeneration. J Tissue Eng Regen Med 9 (2015) 889-902.
[4] E. Farrell, O.P. van der Jagt, W. Koevoet, N. Kops, C.J. van Manen, C.A. Hellingman, H. Jahr, F.J. O'Brien, J.A. Verhaar, H. Weinans, and G.J. van Osch, Chondrogenic priming of human bone marrow stromal cells: a better route to bone repair? Tissue Eng Part C Methods 15 (2009) 285-95.
[5] J.M. Jukes, S.K. Both, A. Leusink, L.M.T. Sterk, C.A. Van Blitterswijk, and J. De Boer, Endochondral bone tissue engineering using embryonic stem cells. Proceedings of the National Academy of Sciences 105 (2008) 6840-6845.
[6] K. Pelttari, A. Winter, E. Steck, K. Goetzke, T. Hennig, B.G. Ochs, T. Aigner, and W. Richter, Premature induction of hypertrophy during in vitro chondrogenesis of human mesenchymal stem cells correlates with calcification and vascular invasion after ectopic transplantation in SCID mice. Arthritis Rheum 54 (2006) 3254-66.
[7] C. Scotti, B. Tonnarelli, A. Papadimitropoulos, A. Scherberich, S. Schaeren, A. Schauerte, J. Lopez-Rios, R. Zeller, A. Barbero, and I. Martin, Recapitulation of endochondral bone formation using human adult mesenchymal stem cells as a paradigm for developmental engineering. Proceedings of the National Academy of Sciences 107 (2010) 7251-7256.
[8] E. Farrell, S.K. Both, K.I. Odörfer, W. Koevoet, N. Kops, F.J. O'Brien, R.J. Baatenburg de Jong, J.A. Verhaar, V. Cuijpers, J. Jansen, R.G. Erben, and G.J. van Osch, In-vivo generation of bone via endochondral ossification by in-vitro chondrogenic priming of adult human and rat mesenchymal stem cells. BMC Musculoskelet Disord 12 (2011) 31.
[9] C.A. Knuth, J. Witte-Bouma, Y. Ridwan, E.B. Wolvius, and E. Farrell, Mesenchymal stem cell-mediated endochondral ossification utilising micropellets and brief chondrogenic priming. Eur Cell Mater 34 (2017) 142-161.
[10] F.E. Freeman, J. Schiavi, M.A. Brennan, P. Owens, P. Layrolle, and L.M. McNamara, Mimicking the Biochemical and Mechanical Extracellular Environment of the Endochondral Ossification Process to Enhance the In Vitro Mineralization Potential of Human Mesenchymal Stem Cells. Tissue Eng Part A 23 (2017) 1466-1478.
[11] D. Kaigler, Z. Wang, K. Horger, D.J. Mooney, and P.H. Krebsbach, VEGF scaffolds enhance angiogenesis and bone regeneration in irradiated osseous defects. J Bone Miner Res 21 (2006) 735-44.
[12] D.H. Kempen, L. Lu, A. Heijink, T.E. Hefferan, L.B. Creemers, A. Maran, M.J. Yaszemski, and W.J. Dhert, Effect of local sequential VEGF and BMP-2 delivery on ectopic and orthotopic bone regeneration. Biomaterials 30 (2009) 2816-25.
[13] E.J. Sheehy, C.T. Buckley, and D.J. Kelly, Chondrocytes and bone marrow-derived mesenchymal stem cells undergoing chondrogenesis in agarose

hydrogels of solid and channelled architectures respond differentially to dynamic culture conditions. J Tissue Eng Regen Med 5 (2011) 747-58.
[14] E. Babaliari, G. Petekidis, and M. Chatzinikolaidou, A Precisely Flow-Controlled Microfluidic System for Enhanced Pre-Osteoblastic Cell Response for Bone Tissue Engineering. Bioengineering (Basel) 5 (2018) 66.
[15] N. Movilla, C. Borau, C. Valero, and J.M. Garcia-Aznar, Degradation of extracellular matrix regulates osteoblast migration: A microfluidic-based study. Bone 107 (2018) 10-17.
[16] A. Hokugo, Y. Kubo, Y. Takahashi, A. Fukuda, K. Horiuchi, K. Mushimoto, Y. Tabata, and S. Morita, Prefabrication of vascularized bone graft using guided bone regeneration. Tissue Engineering 10 (2004) 978-986.
[17] U. Kneser, E. Polykandriotis, J. Ohnolz, K. Heidner, L. Grabinger, S. Euler, K.U. Amann, A. Hess, K. Brune, and P. Greil, Engineering of vascularized transplantable bone tissues: induction of axial vascularization in an osteoconductive matrix using an arteriovenous loop. Tissue engineering 12 (2006) 1721-1731.
[18] O. Tsigkou, I. Pomerantseva, J.A. Spencer, P.A. Redondo, A.R. Hart, E. O'Doherty, Y. Lin, C.C. Friedrich, L. Daheron, C.P. Lin, C.A. Sundback, J.P. Vacanti, and C. Neville, Engineered vascularized bone grafts. Proc Natl Acad Sci U S A 107 (2010) 3311-6.
[19] I. Kocherova, A. Bryja, P. Mozdziak, A. Angelova Volponi, M. Dyszkiewicz-Konwinska, H. Piotrowska-Kempisty, P. Antosik, D. Bukowska, M. Bruska, D. Izycki, M. Zabel, M. Nowicki, and B. Kempisty, Human Umbilical Vein Endothelial Cells (HUVECs) Co-Culture with Osteogenic Cells: From Molecular Communication to Engineering Prevascularised Bone Grafts. J Clin Med 8 (2019) 1602.
[20] C. Bouland, P. Philippart, D. Dequanter, F. Corrillon, I. Loeb, D. Bron, L. Lagneaux, and N. Meuleman, Cross-Talk Between Mesenchymal Stromal Cells (MSCs) and Endothelial Progenitor Cells (EPCs) in Bone Regeneration. Frontiers in cell and developmental biology 9 (2021) 674084.
[21] R. Dreier, Hypertrophic differentiation of chondrocytes in osteoarthritis: the developmental aspect of degenerative joint disorders. Arthritis research & therapy 12 (2010) 1-11.
[22] E. Seeman, Bone modeling and remodeling. Crit Rev Eukaryot Gene Expr 19 (2009) 219-33.
[23] Y. Bando, H. Sakashita, A. Nagasaka, K. Sakiyama, N. Tokuda, S. Iseki, Y. Owada, and O. Amano, Septoclasts expressing epidermal fatty acid-binding protein (E-FABP, FABP5) in endochondral ossification. J Oral Biosci 64 (2022) 18-25.
[24] H. Nagai, and M. Aoki, Inhibition of growth plate angiogenesis and endochondral ossification with diminished expression of MMP-13 in hypertrophic chondrocytes in FGF-2-treated rats. J Bone Miner Metab 20 (2002) 142-7.
[25] E.J. Battegay, Angiogenesis: mechanistic insights, neovascular diseases, and therapeutic prospects. J Mol Med (Berl) 73 (1995) 333-46.
[26] N. Ortega, D. Behonick, D. Stickens, and Z. Werb, How proteases regulate bone morphogenesis. Ann N Y Acad Sci 995 (2003) 109-16.
[27] R.A. Deckelbaum, I.B. Lobov, E. Cheung, G. Halasz, S. Rajamani, J. Lerner, C. Tong, Z. Li, P. Boland, and M. Dominguez, The potassium channel Kcne3 is a VEGFA-inducible gene selectively expressed by vascular endothelial tip cells. Angiogenesis 23 (2020) 179-192.

[28] L. Geris, A. Gerisch, J.V. Sloten, R. Weiner, and H.V. Oosterwyck, Angiogenesis in bone fracture healing: a bioregulatory model. J Theor Biol 251 (2008) 137-58.
[29] W.L. Hunter, and A.L. Arsenault, Vascular invasion of the epithyseal growth plate: Analysis of metaphyseal capillary ultrastructure and growth dynamics. The Anatomical Record 227 (1990) 223-231.
[30] H. Mark, A. Penington, U. Nannmark, W. Morrison, and A. Messina, Microvascular invasion during endochondral ossification in experimental fractures in rats. Bone 35 (2004) 535-42.
[31] Y. Nossin, E. Farrell, W. Koevoet, F. Datema, R.A. Somoza, A.I. Caplan, and G. van Osch, The Releasate of Avascular Cartilage Demonstrates Inherent Pro-Angiogenic Properties In Vitro and In Vivo. Cartilage 13 (2021) 559S-570S.
[32] Y. Nossin, E. Farrell, W.J. Koevoet, R.A. Somoza, A.I. Caplan, B. Brachvogel, and G.J. Van Osch, Angiogenic potential of tissue engineered cartilage from human mesenchymal stem cells is modulated by Indian hedgehog and serpin E1. Frontiers in Bioengineering and Biotechnology 8 (2020) 327.
[33] H. Enomoto, I. Inoki, K. Komiya, T. Shiomi, E. Ikeda, K.-i. Obata, H. Matsumoto, Y. Toyama, and Y. Okada, Vascular endothelial growth factor isoforms and their receptors are expressed in human osteoarthritic cartilage. The American journal of pathology 162 (2003) 171-181.
[34] M. Shakibaei, G. Schulze-Tanzil, A. Mobasheri, T. Beichler, J. Dressler, and W. Schwab, Expression of the vegf receptor-3 in osteoarthritic chondrocytes: Stimulation by interleukin-1β and association with β1-integrins. Histochemistry and cell biology 120 (2003) 235-241.
[35] G.S. Di Marco, M. König, C. Stock, A. Wiesinger, U. Hillebrand, S. Reiermann, S. Reuter, S. Amler, G. Köhler, and F. Buck, High phosphate directly affects endothelial function by downregulating annexin II. Kidney International 83 (2013) 213-222.
[36] G.S. Di Marco, M. Hausberg, U. Hillebrand, P. Rustemeyer, W. Wittkowski, D. Lang, and H. Pavenstadt, Increased inorganic phosphate induces human endothelial cell apoptosis in vitro. American Journal of Physiology-Renal Physiology 294 (2008) F1381-F1387.
[37] F.L. Cals, C.A. Hellingman, W. Koevoet, R.J. Baatenburg de Jong, and G.J. van Osch, Effects of transforming growth factor-beta subtypes on in vitro cartilage production and mineralization of human bone marrow stromal-derived mesenchymal stem cells. J Tissue Eng Regen Med 6 (2012) 68-76.
[38] F.E. Freeman, H.Y. Stevens, P. Owens, R.E. Guldberg, and L.M. McNamara, Osteogenic Differentiation of Mesenchymal Stem Cells by Mimicking the Cellular Niche of the Endochondral Template. Tissue Eng Part A 22 (2016) 1176-1190.
[39] F.E. Freeman, M.A. Brennan, D.C. Browe, A. Renaud, J. De Lima, D.J. Kelly, L.M. McNamara, and P. Layrolle, A Developmental Engineering-Based Approach to Bone Repair: Endochondral Priming Enhances Vascularization and New Bone Formation in a Critical Size Defect. Front Bioeng Biotechnol 8 (2020) 230.
[40] L.F. Bonewald, and S. Dallas, Role of active and latent transforming growth factor β in bone formation. Journal of cellular biochemistry 55 (1994) 350-357.
[41] D.J. Talley-Ronsholdt, E. Lajiness, and K. Nagodawithana, Transforming growth factor-beta inhibition of mineralization by neonatal rat osteoblasts in monolayer and collagen gel culture. In Vitro Cellular & Developmental Biology-Animal 31 (1995) 274-282.

[42] E. Broderick, S. Infanger, T. Turner, and D. Sumner, Depressed bone mineralization following high dose TGF-β1 application in an orthopedic implant model. Calcified tissue international 76 (2005) 379-384.
[43] D.W.D. David Feldman, Jane A. Cauley, Robert Marcus, Osteoporosis, Elsevier Science, Cambridge, Massachusetts, USA, 2013.
[44] S.A. Moody, Principles of developmental genetics, Elsevier Science, Amsterdam, the Netherlands, 2014.
[45] C.A. Knuth, E. Andres Sastre, N.B. Fahy, J. Witte-Bouma, Y. Ridwan, E.M. Strabbing, M.J. Koudstaal, J. van de Peppel, E.B. Wolvius, R. Narcisi, and E. Farrell, Collagen type X is essential for successful mesenchymal stem cell-mediated cartilage formation and subsequent endochondral ossification. Eur Cell Mater 38 (2019) 106-122.
[46] K. Hoshi, S. Kemmotsu, Y. Takeuchi, N. Amizuka, and H. Ozawa, The primary calcification in bones follows removal of decorin and fusion of collagen fibrils. J Bone Miner Res 14 (1999) 273-80.
[47] G. Balasundaram, M. Sato, and T.J. Webster, Using hydroxyapatite nanoparticles and decreased crystallinity to promote osteoblast adhesion similar to functionalizing with RGD. Biomaterials 27 (2006) 2798-2805.
[48] S.G. Rees, D.T. Wassell, R.P. Shellis, and G. Embery, Effect of serum albumin on glycosaminoglycan inhibition of hydroxyapatite formation. Biomaterials 25 (2004) 971-7.
[49] S.G. Rees, R.P. Shellis, and G. Embery, Inhibition of hydroxyapatite crystal growth by bone proteoglycans and proteoglycan components. Biochem Biophys Res Commun 292 (2002) 727-33.
[50] H.C. Blair, M. Zaidi, and P.H. Schlesinger, Mechanisms balancing skeletal matrix synthesis and degradation. Biochem J 364 (2002) 329-41.
[51] S. Otsuki, D.C. Brinson, L. Creighton, M. Kinoshita, R.L. Sah, D. D'Lima, and M. Lotz, The effect of glycosaminoglycan loss on chondrocyte viability: a study on porcine cartilage explants. Arthritis & Rheumatism 58 (2008) 1076-1085.
[52] G. Gibson, Active role of chondrocyte apoptosis in endochondral ossification. Microsc Res Tech 43 (1998) 191-204.
[53] K. Mansfield, B. Pucci, C.S. Adams, and I.M. Shapiro, Induction of apoptosis in skeletal tissues: phosphate-mediated chick chondrocyte apoptosis is calcium dependent. Calcif Tissue Int 73 (2003) 161-72.
[54] D. Magne, G. Bluteau, C. Faucheux, G. Palmer, C. Vignes-Colombeix, P. Pilet, T. Rouillon, J. Caverzasio, P. Weiss, G. Daculsi, and J. Guicheux, Phosphate is a specific signal for ATDC5 chondrocyte maturation and apoptosis-associated mineralization: possible implication of apoptosis in the regulation of endochondral ossification. J Bone Miner Res 18 (2003) 1430-42.
[55] Y. Sabbagh, T.O. Carpenter, and M.B. Demay, Hypophosphatemia leads to rickets by impairing caspase-mediated apoptosis of hypertrophic chondrocytes. Proc Natl Acad Sci U S A 102 (2005) 9637-42.
[56] R.J. McCoy, A. Widaa, K.M. Watters, M. Wuerstle, R.L. Stallings, G.P. Duffy, and F.J. O'Brien, Orchestrating osteogenic differentiation of mesenchymal stem cells—Identification of placental growth factor as a mechanosensitive gene with a pro-osteogenic role. Stem cells 31 (2013) 2420-2431.
[57] T.M. Rodriguez, A. Saldias, M. Irigo, J.V. Zamora, M.J. Perone, and R.A. Dewey, Effect of TGF-beta1 Stimulation on the Secretome of Human Adipose-Derived Mesenchymal Stromal Cells. Stem Cells Transl Med 4 (2015) 894-8.

[58] K. Bittner, P. Vischer, P. Bartholmes, and P. Bruckner, Role of the subchondral vascular system in endochondral ossification: endothelial cells specifically derepress late differentiation in resting chondrocytesin vitro. Experimental cell research 238 (1998) 491-497.
[59] N. Ortega, D.J. Behonick, and Z. Werb, Matrix remodeling during endochondral ossification. Trends in cell biology 14 (2004) 86-93.
[60] R.E. Geuze, F. Wegman, F.C. Oner, W.J. Dhert, and J. Alblas, Influence of endothelial progenitor cells and platelet gel on tissue-engineered bone ectopically in goats. Tissue Eng Part A 15 (2009) 3669-77.
[61] F. Saxer, A. Scherberich, A. Todorov, P. Studer, S. Miot, S. Schreiner, S. Güven, L.A.H. Tchang, M. Haug, M. Heberer, D.J. Schaefer, D. Rikli, I. Martin, and M. Jakob, Implantation of Stromal Vascular Fraction Progenitors at Bone Fracture Sites: From a Rat Model to a First-in-Man Study. Stem Cells 34 (2016) 2956-2966.
[62] L. Wen, Y. Wang, N. Wen, G. Yuan, M. Wen, L. Zhang, Q. Liu, Y. Liang, C. Cai, X. Chen, and Y. Ding, Role of Endothelial Progenitor Cells in Maintaining Stemness and Enhancing Differentiation of Mesenchymal Stem Cells by Indirect Cell-Cell Interaction. Stem Cells Dev 25 (2016) 123-38.

SUPPLEMENTARY MATERIAL

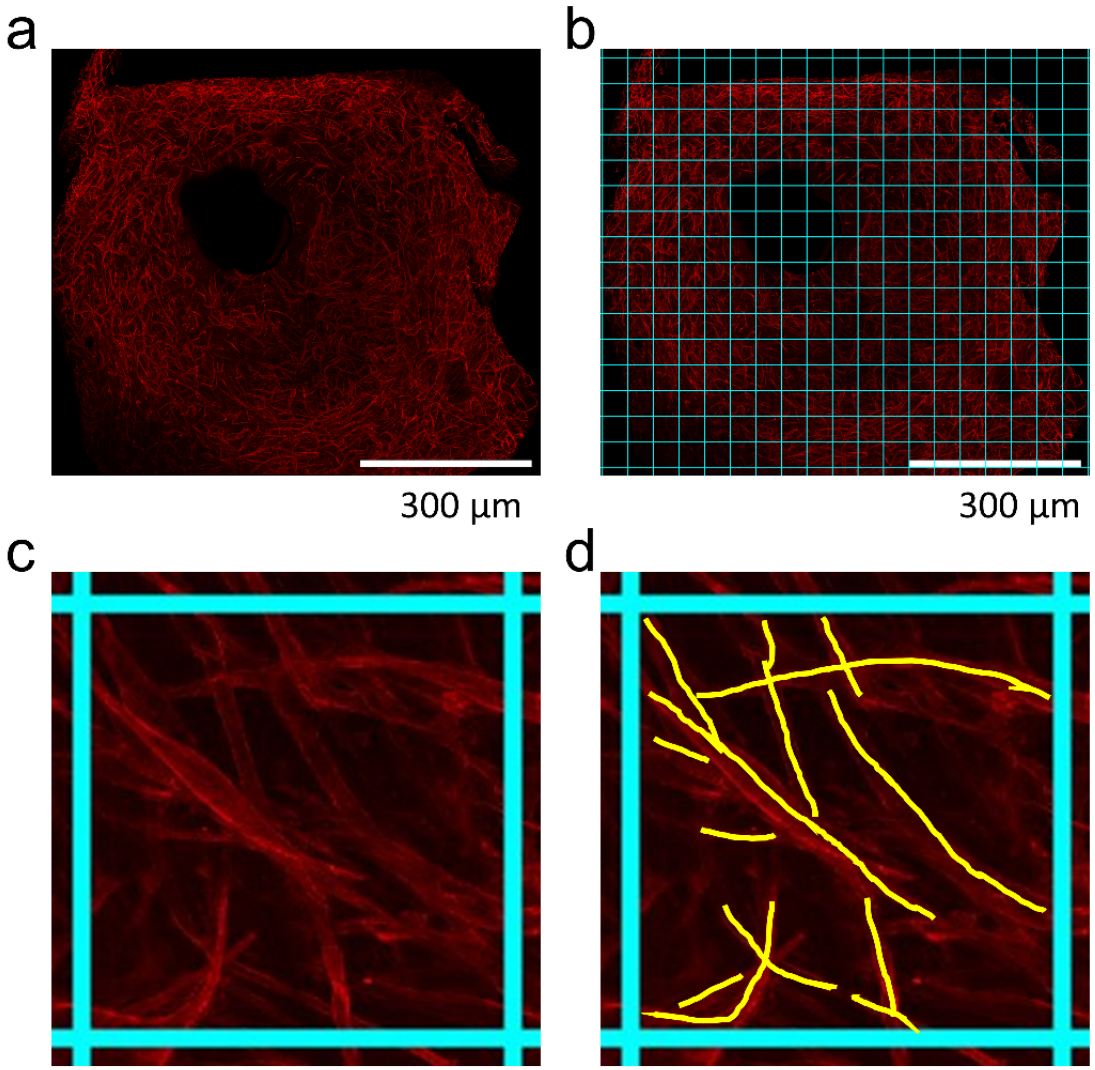

Fig. S1. Schematics of the quantification of the vessel length density (VLD) in 3D tube formation assay. *To evaluate 3D vessel network density,* ***(a)*** *the whole image of the stained vessel network is acquired.* ***(b)*** *Next, the ImageJ software is used to set multiple squares (200000 µm^2 per square) in the image,* ***(c)*** *and 10 squares are randomly selected from the whole image (excluding blank areas).* ***(d)*** *For each square, the tube structures are drawn with freehand line in ImageJ and the total length of these lines is measured. The total VLD (mm/mm^2) is obtained by dividing the total vessel lengths by the area of all the measured squares.*

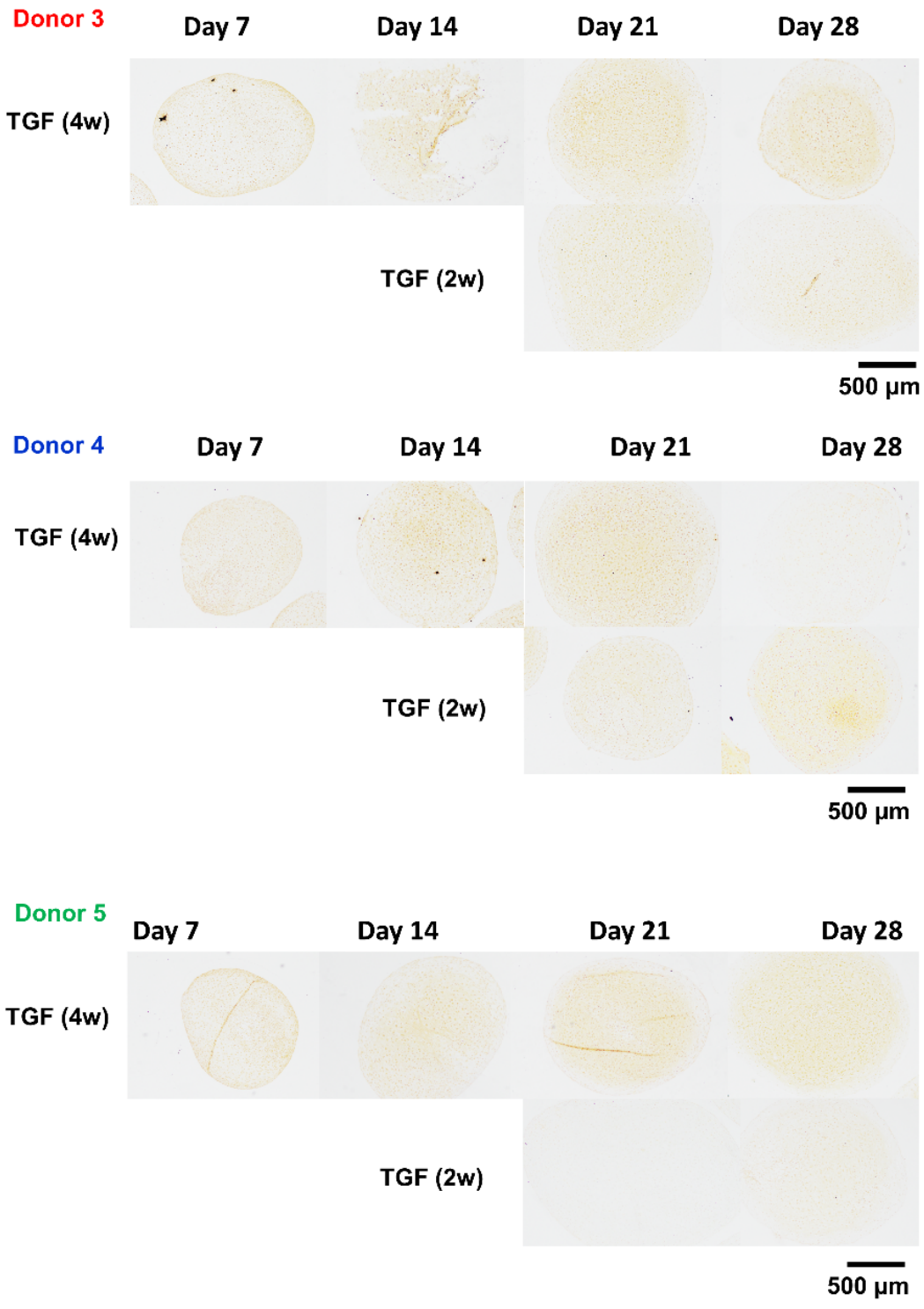

Fig. S2. Von Kossa staining pellets cultured without BGP. *Von Kossa staining of the groups TGF (4w) and TGF (2w) at day 7, 14, 21 and 28 of culture for donor 3, 4 and 5.*

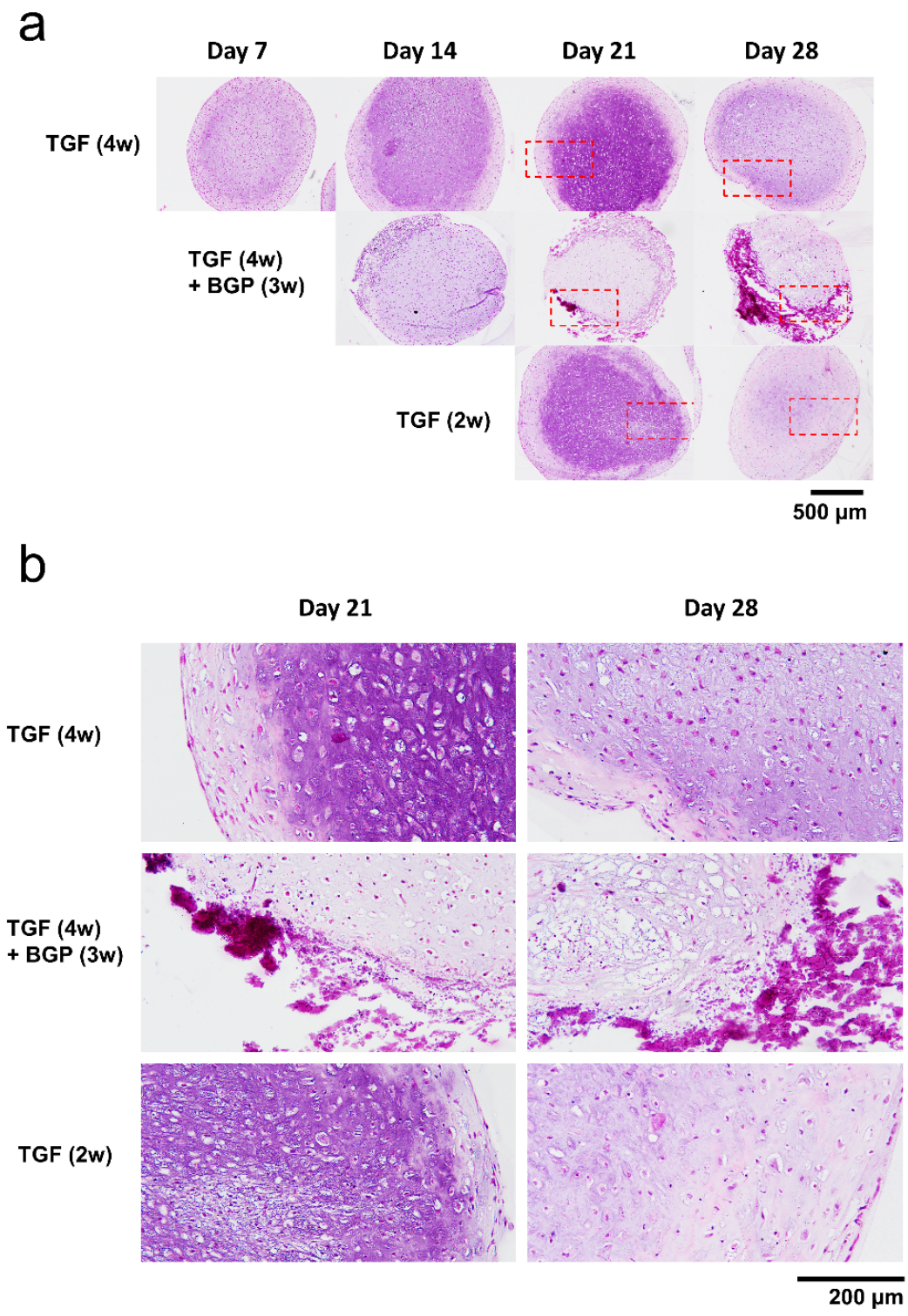

Fig. S3. H&E stained histological sections. *Representative H&E stained histological sections for the different experimental groups for donor 3. Images at low* ***(a)*** *and high* ***(b)*** *magnification are shown.*

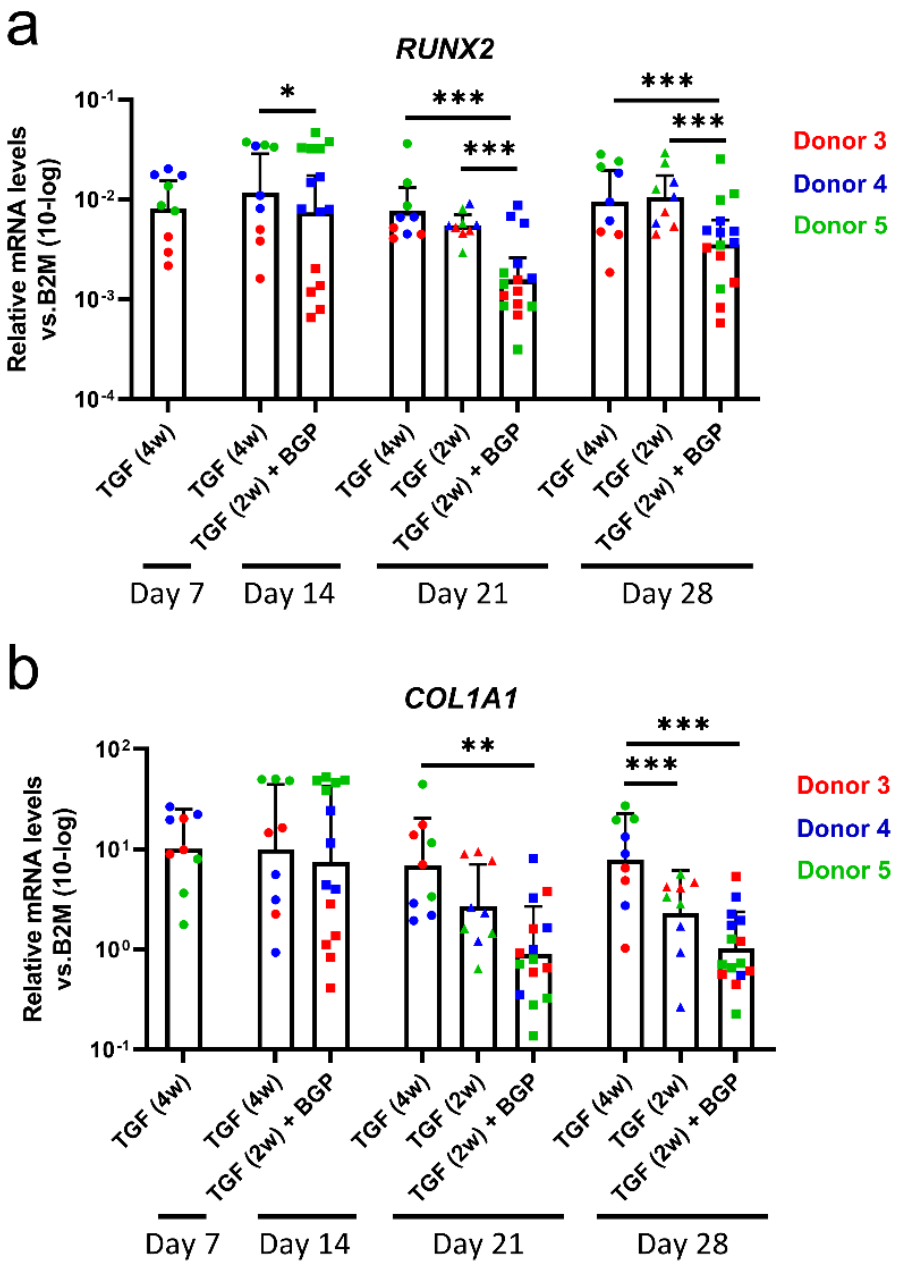

Fig. S4. mRNA expression of RUNX2 and COL1A1. *mRNA expression of RUNX2* ***(a)*** *and COL1A1* ***(b)*** *determined by qRT-PCR. B2M was used as the housekeeper gene. Data are presented as average ± SD (N=3 hMSC donors). *0.01< p < 0.05, **0.01< p < 0.001, ***p < 0.001.*

CHAPTER 4

Development of an advanced human in vitro model of endochondral ossification, comprising mineralised cartilage, osteoclasts and vascular components

Encheng Ji[#], Amaia Garmendia Urdalleta[#], Janneke Witte-Bouma, Gert-Jan Kremers, Nunzia Di Maggio, Andrea Banfi, Eric Farrell*, Andrea Lolli*

#**These authors contributed equally to this work*

Manuscript submitted

CONTRIBUTION STATEMENT

Encheng Ji conducted the experiments related to vessel formation, performed data analysis and visualisation, and jointly drafted and revised the manuscript.

ABSTRACT

During development and regeneration, bone is formed by endochondral ossification (EO) through the remodelling of a cartilage template. This complex process involves multiple cell types and interactions that cannot currently be modelled *in vitro*. This study aimed to develop a novel tissue engineered human *in vitro* model of the early stages of EO by integrating cartilage which undergoes mineralisation, self-assembled vascular networks, and osteoclasts into a single system. We first studied the dynamics of osteoclastogenesis and vascularisation in an *in vivo* model of stromal cell-mediated EO, to inform our *in vitro* system. Next, we aimed to develop a fully human cell-based 3D model of EO by combining human mesenchymal stromal cells (hMSCs) differentiating into chondrocytes, osteoclasts derived from human CD14+ monocytes, and human umbilical vein endothelial cells (HUVECs) and adipose-derived stromal cells (ASCs) as vessel-forming cells. We investigated how mineralising cartilage affects osteoclast and vessel formation *in vitro* through separate cartilage-osteoclasts and cartilage-vessels co-cultures. Finally, we combined these elements and established a complex *in vitro* model that supports the functionality of all these cell types and recapitulates chondrogenesis, cartilage mineralisation, vessel formation and osteoclastogenesis. This integrated approach reaches unprecedented complexity and will allow us to deepen our understanding of cellular interactions during EO, with a number of applications in bone tissue engineering and skeletal disease modelling.

INTRODUCTION

Endochondral ossification (EO) is the natural process of bone formation which occurs in the majority of the bones in the body[1]. Several groups including ours have succeeded in recapitulating endochondral bone formation *in vivo* through a tissue engineering-based approach, allowing the investigation of cellular and molecular mechanisms, or applications in bone regenerative medicine [2-4]. In these studies, a template of hypertrophic cartilage is generally formed from human mesenchymal stromal cells (hMSCs) by inducing chondrogenic differentiation *in vitro*. Upon implantation in animals, the tissue-engineered cartilage undergoes EO and remodels into mature bone which includes all the elements of a functional bone niche, including blood vessels, clastic cells, bone marrow and osteoblasts [5-13]. Recapitulating EO *in vitro* would be highly desirable to establish a highly controlled and completely humanised system, while addressing ethical concerns related to using animals. However, the generation of useful *in vitro* bone models will require the incorporation of many of the aforementioned cellular elements .Current *in vitro* tissue-engineered models are mainly limited to the recapitulation of separate processes, such as the mineralisation of hypertrophic cartilage [14] or the combination of mineralised cartilage only with naïve vessels [15] or osteoclasts [16]. Furthermore, these models often lack a tissue remodelling component. One major challenge is still the difficulty in maintaining the functionality of several cell types and recreating their intricate interplay in a single complex *in vitro* system.

During EO, hypertrophic chondrocytes produce a mineralised cartilage matrix and secrete factors that promote vascular invasion and the recruitment of remodelling osteoclasts [17]. Osteoclasts are important for bone vascularisation and protect blood vessels against senescence [18]. The resorption of the cartilage template and the remodelling of immature bone structures is essential for the formation of a mature bone matrix which can host vasculature and marrow niche. While resorption of unmineralised cartilage is mainly associated with septoclasts [19; 20] and endothelial cells [20; 21], chondroclasts/osteoclasts are thought to be responsible for the resorption of mineralised cartilage and bone [22]. Many studies have shown that when the function of osteoclasts is undermined via knockout of osteoclast-specific genes such as *RANK* or *MMP9* [23-26], the EO process in mice is disrupted, impeding normal bone development and bone remodelling. Recapitulating functional osteoclast activity is therefore essential for the development of a robust *in vitro* EO bone model. In one of our previous studies, we developed a mineralised cartilage co-culture model where *in vitro* invasion of the cartilage matrix by human monocyte derived osteoclasts was shown [16]. However, to date, there have been very few *in vitro* models demonstrating osteoclast-vasculature interactions and none yet in the context of EO.

During EO, vessel network formation is essential to transport nutrients as well as immune and progenitor cells, such as haematopoietic stem cells and osteoprogenitors, to the ossification site. Monocytes migrate through the vessel network and, once reached the mineralisation front, they differentiate into mature clastic cells. Besides providing access to the bone, blood vessels directly contribute to the regulation of signalling pathways involved in osteochondroprogenitor differentiation and cartilage remodelling during EO [27]. This highlights the importance of incorporating vascular components into *in vitro* bone models. Recent efforts have focused on diverse solutions to combine bone cells and vasculature *in vitro*, such as 3D-printed scaffolds with hollow channels [28], self-assembly of vessel-forming cells

[29] and microfluidic devices [30]. However, these studies mainly focus on intramembranous ossification and the interaction between remodelling cartilage and vasculature *in vitro* is still largely unexplored. We recently performed indirect co-culture studies showing how *in vitro* mineralisation affects the pro-angiogenic properties of tissue-engineered cartilage, providing some initial directions for combining these processes *in vitro* [31]. However, replicating the highly dynamic nature of cartilage mineralisation and remodelling, which simultaneously involves vascularisation and osteoclast activity, remains an arduous challenge. We reasoned that the development of a comprehensive *in vitro* model of EO should start with the incorporation of mineralised cartilage, osteoclasts, and blood vessels in a single system, due to their intimate crosstalks and co-dependence. As a first step, the dynamics of osteoclastogenesis and vascularisation were studied in an *in vivo* model of tissue-engineered endochondral bone. This provided temporal information for the recapitulation of these processes *in vitro*. Next, we established direct co-culture systems of cartilage undergoing mineralisation and osteoclasts or vascular networks. Finally, we developed a single complex *in vitro* model of EO that recapitulates chondrogenesis, cartilage mineralisation, osteoclastogenesis and vascular network formation.

RESULTS

hMSC pellets chondrogenically primed for 7 days instruct vascularisation and osteoclastogenesis

We initially investigated the dynamics of vascularisation and osteoclastogenesis *in vivo* in the context of a tissue engineering model of hMSC-mediated endochondral bone formation. Furthermore, we assessed how these processes are affected by the duration of chondrogenic differentiation, since a brief priming protocol would facilitate the development of a complex co-culture system *in vitro*. Sections of available samples from previous *in vivo* experiments of endochondral bone formation performed with 2 hMSC donors were stained to visualise osteoclasts and blood vessels. For these studies, hMSC pellets had been chondrogenically primed *in vitro* for 7 or 21 days, implanted subcutaneously in mice, and retrieved at several time-points up to 84 days post-implantation (Fig. 1A). Endomucin staining of the implanted pellets showed that at the early stages after implantation (3-7 days) vessels were present close to the surface of the pellets for both priming conditions (Fig. 1B). Between 14- and 28-days post-implantation vessel infiltration was more evident for 7-day primed pellets, while only superficial for 21-day primed pellets (Fig. 1B). At the later stages of bone formation (day 56 and 84), large vessel structures were present in the newly formed bone marrow stroma for both 7-day and 21-day primed pellets (Fig. 1B).

TRAP staining evidenced osteoclast recruitment around the pellets as early as 7-14 days post-implantation for both 7-day and 21-day primed pellets (Fig. 1C). While osteoclasts were mainly localised on the surface of the pellets at these early time-points, the late stages of bone formation (day 84) evidenced osteoclasts within the bone marrow at the resorption front of the unresorbed cartilage matrix, supporting their active role in bone remodelling (Fig. 1C). Thus, the comparison of different priming times (7 or 21 days) of hMSC pellets *in vitro* showed the potential of briefly primed cells to instruct vessel and osteoclast formation. In order to further characterise the

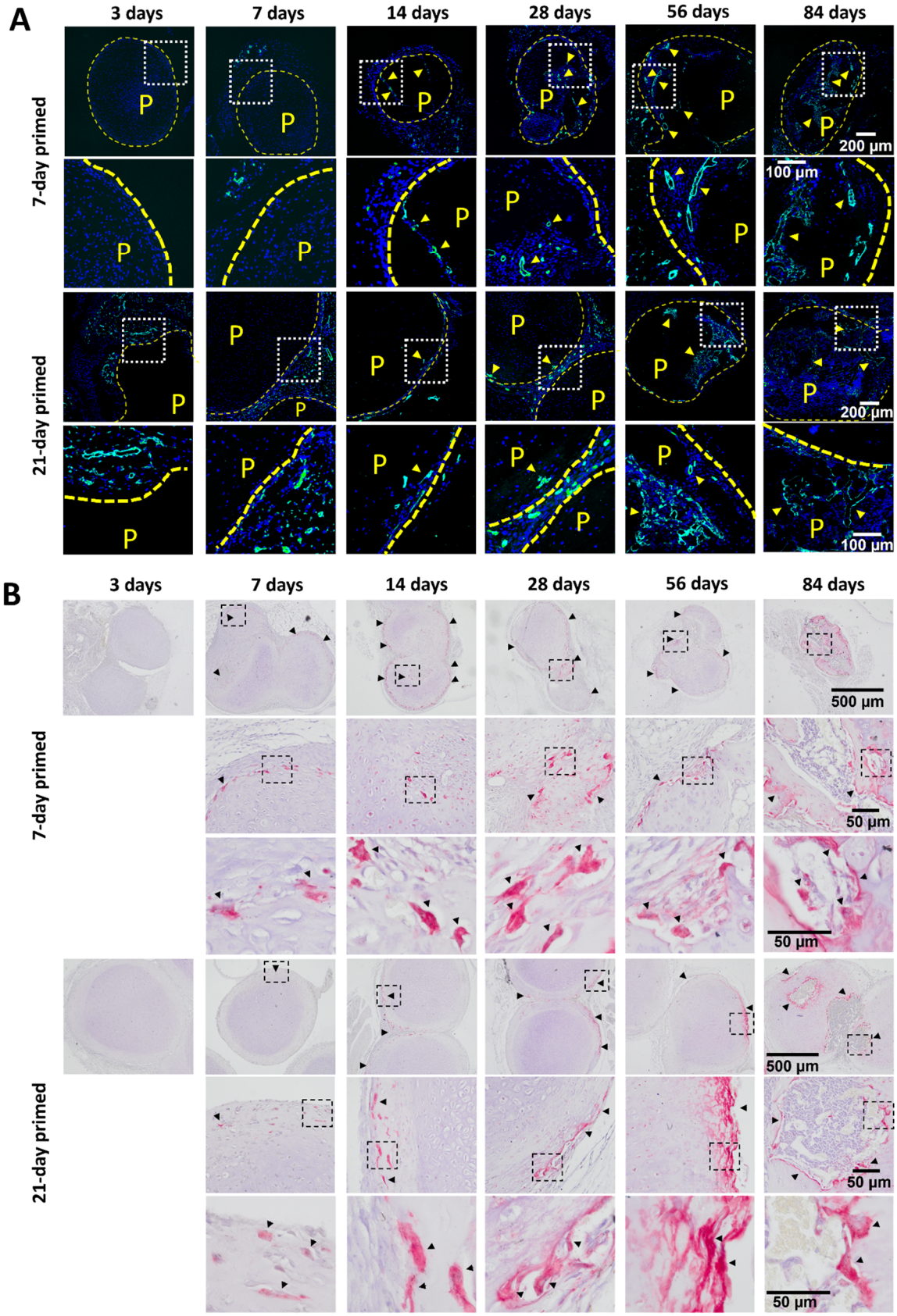

Fig. 1. Vessel and osteoclast recruitment by chondrogenically primed hMSC pellets in vivo. (A) *Experimental scheme for the generation and implantation of 7-day and 21-day chondrogenically primed hMSC pellets.* ***(B)*** *Representative images of*

endomucin stained (green) sections for different time-points post-implantation. The arrowheads indicate vessels; P = pellets. (C) Representative images of TRAP stained (pink) sections for different timepoints post-implantation. The arrowheads indicate osteoclasts. N = 2 hMSC donors.

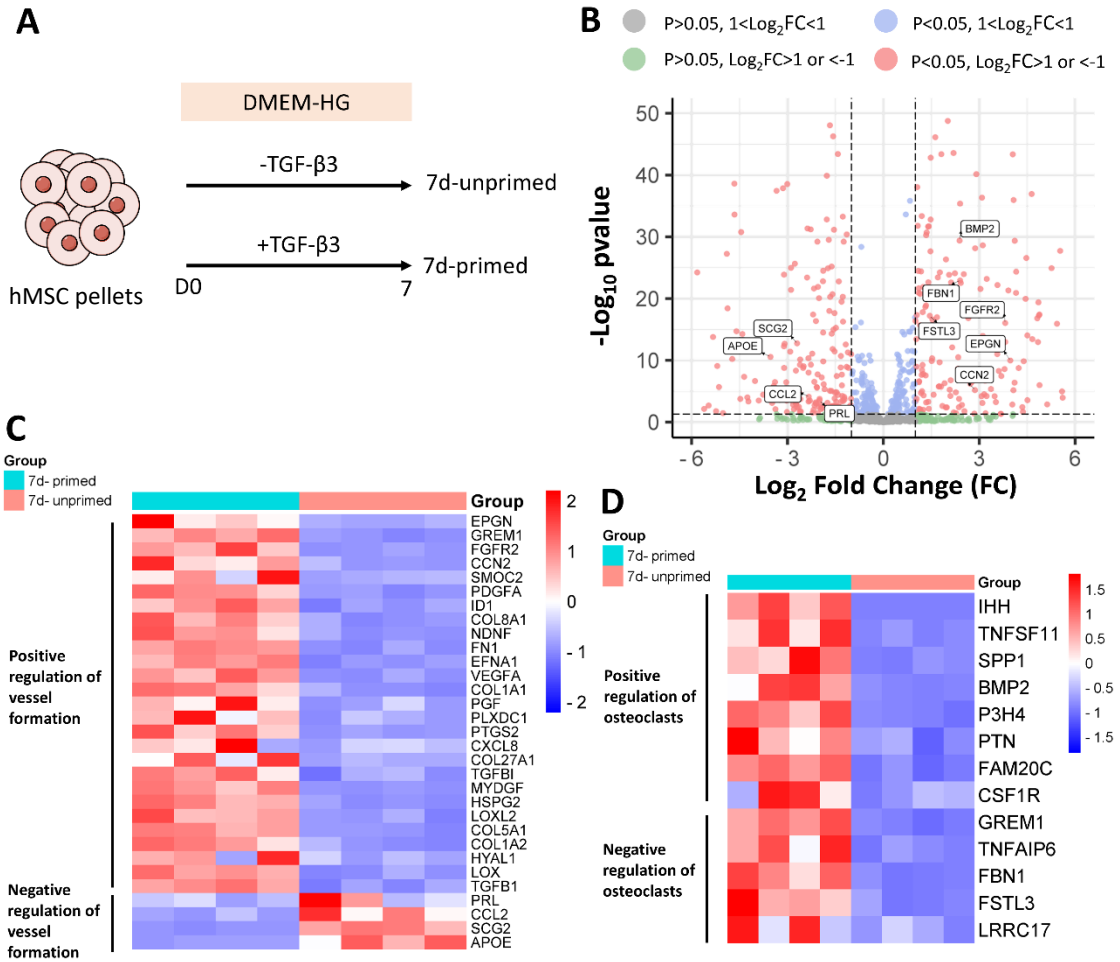

Fig. 2. Bulk RNA-seq analysis of 7-day primed vs 7d-unprimed pellets. (A) *Experimental scheme for the generation of 7d-primed and 7d-unprimed hMSC pellets for bulk RNA-seq analysis.* ***(B)*** *Volcano plot of differentially expressed genes. Several of the genes related regulating vessel formation or osteoclasts were labelled.* ***(C)*** *Heatmap of differentially expressed genes encoding for secreted proteins positively or negatively regulating vessel formation.* ***(D)*** *Heatmap of differentially expressed genes encoding for secreted proteins positively or negatively regulating osteoclasts. N = 4 hMSC donors.*

pro-angiogenic and pro-osteoclastogenic properties of 7-day primed pellets, their full transcriptome was analysed by bulk RNA-seq and compared with unprimed pellets (cultured without TGF-β3 for 7 days (4 hMSC donors)) (Fig. 2A). Differential gene expression analysis showed that 3920 genes were significantly changed (log2 fold change > 1 or <-1) by comparing 7-day primed and 7-day unprimed hMSC pellets, of

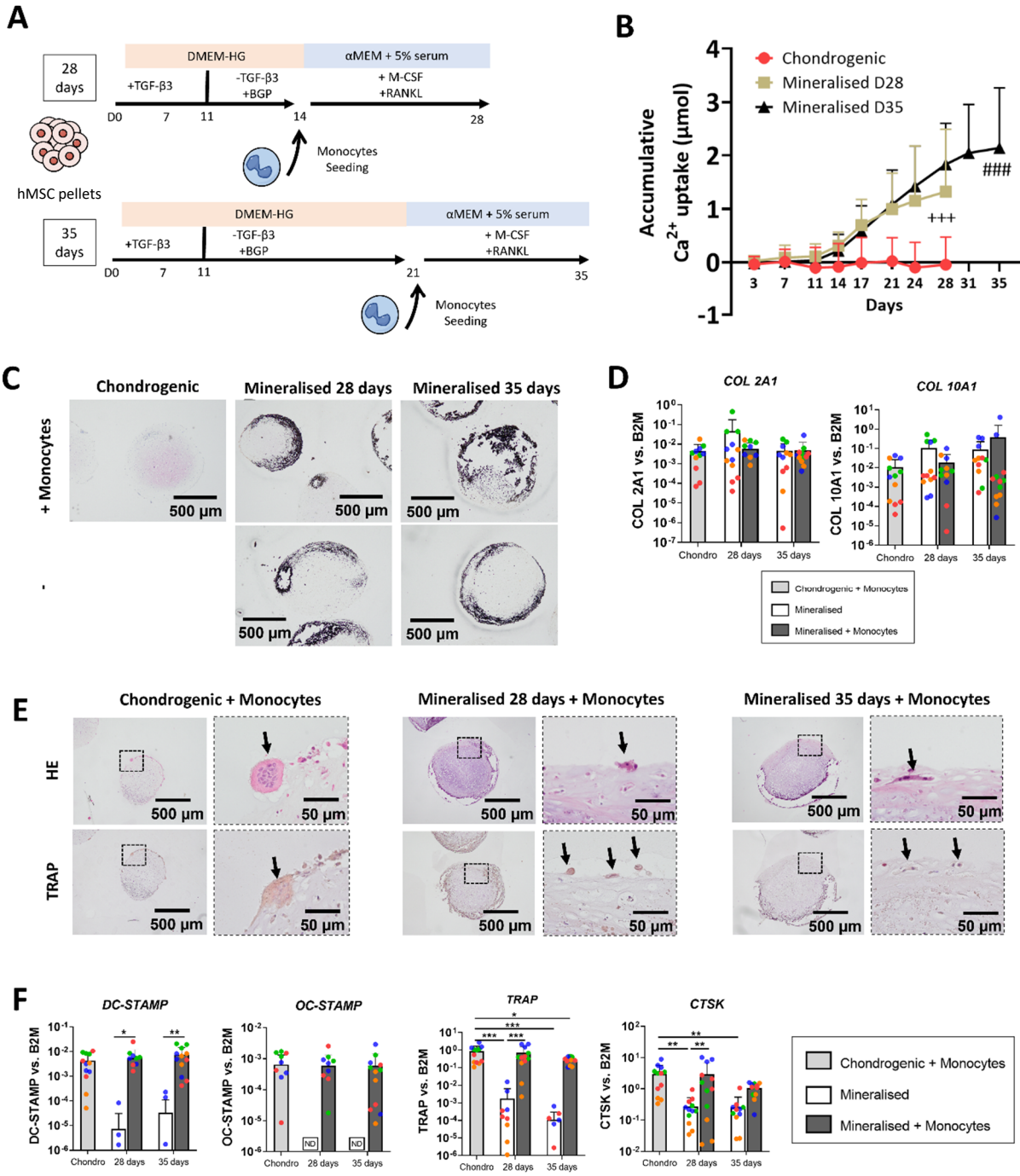

Fig. 3. Co-culture of hMSC pellets undergoing mineralisation with osteoclasts. ***(A)*** *Experimental scheme of the co-culture. BGP was added from day 7 until the end of the culture period.* ***(B)*** *Calcium uptake based determined by the measurement of extracellular calcium levels at different timepoints. # and + indicate statistical difference vs the chondrogenic group.* ***(C)*** *Von Kossa and Thionine co-stainings of hMSC pellets. Representative images are presented.* ***(D)*** *Gene expression analysis of chondrogenesis markers determined by qRT-PCR.* ***(E)*** *HE and TRAP stainings of the pellets.* ***(F)*** *Gene expression analysis of osteoclast markers determined by qRT-PCR. Each colour corresponds to a different donor. All data are presented as average ± SD (N = 4 hMSC donors). *p < 0.05, **p < 0.01, ***p < 0.001.*

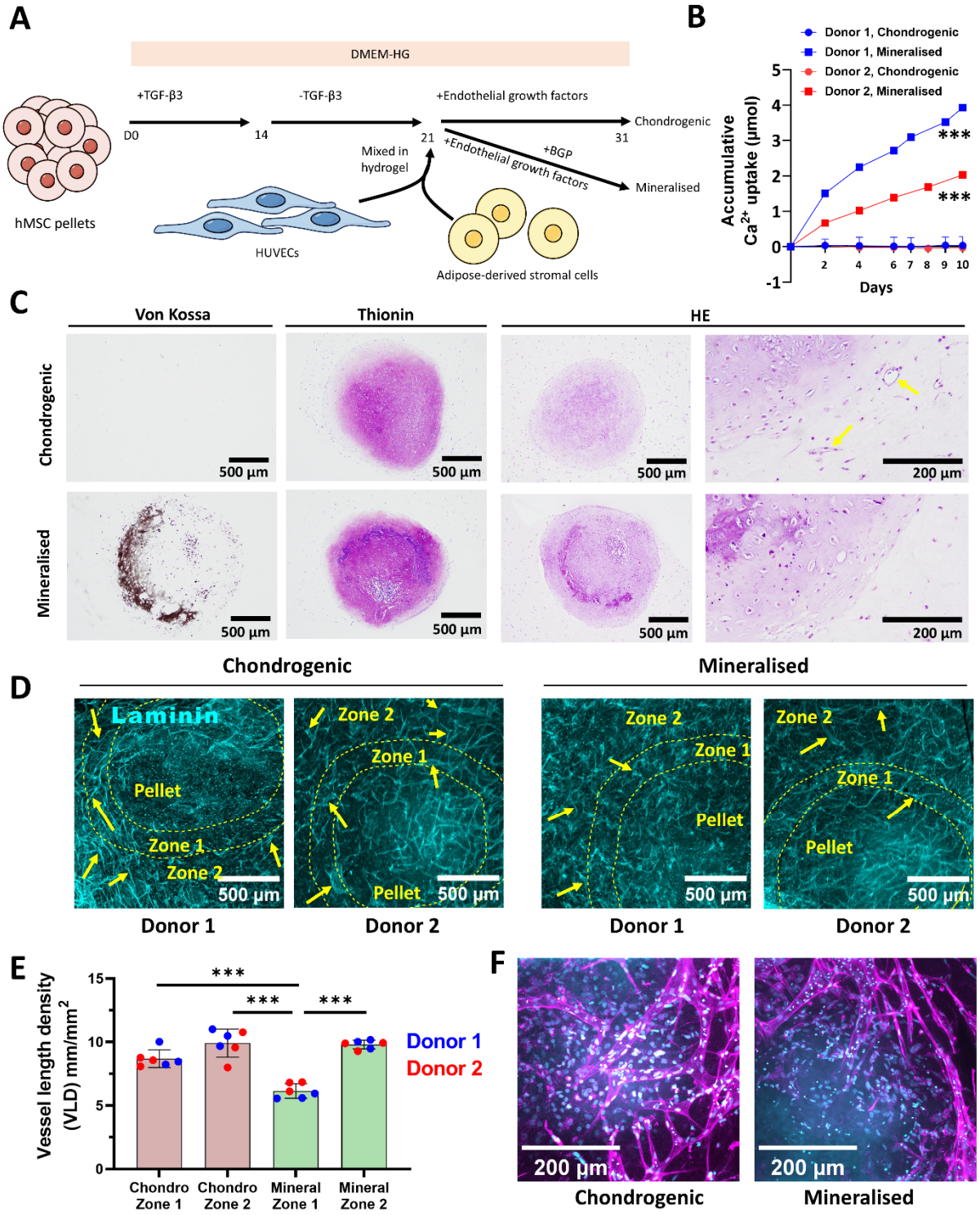

Fig. 4. Co-culture of hMSC pellets undergoing mineralisation with vascular networks. ***(A)*** *Experimental scheme for the co-culture of hMSC (mineralised) pellets with vessel-forming cells in fibrin hydrogels.* ***(B)*** *Calcium uptake based determined by the measurement of extracellular calcium levels at different timepoints. *Indicate statistical difference vs the chondrogenic group.* ***(C)*** *HE, Von Kossa and Thionie stainings of the chondrogenic and mineralised co-culture conditions. Representative images are presented.* ***(D)*** *Confocal imaging of laminin-stained vessels. Representative z-stack images obtained by confocal microscopy are shown.* ***(E)*** *Graph displaying the average VLD values per condition.* ***(F)*** *Confocal imaging of laminin*

*(pink)- and DAPI (blue)-stained vessels in the proximity of the pellets. Representative z-stack images obtained by confocal microscopy are shown. All data are presented as average ± SD (N = 2 hMSC donors). ***p < 0.001.*

which 1969 upregulated and 1951 downregulated (Fig. 2B). Next, we used human secretome data to identify differentially regulated genes that encode for secreted factors [32]. Interestingly, the significantly upregulated genes included several secreted factors known to modulate vascularisation (Fig. 2C) and osteoclastogenesis (Fig. 2D). Altogether these data suggest that hMSC pellets subjected to brief chondrogenic priming may represent a suitable system to support vessel formation and osteoclast differentiation *in vitro*.

Osteoclasts successfully form on chondrogenic pellets at different stages of mineralisation

In order to develop an *in vitro* model with chondrogenic pellets undergoing mineralisation and osteoclasts, hMSC pellets were exposed to BGP after 7 days of chondrogenic priming and subjected to different mineralisation periods (7 or 14 days), prior to monocyte seeding and induction of osteoclast formation for 14 days. The pellets were therefore cultured for 28 or 35 days in total, of which the last 14 days in co-culture with monocytes/osteoclasts (Fig. 3A). Chondrogenic pellets cultured without BGP were included as non-mineralised control. Longitudinal measurements of calcium concentration in the medium revealed significant calcium uptake by mineralising hMSC pellets starting from day 14 (Fig. 3B). Von Kossa staining confirmed the successful formation of mineral deposits within the pellets, which could be maintained in pellets seeded with monocytes (Fig. 3C). Expression levels of the chondrogenic marker *COL2A1* and the hypertrophic marker *COL10A1* were similar for all conditions and not significantly affected by monocyte seeding (Fig. 3D). Osteoclastogenesis was assessed by HE and TRAP staining, revealing the presence of TRAP+ multinucleated cells on the surface of all mineralised pellets seeded with monocytes (Fig. 3E). A certain degree of variability was observed between hMSC donors: 3 out of 4 donors clearly evidenced osteoclasts on the surface of day 28 mineralised pellets, while the size of the osteoclasts formed on the surface of chondrogenic pellets also varied between donors. Induction of the expression of the markers of osteoclast fusion *DC-STAMP* and *OC-STAMP* and the markers of osteoclast activity TRAP and CTSK was found for all mineralised pellets seeded with monocytes in comparison with mineralised pellets not seeded with monocytes (Fig. 3F). Based on these results, we conclude that osteoclasts can be formed and co-cultured with chondrogenic pellets at different stages of *in vitro* mineralisation.

Microvascular networks can be formed and co-cultured with chondrogenic pellets undergoing mineralisation

To establish an *in vitro* model which combines cartilage undergoing mineralisation and vascular networks, we next directly co-cultured hMSC pellets with vessel-forming cells in fibrin hydrogels. Since we previously showed that pellets subjected to prolonged mineralisation have reduced pro-angiogenic properties [31], BGP was added to the medium only at the start of the co-culture (day 21). During initial

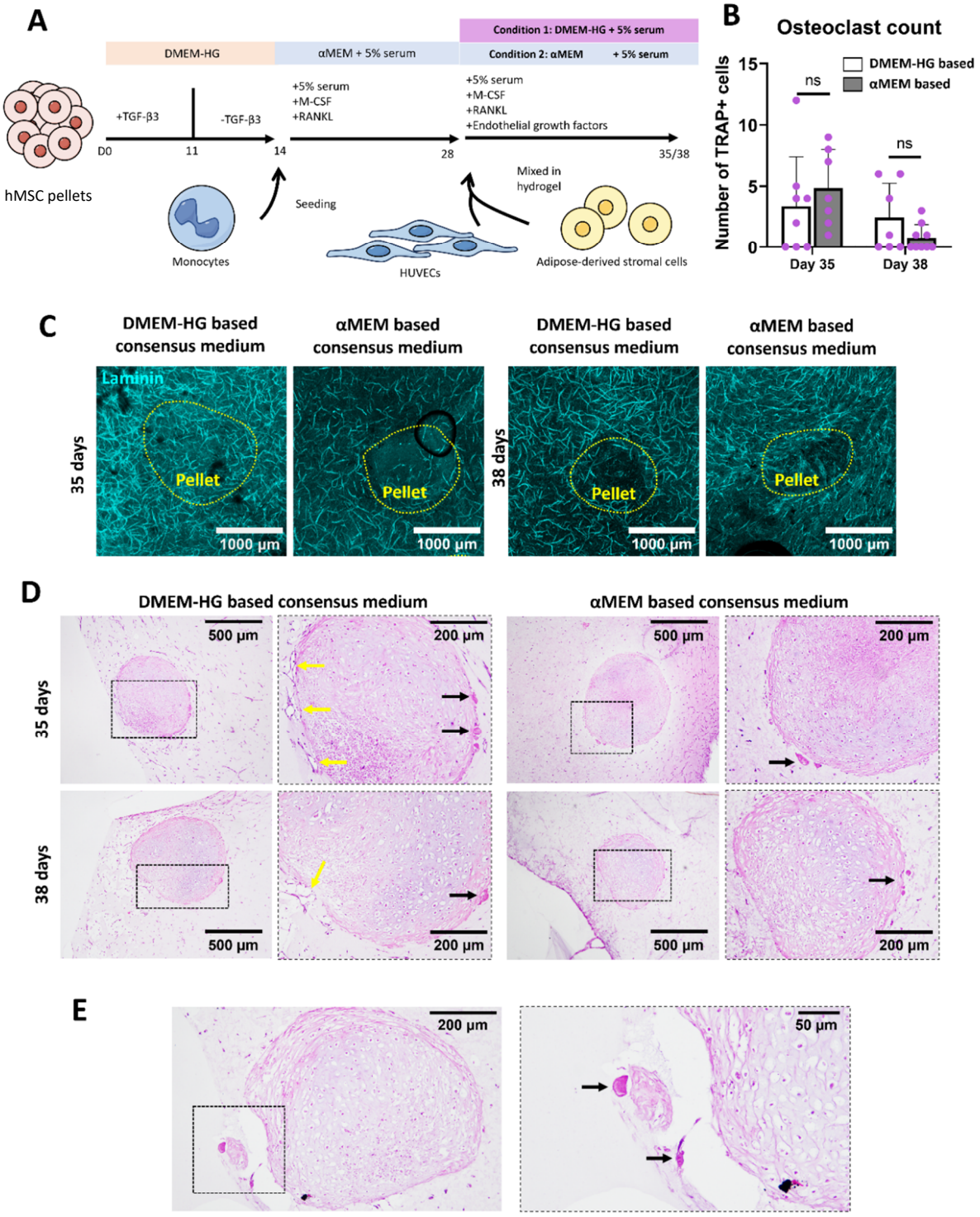

Fig. 5. Co-culture of chondrogenic hMSC pellets, vascular networks and osteoclasts with different consensus media. ***(A)*** *Experimental scheme of the co-culture.* ***(B)*** *Number of TRAP+ cells present on the surface of pellets. All data are presented as average ± SD.* ***(C)*** *Confocal imaging of vessels visualised by laminin staining. Representative z-stack images are shown.* ***(D, E)*** *HE stainings of the co-culture. Representative images are shown. Osteoclasts are indicated by black arrows and vessels by yellow arrows. N = 1 hMSC donor. ns: non-significant*

studies, we also found that the exposure of pellets to TGF-β until the start of the co-culture decreased the efficiency of vascular network formation, likely due to a detrimental effect of TGF-β retained by the pellets (Fig. S1). Based on these observations, we set-up a co-culture scheme where hMSC pellets were chondrogenically primed for 14 days with TGF-β3, then further cultured without TGF-β3 for 7 days. The pellets where then embedded in fibrin hydrogels with ASCs and HUVECs, the components for vascular network formation [33], and cultured until day 31 with or without BGP (Fig. 4A). The calcium measurements demonstrated progressive Ca2+ uptake for pellets exposed to BGP, suggesting that mineralisation of the cartilage matrix can occur during co-culture (Fig. 4B). This was further confirmed by Von Kossa and thionine staining of the pellets (Fig. 4C) HE staining of the hydrogels evidenced the presence of vessel lumina, mainly in the proximity of chondrogenic pellets (Fig. 4C, arrows). To assess vascular network formation, the hydrogels were subjected to whole-mount staining for the endothelial marker laminin (Fig. 4D, F), and the vessel length densities within 200 µm distance from the pellets (zone 1) or further (zone 2) were quantified (Fig. 4E). The results indicated that vascular networks could form around chondrogenic or mineralised pellets. In the case of mineralised pellets, vessel formation in the area close to the pellets (zone 1) was significantly decreased in comparison with zone 2. This effect was due to pellet mineralisation and not uniquely related to BGP addition (Fig. S2). No significant differences were found in zone 2 between chondrogenic and mineralised pellets.

In conclusion, we showed that microvascular networks can be formed and co-cultured with chondrogenic pellets undergoing mineralisation. Under *in vitro* condition s, cartilage mineralisation can locally reduce microvascular assembly.

Integration of chondrogenesis, mineralisation, vascular network formation and osteoclastogenesis into a single 3D co-culture system

We finally aimed to setup a co-culture system which captures cartilage mineralisation, vascular network formation and osteoclastogenesis (Fig. 5A): hMSC pellets were chondrogenically primed with TGF-β3 for 11 days. At day 14 they were seeded with monocytes and osteoclastogenesis was induced via M-CSF and RANKL addition until day 28. Finally, pellet-osteoclast co-cultures were combined with vessel-forming cells (ASCs and HUVECs) in fibrin hydrogels up to day 38. For the last co-culture stage where all cell types are present, we tested consensus media consisting of either DMEM-HG or αMEM supplemented with osteoclastogenic and angiogenic factors. The use of both media generally supported microvascular network formation and osteoclastogenesis under co-culture conditions. A variable but overall similar number of osteoclasts was observed for both conditions at days 35 and 38 (Fig. 5B, D black arrows). While VLDs of the DMEM-HG group showed similar values to the αMEM group (Fig. S3), overall, more vessel branching was observed for DMEM-HG based consensus medium as opposed to αMEM (Fig. 5C, D yellow arrows). Interestingly, some of the histological sections evidenced loose fragments of pellets in close contact with osteoclasts, which may suggest a resorptive effect of these cells (Fig. 5E, black arrows). This phenomenon was observed for both medium types. Based on this study, the DMEM-HG based consensus medium was chosen for further co-cultures.

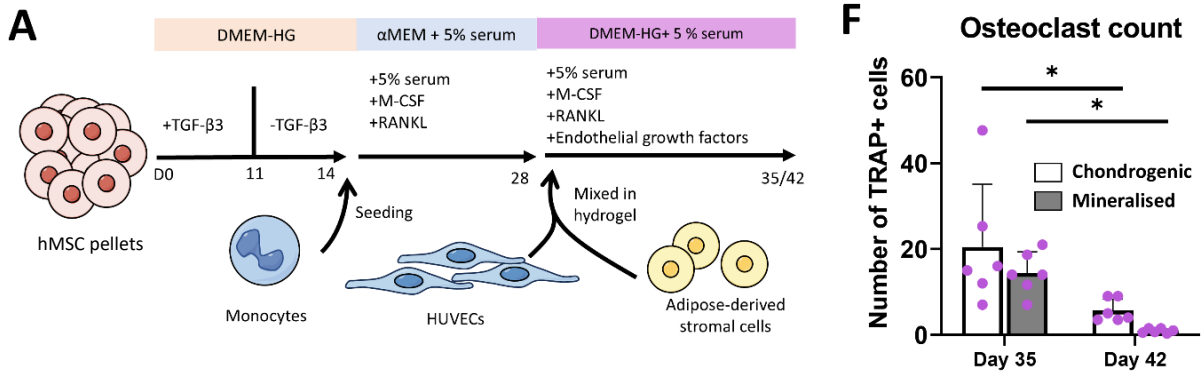
A
DMEM-HG
αMEM + 5% serum
DMEM-HG+ 5 % serum
+TGF-β3
-TGF-β3
+5% serum
+M-CSF
+RANKL
+5% serum
+M-CSF
+RANKL
+Endothelial growth factors
D0
11
14
28
35/42
hMSC pellets
Seeding
Monocytes
HUVECs
Mixed in hydrogel
Adipose-derived stromal cells
F
Osteoclast count
Number of TRAP+ cells
60
40
20
0
*
*
Chondrogenic
Mineralised
Day 35
Day 42

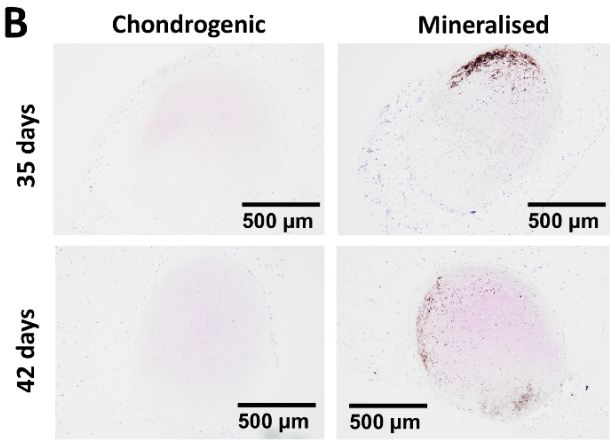
B
Chondrogenic
Mineralised
35 days
42 days
500 µm

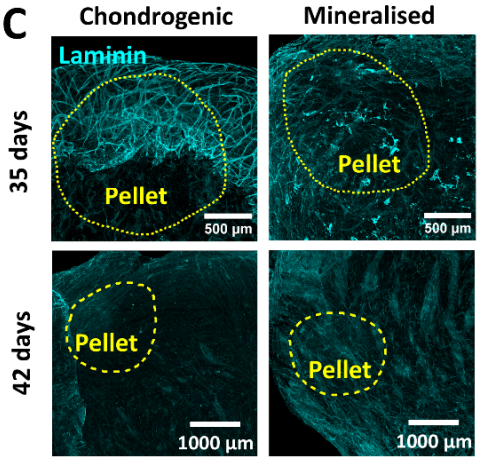
C
Chondrogenic
Mineralised
35 days
42 days
Laminin
Pellet
500 µm
1000 µm

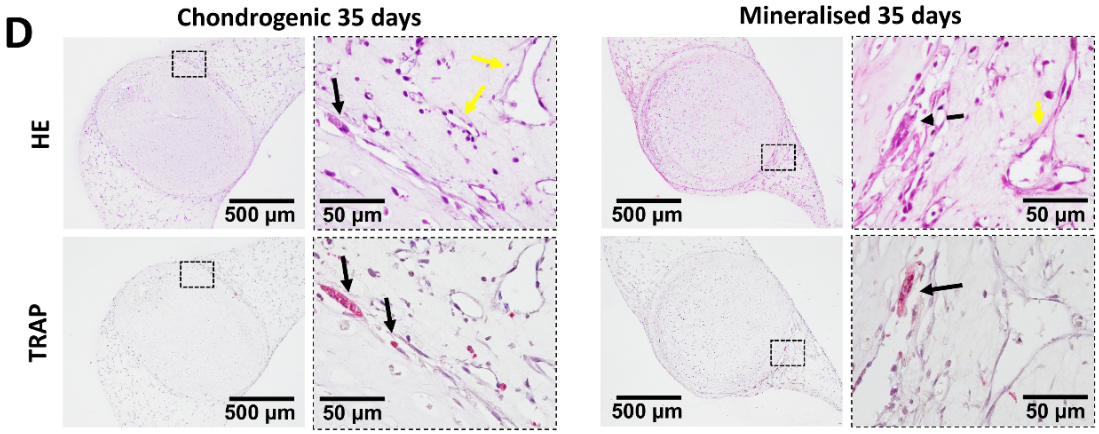
D
Chondrogenic 35 days
Mineralised 35 days
HE
TRAP
500 µm
50 µm

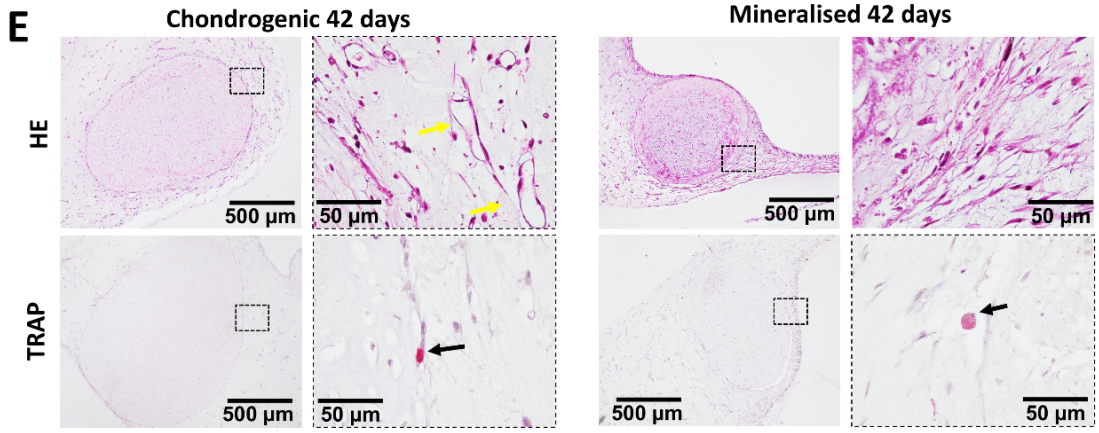
E
Chondrogenic 42 days
Mineralised 42 days
HE
TRAP
500 µm
50 µm

Fig. 6. Co-culture of chondrogenic hMSC pellets undergoing mineralisation, vascular networks and osteoclasts. ***(A)*** *Experimental scheme of the co-culture.* ***(B)*** *Von Kossa and Thionine co-stainings of hMSC pellets. Representative images are presented.* ***(C)*** *Confocal imaging of vessels visualised with laminin staining. Representative z-stack images are shown.* ***(D, E)*** *Adjacent histological sections of the co-culture at 35* ***(D)*** *and 42* ***(E)*** *days subjected to HE and TRAP stainings. Representative images are shown. Osteoclasts are indicated by black arrows and vessels by yellow arrows. N = 1 hMSC donor.* ***(F)*** *Number of TRAP+ cells present on the surface of pellets. All data are presented as average ± SD. * 0.01 < p < 0.05*

As a last step, the induction of cartilage mineralisation was introduced in the co-culture system to add a further level of complexity to the model. This was achieved by the addition of BGP from day 28 onwards, while the co-culture was continued until day 35 or day 42 to allow sufficient time for mineralisation (Fig. 6A). Mineralisation of chondrogenic pellets was confirmed via Von Kossa/Thionine staining at both time-points of analysis (Fig. 6B). At day 35 we observed the characteristic vessel structures around chondrogenic pellets, while mineralisation caused a decrease in the amount of laminin+ vessels observed within the gels (Fig. 6C). Prolonging the culture time to 42 days had a detrimental effect on the vascular networks as evidenced by the faint laminin signal (Fig. 6C). This was particularly noticeable for the mineralised group where no vessels could be observed by HE staining, as opposed to the chondrogenic group (Fig. 6D yellow arrows). In terms of osteoclast formation, HE and TRAP staining of adjacent sections of the hydrogels showed successful formation of multinucleated osteoclasts and their presence in close contact with the surface of the pellets and close to the vessels (Fig. 6D, E, black arrows). No significant differences in terms of number of formed osteoclasts were observed between chondrogenic and mineralised pellets for 35-day cultures (Fig. 6F). Prolonging the culture until day 42 led to significantly reduced osteoclast numbers, further highlighting the need to select proper culture periods for such a complex system.

DISCUSSION

In this study, we successfully established a complex *in vitro* model of EO where the functionality of multiple cell types is supported. This model provides a controlled environment that mimics the early physiological steps of EO, including the formation and calcification of the cartilage template, the recruitment of monocytes and their differentiation into osteoclasts, and the formation of microvascular networks. We thus provide a platform to study the interplay of these processes in physiology or bone-related diseases. Such model can not only enhance our fundamental understanding of bone biology but also serve as a valuable tool for testing potential therapeutic interventions, drug screening, and exploring the pathogenesis of skeletal disorders.

To design an *in vitro* model of EO with physiological relevance, we initially investigated how vessels and osteoclasts are recruited *in vivo* after the implantation of chondrogenically-primed pellets. After implantation of hMSC-derived cartilage in an animal, mineralisation starts already within 7 days post-implantation and continues henceforth (chapter 2 of this thesis). Here we found that during the early stages of the bone formation process, osteoclasts are rapidly recruited to the surface of the pellets

and vessels start to form in close proximity. This led us to reason that a relevant *in vitro* model of the early stages of EO should necessarily integrate cartilage mineralisation, osteoclast formation and activity, and angiogenesis. The *in vivo* data showed that these processes occur simultaneously and capturing the cross-talks between these cell types will likely affect the response of these cells to stimuli or drugs. In the context of these *in vivo* analyses, we also took into account the effect of the duration of the chondrogenic priming on the dynamics of bone formation. The chondrogenic differentiation phase leads to the formation of a mature cartilage template for implantation, and it is generally achieved by culturing hMSCs in the presence of chondrogenic growth factors for a period of 3-6 weeks. Such an extensive period is obviously not practical as a starting point to develop a model where multiple cell types need to be added and further differentiation stages are required. Furthermore, there are indications that a prolonged chondrogenic priming (5-6 weeks) which leads to the formation of a mature and very dense cartilaginous matrix may potentially reduce *in vivo* remodelling and be overall detrimental for bone formation [34]. We found that 7 days of chondrogenic priming are sufficient to induce osteoclast recruitment and vessel invasion after implantation, with similar dynamics in comparison to 21 days of priming. In the case of 7 days of priming, vessel infiltration reached further depth at the earlier stages of bone formation, possibly due to smaller size of the construct and presence of less (dense) cartilage matrix. Based on this evidence, we concluded that in the setting up of the *in vitro* model a minimum of 7 days priming with TGF-β is necessary prior to the stimulation of other processes and the addition of other cell types. We then corroborated this evidence by showing that 7 days of *in vitro* chondrogenic priming are sufficient to induce the expression of a number of genes related to the modulation of angiogenesis and osteoclastogenesis. These include well known pro-angiogenic genes such as *VEGF* and *PDGFA*, which are significantly increased with 7 days of chondrogenic priming, as well as genes relevant to osteoclastic activity such as *TNFSF11* (*RANKL*) and *CSF1R*. Overall, this suggested that chondrogenically primed pellets may contribute to the establishment of a supportive environment for the co-existence of vasculature, osteoclasts and mineralised cartilage in an *in vitro* model.

Setting-up a co-culture of several human primary cell types and guaranteeing their functionality is a complex task. Of note, culture media to induce cartilage formation, vascular network formation and osteoclastogenesis all include a number of factors which may affect the viability and activity of the other cell types. We thus decided to establish first separate co-cultures of (mineralised) cartilage with osteoclasts or vascular networks, as these would provide relevant information on how all these processes can be combined in a later stage. Monocyte seeding on mineralised pellets and culture with M-CSF and RANKL led to the successful formation of TRAP+ osteoclasts at the pellet surface. This is a very similar pattern to those observed for *in vivo* implanted pellets where osteoclasts are mainly localised on the edge of the pellets at the early stages of bone formation. Interestingly, smaller and less multinucleated osteoclasts formed on the surface of mineralised pellets in comparison to chondrogenic pellets. This is not necessarily a detrimental phenomenon for our model as very large osteoclasts may represent culture artifacts. However, in order to provide a more controlled environment *in vitro*, it is necessary to further understand the exact interactions of osteoclasts with mineralised and unmineralised cartilage and how this regulates their formation and resorption activity. Future studies could employ the model developed in this study to that specific purpose.

By co-culturing self-assembled vessel structures with lumen and mineralised cartilage *in vitro*, we next established a model that allows recapitulation of the intricate interplay between vascularisation and cartilage mineralisation *in vitro*. Of note, this process is normally studied *in vivo* as *in vitro* models of tissue vascularisation still face many challenges. By applying our *in vitro* co-culture system of cartilage and vascular networks, we demonstrated that cartilage mineralisation leads to a local decrease in vessel formation. This is in line with our previous work showing that the transition from hypertrophic to mineralised cartilage involves a certain level of chondrocyte cell death with a decrease in the expression and production of pro-angiogenic factors such as VEGF, which could explain the reduced vessel formation [31]. Furthermore, increased concentrations of calcium and phosphate have been shown to increase oxidative stress and apoptosis in endothelial cells [35]. Future mechanistic studies could make use of our newly developed model to investigate the exact cellular and molecular mechanisms by which cartilage mineralisation can negatively impact angiogenesis in the context of the early stages of EO. These may be highly relevant for the tissue engineering field, where the ability to better control cartilage vascularisation and remodelling after implantation could lead to more effective or more rapid bone formation in the context of a large bone defect.

In the last step of the work, we succeeded in incorporating all of the selected processes into a single *in vitro* model of EO. Co-cultures of chondrogenic/mineralised pellets, monocytes and vessel-forming cells led to the formation of TRAP+ osteoclasts and vessels in close proximity and in contact with the pellets. To the best of our knowledge, this represents unprecedented complexity for an *in vitro* model of bone formation via EO. This model thus opens up a new range of possibilities to investigate a complex cross-talk between chondrocytes, osteoclasts and vascular cells in a controlled environment. Of note, a longer culture period led to reduced osteoclast and vessel network formation, particularly for mineralised pellets. These findings highlight the complexity of recapitulating a bone-like environment *in vitro*, where a delicate balance between mineral deposition and osteoclast and vascular network formation needs to be achieved. It should be considered that the current absence of the renewal of existing osteoclasts and vessels *in vitro* by fresh cells sets a time limit to the survival of these cells. We expect that further developments of the *in vitro* model, which could include dynamic fluidic system with periodic cell renewal, will allow to guarantee cell functionality for more extended periods of time, ultimately allowing the recapitulation of later stages of the bone formation process.

Within this study we mainly focused on establishing a complex co-culture which could capture the early processes which normally occur after implantation of tissue-engineered cartilage templates, and guarantee the functionality of the cell types involved. Future steps could focus on the subsequent stages of EO where the cartilage is resorbed and osteoprogenitors home via the vasculature leading to osteoblast differentiation and generation of a bone matrix. It is very promising that we already observed the formation of loose cartilage fragments in proximity to osteoclasts in our co-cultures, which may be indicative of resorptive phenomena. Optimisation of culture conditions to further stimulate remodelling may allow to create space for the vessels to invade the dense cartilage matrix, eventually providing a mean to deliver cells, factors and drugs to the forming bone niche. Importantly, this growing level of *in vitro* complexity can be of enormous value for research on the physiology of EO or bone formation-related diseases. Potential research applications include, but are not limited to, the study of undesired cartilage hypertrophy and vascularisation in osteoarthritis,

disturbances of endochondral bone formation in growth and metabolic diseases, or the migration of metastatic cancer cells to the bone. For all these conditions, *in vitro* models of higher complexity and relevance are of vital importance.

CONCLUSION

This study presents a novel *in vitro* model that integrates mineralised cartilage, vascular structures, and osteoclasts to recapitulate the early stages of EO. Inspired by the *in vivo* dynamics of EO in the tissue engineered setting, we adopted a systematic approach to develop co-cultures of increasing complexity, finally combining all processes into a single *in vitro* platform. These models will contribute to our understanding of bone formation and remodelling, offering a valuable tool for future research into skeletal-related disorders and potential therapeutic strategies.

MATERIALS AND METHODS

Cell isolation and culture

Human mesenchymal stromal cells (hMSCs) (N=5 donors in total) were isolated from leftover iliac crest bone chips of patients (ages 9-12) undergoing alveolar reconstruction surgery and expanded, as previously described [36]. Passage 3-4 cells were used for the experiments. Material collection was performed with the approval of the Erasmus Medical Centre Ethics Committee (MEC-2014-106 and MEC-2022-0163).

Human CD14+ monocytes were acquired from buffy coats provided by Sanquin blood bank (Sanquin blood bank, Amsterdam, The Netherlands; contract number: NVT0053.01) after receiving ethical approval (N=5 donors). Monocytes were isolated as previously described [37]. Once isolated, cells were frozen and stored in liquid nitrogen in freezing medium consisting of 1:1 osteoclast medium (alpha minimum essential medium (αMEM, ThermoFisher Scientific, Waltham, MA, USA)) supplemented with 15% v / v heat inactivated foetal bovine serum (FBS, Sigma Aldrich, Saint Louis, MO, USA, lot #BCCD0778), 50 µg / mL gentamicin (ThermoFisher Scientific), 0.25 µg / mL Amphothericin B (ThermoFisher Scientific)) and dimethyl sulfoxide (DMSO, Sigma Aldrich) diluted 1:5 with v / v FBS.

Adipose-derived stromal/stem cells (ASCs) were isolated from human adipose tissue obtained from a healthy patient undergoing plastic surgery, following informed consent and approval from the Ethical Committee of the Basel University Hospital (Ethikkommission beider Basel [EKKB], Ref. 78/07). The isolation procedure involved tissue mincing, collagenase digestion, centrifugation, and filtration steps as previously described [31]. Isolated cells were cultured in αMEM supplemented with 10% v / v FBS, 50 µg / mL gentamicin, 1.5 µg / mL Amphothericin B, 1% v / v HEPES (ThermoFisher Scientific), 1% v / v glutamine (ThermoFisher Scientific), 1% v / v sodium pyruvate (ThermoFisher Scientific) and 5 ng/mL fibroblast growth factor 2 (FGF-2, R&D System, Abingdon, UK). Passage 2 cells were used for the experiments.

Human umbilical vein endothelial cells (HUVECs) were purchased from Promocell (Heidelberg, Germany; C-12203; 3 pooled donors) and expanded with a seeding density of 3300 cells/cm², as previously described [31]. Endothelial cell growth medium-2 (EGM2, Lonza, Basel, Switzerland) was used for HUVEC expansion. Cells were subcultured at 85–90% confluence, until passage 4.

Chondrogenic differentiation and mineralisation of hMSC pellets

200.000 hMSCs were transferred to individual 15 mL polypropylene tubes containing 500 µL complete chondrogenic medium consisting of dulbecco's modified eagle medium high glucose (DMEM HG, ThermoFisher Scientific) supplemented with 50 µg / mL gentamicin, 1.5 µg / mL Amphothericin B, 1 mM sodium pyruvate, 40 µg / mL L-proline (Sigma Aldrich), 1:100 v /v insulin-transferrin-selenium (ITS+, BD Biosciences, Drachten, The Netherlands), 25 µg / mL as L-ascorbic acid 2-phosphate (Ascorbic acid, Sigma Aldrich), 100 nM dexamethasone (Sigma Aldrich) and 10 ng / mL transforming growth factor- β3 (TGF-β3, R&D Systems). Each tube was centrifuged at 300g for 8 minutes. Pellets were cultured at 37ºC and 5% CO_2 in a humidified atmosphere for the number of days specified for each experiment. Pellet mineralisation was induced by the addition of 10mM β-glycerophosphate (BGP, Sigma Aldrich) to the medium.

Co-culture of hMSC pellets and osteoclasts

hMSC pellets were formed and cultured for 14 or 21 days prior to the start of the co-culture. For all the pellets, TGF-β and dexamethasone were removed at day 11 to prevent negative effects on osteoclast formation. BGP addition started at day 7 and lasted until the end of the co-culture. CD14+ monocytes were thawed and 500.000 cells were resuspended into 300 µL of osteoclast medium (αMEM, 50 µg / mL gentamicin, 1.5 µg / mL Amphothericin B, 5% v / v FBS, 25 µg / mL ascorbic acid) supplemented with 25 ng / mL macrophage colony stimulating factor (M-CSF, R&D Systems). These were seeded into individual 15ml-tubes each containing a pellet. Tubes were placed in a shaker at low agitation (100 $\mathbf{min^{-1}}$) and incubated for 1 hour at 37ºC. Then, 200 µL of osteoclast medium were added per tube to reach a total volume of 500 µL. Samples were cultured for 14 days at 37ºC and 5% CO_2 in a humidified atmosphere. From day 3 of co-culture, 30 ng / mL receptor activator of nuclear factor kappa-β ligand (RANKL, ThermoFisher Scientific) was added to the medium.

Co-culture of hMSC pellets and vascular networks

hMSC pellets were cultured for 14 days in chondrogenic medium. Then, TGF-β3 was removed and culture continued until day 21. 300,000 HUVECs and 300,000 ASCs were resuspended in 50 µL of 20 mg/mL fibrinogen in 0.9% w/v NaCl (plasminogen, vWF and fibronectin-depleted human fibrinogen, MILAN Analytica AG). For the enzyme solution, human thrombin (Sigma-Aldrich) and Factor XIII (CSL Behring, King of Prussia, PA, USA) were added at a concentration of 6 U/mL to 50 µL of 40 mM CaCl2 solution. Then, the cell suspension, enzymes and 3 chondrogenic pellets were mixed to generate 100 µL fibrin hydrogels in an ibidi 12-well chamber (ibidi, Gräfelfing, Germany) and incubated for 15 min at 37 °C to allow crosslinking. The hydrogels were cultured in 270 µL of vessel consensus medium (DMEM HG, 50 µg / mL gentamicin, 1.5 µg / mL Amphothericin B, 1 mM sodium pyruvate, 40 µg / mL L-proline, 1:100 v /v ITS+ and endothelial factors mix (Lonza, Basel, Switzerland)). To induce pellet mineralisation, 10 mM BGP was added to the culture medium. The medium was renewed every 2 days and samples were cultured in a humidified atmosphere at 37 °C and 5% CO2 for 10 days.

Co-culture of hMSC pellets, osteoclasts and vascular networks

hMSC pellets were cultured for 11 days with chondrogenic medium, then TGF-β3 and dexamethasone were removed from day 11 to day 14. Next, CD14+ monocytes were seeded on and co-cultured with the pellets from day 14 to day 28 with osteoclast medium supplemented with 25 ng/mL M-CSF (from day 14) and 30 ng/mL RANKL (from day 17). On day 28, HUVECs, ASCs and pellets seeded with differentiated osteoclasts were embedded in fibrin hydrogels as described in 2.4. The samples were cultured with vessel consensus medium described in section 5.4, further supplemented with 5% FBS, 25 ng / mL M-CSF and 30 ng / mL RANKL. An alternative consensus medium was tested where DMEM-HG was replaced by αMEM. For those samples where pellet mineralisation was induced, 10mM BGP was added to the medium. The medium was renewed every 2 days, and cultures were kept in a humidified atmosphere at 37 °C and 5% CO2 until day 42.

Histological analysis

Pellets and fibrin hydrogels were fixed with 4% formalin overnight followed by dehydration and paraffin-wax embedding. Then, paraffin blocks were sectioned at 6 µm thickness and slides deparaffinised before staining. Optical imaging of slides post-staining was performed with an Olympus BX50 microscope (Olympus Corporation, Shinjuku, Tokyo, Japan).

Von Kossa / Thionine co-staining

Slides were incubated for 15 minutes in 5% Silver nitrate solution (Sigma Aldrich) under a desk light (> 60 W). Slides were counterstained with 0.4% thionine (Sigma Aldrich) in 0.01 M sodium acetate (Sigma Aldrich), pH 4.5) for 5 minutes. Slide dehydration was performed by immersion in increasing gradients of ethanol: 70% (10 seconds), 96% (30 seconds), 100% (1 minute). Slides were finally immersed in xylene (twice, 1 minute) and mounted in mounting solution (Entellan, Merck Life Science NV, Amsterdam, The Netherlands).

Haematoxylin and eosin

Slides were stained with Gill's haematoxylin (Sigma Aldrich) for 5 minutes and placed in running tap water for 10 minutes. Co-staining with Eosin Y (Merck Life Science NV) was performed for 45 seconds and was followed by slide dehydration and mounting as detailed in section Von Kossa / Thionine co-staining.

TRAP staining and osteoclast counting

Slides were incubated with freshly prepared acetate-tartaric acid buffer for 20 minutes at room temperature. This buffer was composed of 0.2 M Sodium acetate (Sigma Aldrich) and 100 mM L (+) tartaric acid (Sigma Aldrich) diluted in distilled water and pH adjusted to 5.0. After incubation, 0.5 mg / mL Naphtol AS-BI phosphate (Sigma Aldrich) and 1.1 mg / mL Fast red TR salt (Sigma Aldrich) were added to the acetate-tartaric acid buffer and slides were further incubated at 37ºC for 3 hours at low agitation. Counterstaining of samples was performed by incubation in Gill's haematoxylin (Sigma

Aldrich) and following immersion in running tap water. Finally, slides were mounted with mounting solution (VectaMount, Vector Laboratories, Newark, NewJersey, USA). Number of TRAP + cells on the surface of pellets were counted at 3 different depths and in triplicates per group.

Endomucin staining (immunofluorescence)

Vascularisation of implanted pellets was assessed by immunofluorescent staining of endomucin. Before staining, antigen retrieval was performed with a microwave tissue processor at 95° for 20 minutes in a Tris-EDTA buffer solution (pH=9). Tissue sections were then incubated overnight with a primary rat anti-Endomucin antibody (Santa Cruz, sc-65495, 1:100). A Goat fluorescently labelled anti-rat secondary antibody was then used (Thermo Fisher Scientific, 1:200). To remove red blood cell autofluorescence, tissue sections were treated with Vector TrueVIEW quenching kit (Vector Laboratories, sp-8400) following manufacturer's instructions. Images were acquired with a Nikon Ti2 Eclipse microscope (Nikon, Tokyo, Japan).

Calcium uptake assay

Calcium concentration in culture medium supernatants was calculated using a standard curve of 0–3.0 mM CaCl2 (Sigma-Aldrich) in calcium-free DMEM (ThermoFisher). 100 µL of reagent [1:1 of reagent 1 (1M ethanolamine pH 10.5 (Sigma-Aldrich)) and reagent 2 (0.35 mM o-cresolphthalein complexone (Sigma-Aldrich), and 19.8 mM 8-hydroxyquinoline (Sigma-Aldrich), 0.6 M hydrochloric acid)] were mixed with 10 µL medium or standard. Samples were measured at 570 nm on a Versamax spectrophotometer. Medium only (no cells) samples were taken during culture and used for data normalisation.

Gene expression analysis

Pellet samples were manually homogenised, lysed with 400 µL RNA STAT-60 (Tel-Test Inc., Friendswood, Texas, USA) and stored at -80ºC. To isolate RNA, 80 µ L chloroform (Sigma Aldrich) were added and the samples were centrifuged for 15 mi nutes at 12,000g. The aqueous phase containing RNA was mixed with an equal volu me of 70 % v/v ethanol and loaded into a RNeasy micro-column (Qiagen, Hilden, Ger many). Total RNA was isolated following the manufacturer's instructions and RNA yie ld and purity was measured with a spectrophotometer/fluorometer (DSS-11 Series S pectrophotometer/fluorometer, DeNovix, Wilmington, USA) at 260/280 nm. cDNA syn thesis was performed with the RevertAid First Strand cDNA kit (ThermoFisher Scienti fic), according to the Manufacturer's instructions. 0.24 µg RNA were used per sampl e. Expression of the genes of interest (Table. 1) was measured by RT-qPCR analysis using TaqMan assays and master mix (ThermoFisher Scientific) or unlabelled primer s and SYBR Green master mix (ThermoFisher Scientific). A Bio-Rad CFX96 Real-Ti me PCR Detection system (Bio-Rad, Lunteren, The Netherlands) was used. B2M wa s used as housekeeping gene, since it was found to be the most stable out of the 3 h ousekeepers that were tested (B2M, UBC and GAPDH). The ΔCt method was used f or the calculation of gene expression as follows: Gene Expression = 2^(-ΔCt) and ΔC t = Ct gene of interest – Ct B2M.

Types of gene	Target gene	Forward sequence (5'-3')	Reverse sequence (5'-3')	Probe (FAM, 5'-3')
Housekeeper	***B2M***	TGCTCGCGCTACTCTCTCTTT	TCTGCTGGATGACGTGAGTAAAC	
	UBC	ATTTGGGTCGCGGTTCTTG	TGCCTTGACATTCTCGATGGT	
	GAPDH	ATGGGGAAGGTGAAGGTCG	TAAAAGCAGCCCTGGTGACC	CGCCCAATACGACCAAATCCGTTGAC
Osteoclast markers	***DC-STAMP***	AAGCAGCCGCTGGGAGT	TTTTCAGGACTGGAAGCCAGAAATGAA	
	OC-STAMP	GCCTGAAACCACTGCCATTTG	AGGACCTCCACCCGGTCT	
	CTSK	GGGAGCTATGGAAGAAGACCC	CCAGGTGGTTCATAGCCAGT	
	TRAP	GACTGTGCAGATCCTGGGTG	GAGCGGTCAGAGAATACGTCC	
Collagen markers	***COL2A1***	GGCAATAGCAGGTTCACGTACA	CGATAACAGTCTTGCCCCACTT	CCGGTATGTTTCGTGCAGCCATCCT
	COL10A1	CAAGGCACCATCTCCAGGAA	AAAGGGTATTTGTGGCAGCATATT	TCCAGCACGCAGAATCCATCTGA

Table. 1. List of genes of interest used for RT-qPCR analysis in this study.

RNA sequencing data analysis

The RNA sequencing dataset analysed in this study was previously generated by culture of hMSC pellets for 7 days with TGF-β (7d-primed pellets) or without TGF-β (7d-unpirmed pellets) (N = 4 hMSC donors) (see Chapter 2 of this thesis). Differential expression analysis was performed using DESeq2. A pre-filtering heuristic was used prior to running DESeq2 to remove single strong outliers in either one of the classes. Among these, genes encoding for secreted factors related to vascularisation and osteoclastogenesis were identified based GO terms. The terms related with the positive regulation of vessel formation are GO:0001938, positive regulation of endothelial cell proliferation; GO:1905564, positive regulation of vascular endothelial cell proliferation; GO:0043536, positive regulation of blood vessel endothelial cell

migration; GO:2001214, positive regulation of vasculogenesis. The terms related with the negative regulation of vessel formation are GO:0001937, negative regulation of endothelial cell proliferation; GO:1905563, negative regulation of vascular endothelial cell proliferation; GO:0010596, negative regulation of endothelial cell migration; GO:2001213, negative regulation of vasculogenesis. The terms related with the positive regulation of osteoclasts are GO:2001206, positive regulation of osteoclast development; GO:0090290 positive regulation of osteoclast proliferation; GO:0045453 bone resorption; GO:0046849, bone remodelling. The terms related with the negative regulation of osteoclasts are GO:2001205, negative regulation of osteoclast development and GO:0090291, negative regulation of osteoclast proliferation.

Confocal imaging and vessel length density (VLD) quantification

Fibrin hydrogels were fixed with 1% paraformaldehyde overnight at 4°C. To block non-specific binding, 3% BSA and 5% donkey serum (Sigma-Aldrich) in PBS were added overnight. The gels were subsequently incubated with 1:100 anti-human laminin antibody (0.7 mg/mL stock, Abcam, Cambridge, UK) in PBS with 3% BSA and 5% donkey serum (Sigma-Aldrich) overnight. Samples were then incubated with 1:200 Alexa fluor 647 secondary antibody (2 mg/mL stock, ThermoFisher Scientific) and DAPI (1:10000) at 4 °C overnight. The hydrogels were imaged using Leica Stellaris 5 low-incidence angle upright microscope or Leica TCS SP5 microscope, with an excitation wavelength of 638nm and a long-pass emission filter for laminin signal. The gels were optically scanned (distance between every scanned layer: 6 µm), and all the images were stacked through a Z-stack program in ImageJ for Vessel length density (VLD) analysis. Vessel lengths were measured by overlaying captured microscopic images with a square grid (field size = 200,000 µm2). Squares were randomly chosen and the length of each vessel (if any) in the selected squares was measured and summed up. For each sample, 10 fields of the whole image for vessel length measurements were obtained, with triplicate samples for each experimental group.

Statistical analysis

Data representation was performed using GraphPad Prism (software version 8.0), and statistical analyses was performed with SPSS 24 (IBM). Subsequently, for all multiple comparisons, a linear mixed model with Bonferroni correction was used; the different conditions were considered as a fixed parameter and the donor as a random factor. Statistical significance was evaluated between conditions within the same time-point and defined as $p < 0.05$. All results are presented as mean ± standard deviation (SD).

REFERENCES

[1] C. Kiernan, C. Knuth, and E. Farrell, Chapter 6 - Endochondral Ossification: Recapitulating Bone Development for Bone Defect Repair. in: M.J. Stoddart, A.M. Craft, G. Pattappa, and O.F.W. Gardner, (Eds.), Developmental Biology and Musculoskeletal Tissue Engineering, Academic Press, Boston, 2018, pp. 125-148.

[2] N.C. Foster, J.R. Henstock, Y. Reinwald, and A.J. El Haj, Dynamic 3D culture: Models of chondrogenesis and endochondral ossification. Birth Defects Research Part C: Embryo Today: Reviews 105 (2015) 19-33.

[3] F.E. Freeman, and L.M. McNamara, Endochondral Priming: A Developmental Engineering Strategy for Bone Tissue Regeneration. Tissue Engineering Part B: Reviews 23 (2016) 128-141.

[4] C. Kiernan, C. Knuth, and E. Farrell, Endochondral ossification: Recapitulating bone development for bone defect repair, Developmental Biology and Musculoskeletal Tissue Engineering: Principles and Applications, 2018, pp. 125-148.

[5] E. Farrell, O.P. van der Jagt, W. Koevoet, N. Kops, C.J. Van Manen, C.A. Hellingman, H. Jahr, F.J. O'Brien, J.A.N. Verhaar, H. Weinans, and G.J.V.M. van Osch, Chondrogenic Priming of Human Bone Marrow Stromal Cells: A Better Route to Bone Repair? Tissue Engineering Part C: Methods 15 (2009) 285-295.

[6] C. Scotti, B. Tonnarelli, A. Papadimitropoulos, A. Scherberich, S. Schaeren, A. Schauerte, J. Lopez-Rios, R. Zeller, A. Barbero, and I. Martin, Recapitulation of endochondral bone formation using human adult mesenchymal stem cells as a paradigm for developmental engineering. Proceedings of the National Academy of Sciences 107 (2010) 7251-7256.

[7] J.M. Jukes, S.K. Both, A. Leusink, L.M.T. Sterk, C.A. van Blitterswijk, and J. de Boer, Endochondral bone tissue engineering using embryonic stem cells. Proceedings of the National Academy of Sciences 105 (2008) 6840-6845.

[8] A.A. Winter, A.S. Pollack, and R.B. Odrich, Sinus/alveolar crest tenting (SACT): a new technique for implant placement in atrophic maxillary ridges without bone grafts or membranes. International Journal of Periodontics & Restorative Dentistry 23 (2003).

[9] G. Nilsson Hall, L.F. Mendes, C. Gklava, L. Geris, F.P. Luyten, and I. Papantoniou, Developmentally Engineered Callus Organoid Bioassemblies Exhibit Predictive In Vivo Long Bone Healing. Advanced Science 7 (2020) 1902295.

[10] W.L. Tam, L. Freitas Mendes, X. Chen, R. Lesage, I. Van Hoven, E. Leysen, G. Kerckhofs, K. Bosmans, Y.C. Chai, A. Yamashita, N. Tsumaki, L. Geris, S.J. Roberts, and F.P. Luyten, Human pluripotent stem cell-derived cartilaginous organoids promote scaffold-free healing of critical size long bone defects. Stem Cell Research & Therapy 12 (2021) 513.

[11] S.C. Dennis, C.J. Berkland, L.F. Bonewald, and M.S. Detamore, Endochondral ossification for enhancing bone regeneration: converging native extracellular matrix biomaterials and developmental engineering in vivo. Tissue Eng Part B Rev 21 (2015) 247-66.

[12] N. Fahy, V. Palomares Cabeza, A. Lolli, J. Witte-Bouma, A. Merino, Y. Ridwan, E.B. Wolvius, M.J. Hoogduijn, E. Farrell, and P.A.J. Brama, Chondrogenically Primed Human Mesenchymal Stem Cells Persist and Undergo Early Stages of

Endochondral Ossification in an Immunocompetent Xenogeneic Model. Front Immunol 12 (2021) 715267.
[13] V. Palomares Cabeza, N. Fahy, C.H. Kiernan, A. Lolli, J. Witte-Bouma, S. Fahmy Garcia, A. Merino, N. Kops, Y. Ridwan, E.B. Wolvius, P.A.J. Brama, M.J. Hoogduijn, and E. Farrell, Bone formation by human paediatric marrow stromal cells in a functional allogeneic immune system. Biomaterials 306 (2024) 122471.
[14] D. Bicho, S. Pina, J.M. Oliveira, and R.L. Reis, In Vitro Mimetic Models for the Bone-Cartilage Interface Regeneration. in: J.M. Oliveira, S. Pina, R.L. Reis, and J. San Roman, (Eds.), Osteochondral Tissue Engineering: Challenges, Current Strategies, and Technological Advances, Springer International Publishing, Cham, 2018, pp. 373-394.
[15] F.E. Freeman, M.G. Haugh, and L.M. McNamara, An In Vitro Bone Tissue Regeneration Strategy Combining Chondrogenic and Vascular Priming Enhances the Mineralization Potential of Mesenchymal Stem Cells In Vitro While Also Allowing for Vessel Formation. Tissue Engineering Part A 21 (2015) 1320-1332.
[16] A. Garmendia Urdalleta, Witte-Bouma, J., Kops, N., Lolli, A., Farrell, E., Osteoclast incorporation in an *in vitro* 3D model of endochondral ossification. *Tissue Engineering part A* (Online ahead of print).
[17] J. Kodama, K.J. Wilkinson, M. Iwamoto, S. Otsuru, and M. Enomoto-Iwamoto, The role of hypertrophic chondrocytes in regulation of the cartilage-to-bone transition in fracture healing. Bone Rep 17 (2022) 101616.
[18] F.C. Cackowski, J.L. Anderson, K.D. Patrene, R.J. Choksi, S.D. Shapiro, J.J. Windle, H.C. Blair, and G.D. Roodman, Osteoclasts are important for bone angiogenesis. Blood 115 (2010) 140-149.
[19] K.K. Sivaraj, P.G. Majev, H.W. Jeong, B. Dharmalingam, D. Zeuschner, S. Schröder, M.G. Bixel, M. Timmen, R. Stange, and R.H. Adams, Mesenchymal stromal cell-derived septoclasts resorb cartilage during developmental ossification and fracture healing. Nat Commun 13 (2022) 571.
[20] P.R. Odgren, H. Witwicka, and P. Reyes-Gutierrez, The cast of clasts: catabolism and vascular invasion during bone growth, repair, and disease by osteoclasts, chondroclasts, and septoclasts. Connect Tissue Res 57 (2016) 161-74.
[21] S.G. Romeo, K.M. Alawi, J. Rodrigues, A. Singh, A.P. Kusumbe, and S.K. Ramasamy, Endothelial proteolytic activity and interaction with non-resorbing osteoclasts mediate bone elongation. Nat Cell Biol 21 (2019) 430-441.
[22] C. Maes, and H.M. Kronenberg, Chapter 60 - Bone Development and Remodeling. in: J.L. Jameson, L.J. De Groot, D.M. de Kretser, L.C. Giudice, A.B. Grossman, S. Melmed, J.T. Potts, and G.C. Weir, (Eds.), Endocrinology: Adult and Pediatric (Seventh Edition), W.B. Saunders, Philadelphia, 2016, pp. 1038-1062.e8.
[23] N. Ortega, K. Wang, N. Ferrara, Z. Werb, and T.H. Vu, Complementary interplay between matrix metalloproteinase-9, vascular endothelial growth factor and osteoclast function drives endochondral bone formation. Dis Model Mech 3 (2010) 224-35.
[24] W.C. Dougall, M. Glaccum, K. Charrier, K. Rohrbach, K. Brasel, T. De Smedt, E. Daro, J. Smith, M.E. Tometsko, C.R. Maliszewski, A. Armstrong, V. Shen, S. Bain, D. Cosman, D. Anderson, P.J. Morrissey, J.J. Peschon, and J. Schuh, RANK is essential for osteoclast and lymph node development. Genes Dev 13 (1999) 2412-24.

[25] J. Li, S. Mori, Y. Kaji, J. Kawanishi, T. Akiyama, and H. Norimatsu, Concentration of bisphosphonate (incadronate) in callus area and its effects on fracture healing in rats. J Bone Miner Res 15 (2000) 2042-51.
[26] B. Tosun, L.I. Wolff, A. Houben, S. Nutt, and C. Hartmann, Osteoclasts and Macrophages-Their Role in Bone Marrow Cavity Formation During Mouse Embryonic Development. J Bone Miner Res 37 (2022) 1761-1774.
[27] S.K. Ramasamy, A.P. Kusumbe, M. Schiller, D. Zeuschner, M.G. Bixel, C. Milia, J. Gamrekelashvili, A. Limbourg, A. Medvinsky, M.M. Santoro, F.P. Limbourg, and R.H. Adams, Blood flow controls bone vascular function and osteogenesis. Nature Communications 7 (2016) 13601.
[28] Y. Zhang, Y. Yu, and I.T. Ozbolat, Direct Bioprinting of Vessel-Like Tubular Microfluidic Channels. Journal of Nanotechnology in Engineering and Medicine 4 (2013).
[29] A.L. Torres, S.J. Bidarra, D.P. Vasconcelos, J.N. Barbosa, E.A. Silva, D.S. Nascimento, and C.C. Barrias, Microvascular engineering: Dynamic changes in microgel-entrapped vascular cells correlates with higher vasculogenic/angiogenic potential. Biomaterials 228 (2020) 119554.
[30] G. Borciani, G. Montalbano, N. Baldini, G. Cerqueni, C. Vitale-Brovarone, and G. Ciapetti, Co–culture systems of osteoblasts and osteoclasts: Simulating in vitro bone remodeling in regenerative approaches. Acta Biomaterialia 108 (2020) 22-45.
[31] E. Ji, L. Leijsten, J. Witte-Bouma, A. Rouchon, N. Di Maggio, A. Banfi, G. van Osch, E. Farrell, and A. Lolli, In Vitro Mineralisation of Tissue-Engineered Cartilage Reduces Endothelial Cell Migration, Proliferation and Tube Formation. Cells 12 (2023).
[32] Y. Nossin, E. Farrell, W.J.L.M. Koevoet, F. Datema, R.A. Somoza, A.I. Caplan, and G.J.V.M. van Osch, The Releasate of Avascular Cartilage Demonstrates Inherent Pro-Angiogenic Properties In Vitro and In Vivo. CARTILAGE 13 (2021) 559S-570S.
[33] A. Rouchon, VEGF decoration of fibrin scaffolds for in vitro and in vivo engineering of vascularized tissues, University_of_Basel, 2022.
[34] C.A. Knuth, J. Witte-Bouma, Y. Ridwan, E. Wolvius, and E. Farrell, Mesenchymal stem cell-mediated endochondral ossification utilising micropellets and brief chondrogenic priming. European Cells & Materials 34 (2017) 142-161.
[35] N.T. Nguyen, T.T. Nguyen, and K.S. Park, Oxidative Stress Related to Plasmalemmal and Mitochondrial Phosphate Transporters in Vascular Calcification. Antioxidants (Basel) 11 (2022).
[36] C. Knuth, C. Kiernan, V. Palomares Cabeza, J. Lehmann, J. Witte-Bouma, D. ten Berge, P. Brama, E. Wolvius, E. Strabbing, M. Koudstaal, R. Narcisi, and E. Farrell, Isolating paediatric mesenchymal stem cells with enhancedexpansion and differentiation capabilities. Tissue Engineering Part C Methods 24 (2018) 313-321.
[37] A. Garmendia Urdalleta, M. Van Poll, N. Fahy, J. Witte-Bouma, W. Van Wamel, I. Apachitei, A.A. Zadpoor, L.E. Fratila-Apachitei, and E. Farrell, The response of human macrophages to 3D printed titanium antibacterial implants does not affect the osteogenic differentiation of hMSCs. Front Bioeng Biotechnol 11 (2023) 1176534.

SUPPLEMENTARY MATERIAL

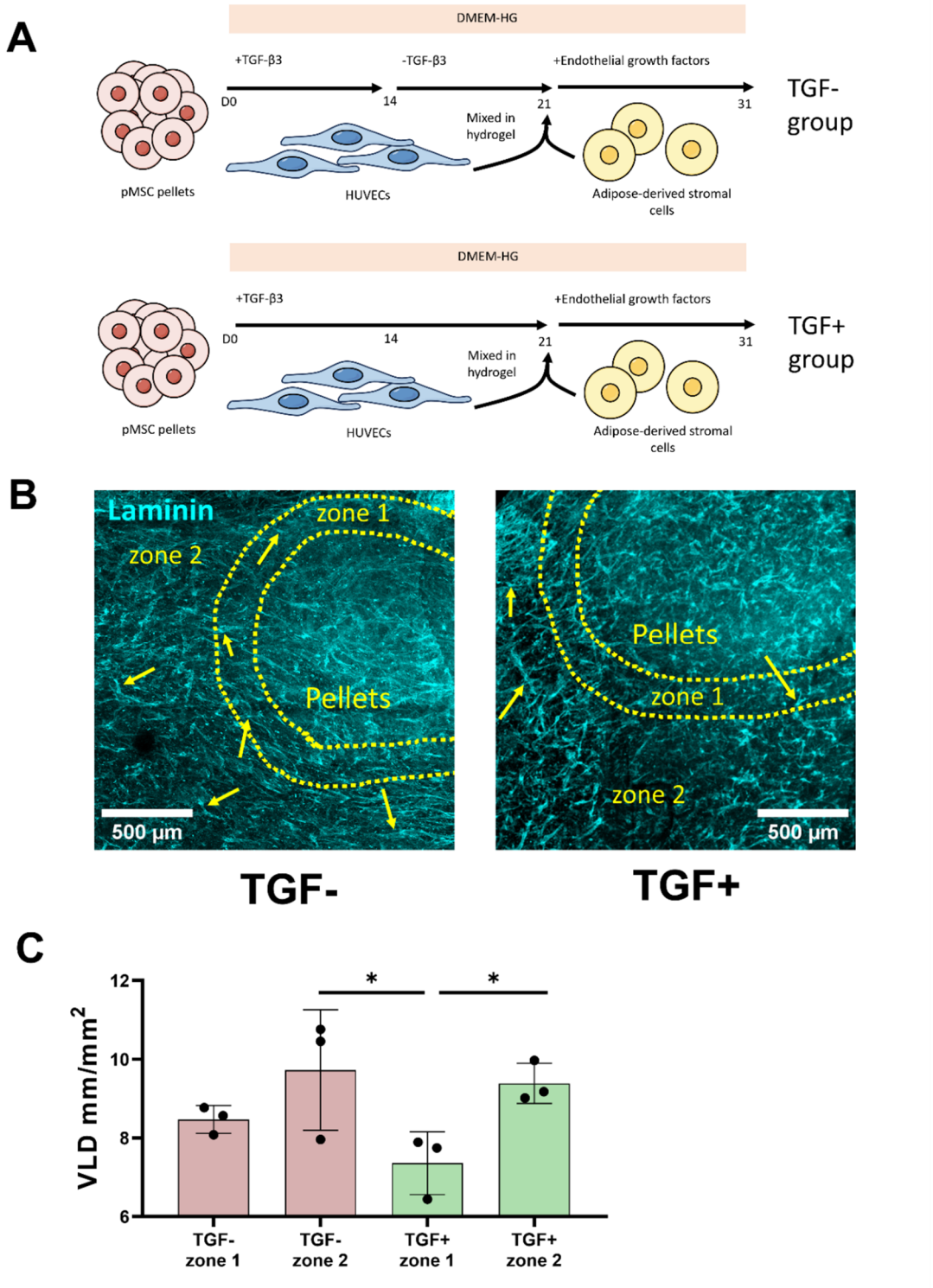

Fig. S1. The effect of TGF addition and removal on vessel formation (A) *The cultural scheme for TGF addition (TGF+) and TGF removal (TGF-) strategies.* ***(B)*** *Confocal imaging of laminin-stained vessels. Representative z-stack images obtained by confocal microscopy are shown.* ***(C)*** *Graph displaying the average VLD values per condition. All data are presented as average ± SD. * 0.01 < p < 0.05*

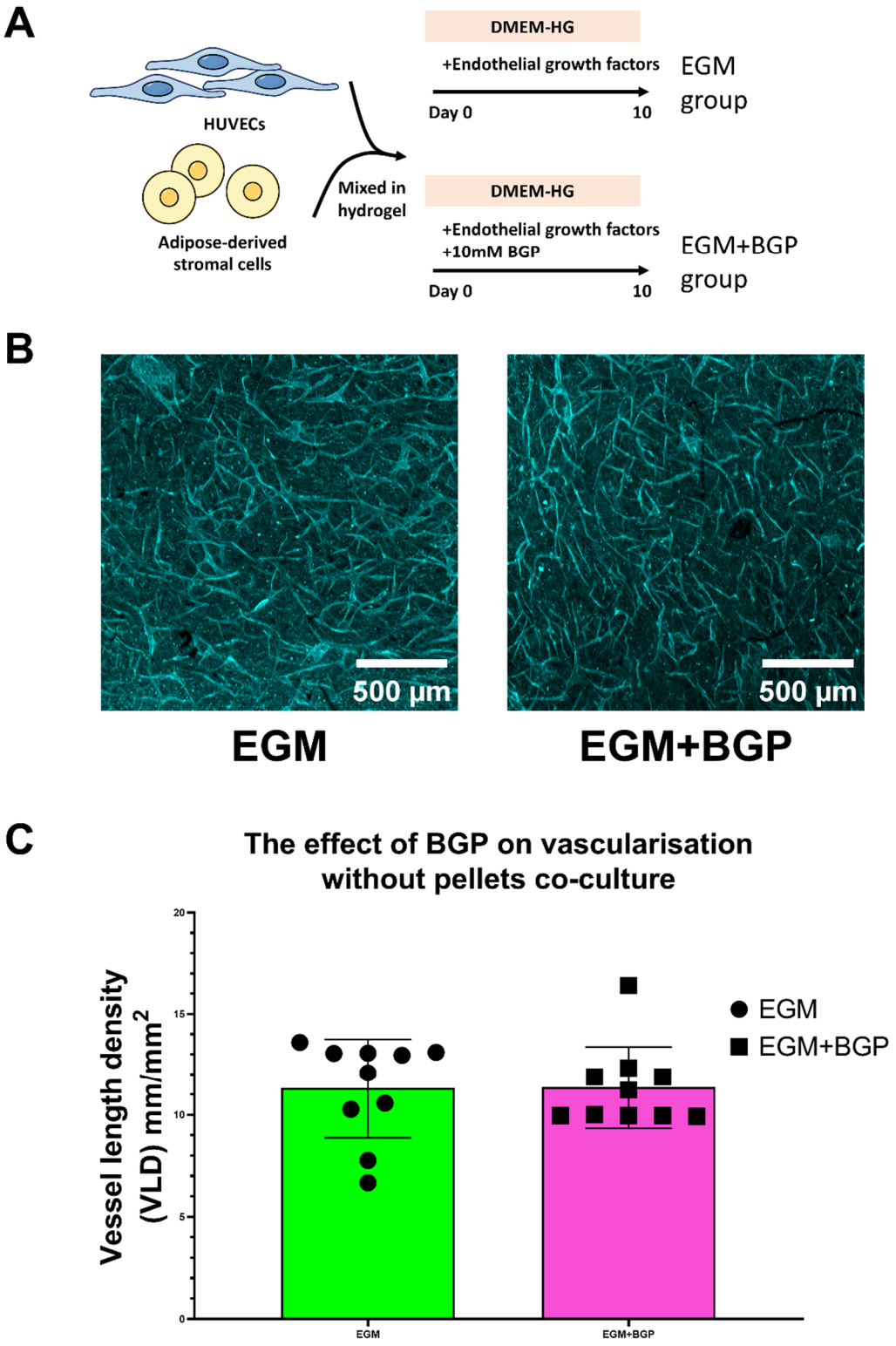

Fig. S2. The effect of BGP addition on vessel formation. (A) *The cultural scheme for condition only with EGM (EGM) and the condition with both EGM and BGP addition (EGM+BGP).* ***(B)*** *Confocal imaging of laminin-stained vessels. Representative z-stack images obtained by confocal microscopy are shown.* ***(C)*** *Graph displaying the average VLD values per condition. All data are presented as average ± SD.*

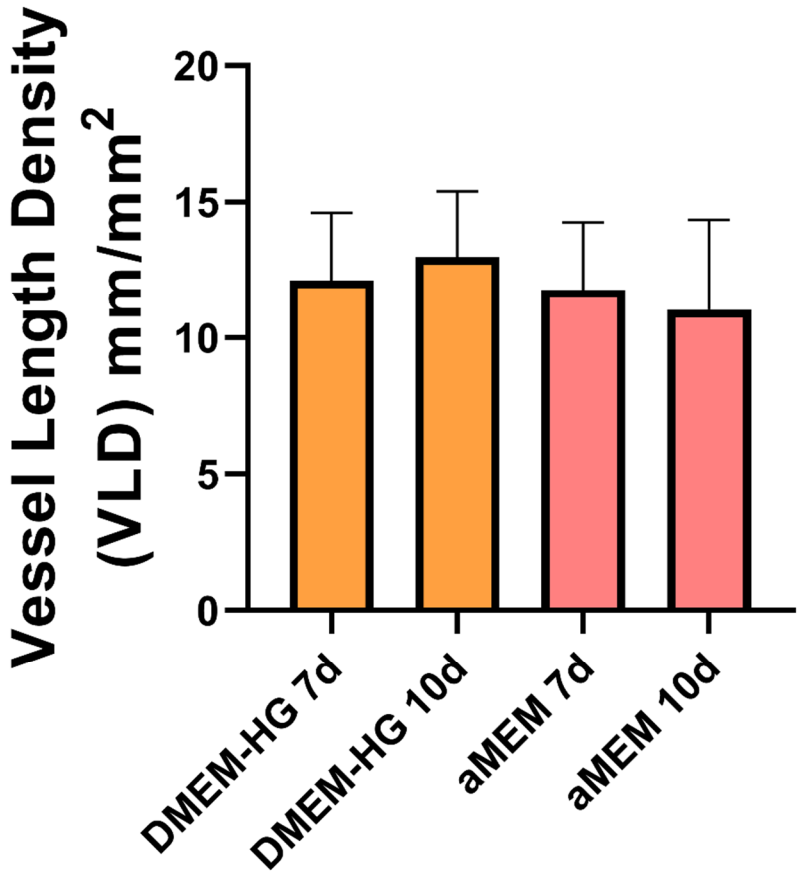

Fig. S3. The effect of DMEM-HG- and aMEM-based consensus medium on vessel formation. *The graph displays the average VLD values with DMEM-HG- or aMEM-based consensus medium.*

CHAPTER 5

Metastasis to the bone: new in vitro models of bone formation to study migration and proliferation of metastatic cancer cells

Marta Cecchi, Encheng Ji, Janneke Witte – Bouma, Mathieu M.E. Wijffels, Michiel H.J. Verhofstad, Silvia Scaglione, Astrid Parenti, Andrea Lolli, Eric Farrell

Manuscript in preparation.

CONTRIBUTION STATEMENT

Encheng Ji performed the experiments with fluid flow, contributed to the experiments with *in vitro* pellets and cancer cells, performed data analysis and visualisation and substantially revised the manuscript.

CHAPTER 6

DISCUSSION AND CONCLUSIONS

CONTRIBUTION STATEMENT

Encheng Ji drafted and revised the chapter.

DISCUSSION

Key findings

Endochondral ossification is essential for bone formation during embryonic development and fracture healing. Thus, developing *in vitro* models that recapitulate endochondral ossification can help us advance our understanding of skeletal development, bone regeneration and treating skeletal diseases. These models may eventually provide a fully controlled environment to investigate the intricate cellular and molecular processes underlying the transformation of cartilage into bone. By mimicking this natural process *in vitro*, researchers could gain invaluable insights into the key regulators and signalling pathways that are still only partially understood, potentially leading to novel therapeutic strategies for bone disorders, including cancer metastasis.

In the work of this thesis, we focused on the early stages of endochondral ossification, whereby blood vessels invade the mineralised template of hypertrophic cartilage, and osteoclasts contribute to tissue resorption and remodelling. Such interplay still needs an appropriate *in vitro* platform where cellular interactions can be dissected and studied. To address this need, we explored a new *in vitro* strategy inspired by tissue engineering-based models of endochondral ossification, which generally require the implantation of cartilage constructs into animals. We focused on the hMSC pellet model since hMSCs are a clinically relevant cell source with well-established chondrogenic and osteogenic potential, making them ideal for modelling endochondral ossification. The pellet culture system provides a three-dimensional microenvironment that closely mimics the condensation of mesenchymal cells at the start of bone formation. This approach offers not only scalability and reproducibility, crucial factors for developing robust *in vitro* models but also versatility as it can be implemented with additional cell types and various culture conditions. We began in **Chapter 2** by studying the process of hMSC-based endochondral ossification *in vivo*, characterising the sequence of events that cause a cartilage template to remodel into mature bone. This study provided crucial insights into the key gene regulatory networks in chondrocytes that instruct tissue remodelling and vascularisation, informing the development of our subsequent *in vitro* models. We next sought to develop *in vitro* models that could recapitulate key aspects of the early stages of endochondral ossification. We initially focused on the interplay between mineralised cartilage and angiogenesis, as these phenomena occur early and simultaneously after cartilage implantation. In **Chapter 3**, we specifically investigated how the mineralisation of tissue-engineered cartilage affects its pro-angiogenic potential. We demonstrated that *in vitro* cartilage mineralisation induced by β-glycerophosphate leads to decreased VEGFA production by the chondrocytes, and reduced ability to stimulate endothelial cell migration and proliferation. This showed that the pro-angiogenic potential of transient cartilage is stage-dependent, and this aspect must be carefully considered in the design of *in vitro* models of bone formation. In **Chapter 4**, we developed an *in vitro* co-culture model directly incorporating the interactions between chondrogenic pellets, vessels, and osteoclasts during cartilage mineralisation, thus recapitulating *in situ* osteoclastogenesis and vascular network formation. Such findings evidenced the potential of this model to serve as a platform for studying bone biology and testing therapeutic interventions. Finally, in **Chapter 5** we co-cultured mineralised pellets with metastatic breast and melanoma cancer cells to setup *in vitro* systems for the study of bone metastasis.

Bones reimagined: crafting novel in vitro bone models by a stepwise approach

In vitro bone models have emerged as crucial tools for studying bone formation, offering advantages over animal models in terms of reproducibility, controllability, and potential for completely humanised cellular environments. However, the development of these models faces significant challenges in recapitulating the complexity of the mature bone environment. While various approaches have been developed, from simple co-culture systems to complex 3D bioprinted constructs, each has limitations in representing the native bone microenvironment. Furthermore, the intricate coupling between angiogenesis, remodelling and osteogenesis in bone formation adds another layer of complexity to the creation of physiologically relevant *in vitro* bone models [1]. Unlike most common models which rely mainly on osteoblast cultures or direct mineralisation of osteogenically differentiated hMSCs, our approach took a different direction by utilising the endochondral route of bone formation. Instead of attempting to directly mimicking the architecture of native bone, we thus focused on recapitulating the physiological steps that lead to bone formation. We chose to start with hMSC pellets since these can be easily cultured with chondrogenic growth factors (TGF-β) to generate cartilage templates. Much research has shown that when these constructs are implanted *in vivo*, mature bone is generated via endochondral ossification, accurately recapitulating the processes of cartilage mineralisation, vessel invasion, and osteoclast-mediated remodelling [2-6]. While this system closely mimics the developmental process of bone formation, there are ethical concerns, regarding the use of experimental animals, and the cellular and molecular dynamics that underlie bone formation remain challenging to investigate. This is because several processes of tissue formation and remodelling occur at the same time, making it difficult to dissect the contribution of each cell type or single factors. Furthermore, the cellular contribution from the host animal leads to the generation of chimeric bone, potentially impacting its properties and response to stimuli. In this thesis we took an important step towards addressing these limitations by developing an advanced and fully humanised *in vitro* model that incorporates key aspects of endochondral ossification, including cartilage mineralisation, remodelling, and vascular network formation. This was realised by gradually complicating the system and by first establishing an *in vitro* model of mineralised cartilage (**Chapter 3**), then separate cartilage-vessels and cartilage-osteoclasts co-cultures, with or without mineralisation, and finally a complete cartilage-vessels-osteoclasts co-culture (**Chapter 4**).

Overall, we thus provided the field with a set of new models with different degree of complexity that could be applied to answer questions related to physiological or pathological events in the context of bone formation. Different components of the model could be tailored to simulate various conditions, and a suitable level of complexity could be chosen depending on the research question. A relatively simple co-culture of cartilage and osteoclasts may be sufficient to study aspects of the chondrocyte-osteoclast crosstalk. The study of altered cartilage remodelling may instead require higher complexity and the simultaneous presence of mineralised cartilage, vessels and osteoclasts. Many are the diseases which could benefit from such models, due to altered bone formation as in the context of growth diseases, or due to aspects of the bone microenvironment supporting the pathological process, as in the case of bone metastasis. For example, osteochondrosis is characterised by focal disturbances in endochondral ossification, often due to impaired vascularisation of the epiphyseal growth cartilage. This vascular failure leads to ischemic chondronecrosis, which can manifest as lesions detectable through imaging

techniques like CT and MRI [7]. By using the *in vitro* model, we may investigate the mechanisms behind vascular failure and its relationship to cartilage necrosis, potentially identifying therapeutic targets for enhancing blood supply to affected areas. Other opportunities may include the study of osteoclast deficiency in the context of cartilage resorption during growth or repair, which can lead to skeletal deformities, short stature, and disrupted fracture repair. The model could represent a tool to investigate dysregulated crosstalk between hypertrophic cartilage/chondrocytes and osteoclasts or endothelial cells, e.g. in the context of poor fracture healing due to infections, diabetes or malnutrition These studies could potentially help elucidating the signalling pathways involved in defective osteoclast or endothelial function during ossification, potentially leading to novel therapeutic approaches for managing these disorders [8; 9].

Optimising the chondrogenic priming duration for efficient in vitro modelling of bone formation with hMSC pellets

To begin assembling complex *in vitro* models, we first needed to better understand the process involved in endochondral ossification upon which we planned to build *in vitro* co-cultures: the generation of the cartilage template. It is well established that after implantation this provides an excellent substrate for the formation of endochondral bone. However, we still knew relatively little about how the properties of the cartilage related to the induction of mineralisation-vascularisation-remodelling processes after implantation. Understanding specifically whether cartilage of a certain amount or maturity is required for endochondral bone formation to occur was of primary importance for developing *in vitro* bone formation models. Since these properties are mainly determined by the duration of chondrogenic priming (with TGF-β), in **Chapter 2** we examined the bone formation potential of hMSC pellets at different stages of chondrogenic priming, via *in vivo* transplantation experiments. We found that a short chondrogenic priming (7 days) is sufficient for hMSCs to acquire bone formation potential, and a mature cartilage template is not a hard requirement for bone formation to occur. By studying the transcriptome of chondrogenically-primed cells, we showed that this brief chondrogenic stimulus does not only trigger the expression of genes related to bone formation and remodelling but also several regulators of vascularisation and osteoclastogenesis.

The aforementioned evidence informed us that the short priming procedure is adequate to support endochondral ossification. This choice is obviously desirable for an *in vitro* model of bone formation which involves multiple phases and cell types. In **Chapter 3** we investigated whether such short chondrogenic priming could be coupled with cartilage mineralisation *in vitro*. We found that BGP could be successfully introduced on day 7 of priming to induce mineralisation, which was overall improved when TGF-β was withdrawn from the culture medium on day 14. In addition, we showed that the expression of pro-angiogenic markers and the positive effect of conditioned medium derived from pellets after 7 days of chondrogenic priming on vessel formation was not further enhanced by longer priming. Altogether, our data demonstrate that short chondrogenic priming is adequate to establish *in vitro* models of endochondral ossification. Of note, our new insights into the effect of the duration of chondrogenic priming on endochondral bone formation are also particularly relevant for the bone tissue engineering field and the implantation of chondrogenic constructs to regenerate bone. From a translation perspective, the extensive cell handling

required during the priming drastically increases the costs and time of the procedure, causing significant hurdles in view of translation. Our data can aid the development of new strategies to minimise the need for chondrogenic pre-differentiation of hMSCs while preserving their bone formation potential.

Bridging processes: the challenge of modelling mineralisation, vascularisation, and osteoclast activity in endochondral ossification

Setting up an *in vitro* model that supports the functionality of several cell types of primary origin and allows to recreate their interplay is no easy task. In this thesis, we mainly focused on identifying suitable *in vitro* conditions to support vessel formation in combination with a cartilage template undergoing mineralisation and remodelling. As shown in **Chapter 2** and **Chapter 4**, vessel infiltration occurs early after cartilage implantation and it is thus expected to play a central role in bone formation since the very early stages. To establish an *in vitro* bone formation model that includes a vascular network, we decided to utilise a strategy of self-assembly of vessel-forming cells (endothelial cells and pericyte-like cells) and combine it with hMSC pellets. In **Chapter 3**, we performed a conditioned medium study and found that the pro-angiogenic potential of hMSC pellets is achieved after 7days of chondrogenic priming and it is negatively affected by prolonged mineralisation. In **Chapter 4**, we moved to direct co-cultures and developed a system combining mineralised/chondrogenic pellets and tissue-engineered vessels. We observed that vessels with lumen were formed under such co-culture conditions and they could physically interact with the surface of hMSC pellets. Both indirect and direct cultures indicated that vessel formation can be achieved in the presence of tissue-engineered cartilage that undergoes mineralisation. It is thus feasible to apply such a model to investigate cell-cell interaction between hypertrophic chondrocytes and endothelial cells. Since we did not observe direct vessel invasion under this setting, we hypothesised that the dense cartilage matrix could prevent vessel infiltration. In the next step, we decided to incorporate osteoclasts as the main cells capable of effective cartilage degradation and due to their documented ability to promote vascular invasion.

In **Chapter 4**, we built a complex 3D co-culture system with (mineralised) pellets, osteoclasts forming in the pellets, and vessels assembled in the fibrin hydrogel. Under *in vivo* conditions, osteoclasts in remodelling bone are formed from monocyte/macrophage precursors under the influence of signalling molecules such as macrophage-colony stimulating factor (M-CSF) and receptor activator of nuclear factor kappa-B ligand (RANKL) [10; 11]. We recapitulated this process *in vitro* and finally achieved the formation of vasculature, osteoclasts and chondrogenic/mineralised cartilage in a single system. While we did not observe clear signs of vessel infiltration, we found osteoclasts residing inside the pellets, in addition to loose pellet fragments in close contact with osteoclasts [12]. This suggests that these cells may be actively engaged in a matrix degradation process. To the best of our knowledge, this is the first time that this evidence is provided in the context of such a complex co-culture system recapitulating endochondral ossification. This is consistent with hMSC pellets contributing to the digesting ability of osteoclasts and the coupling of vessel network formation and osteoclastogenesis. As we showed in **Chapter 4**, upregulated genes in chondrogenic pellets included secreted factors relevant to osteoclastic activity, like *TNFSF11* (*RANKL*) and *CSF1R*, and angiogenic genes, e.g. *VEGF* and *PDGFA*, which can also affect osteoclasts behaviour. Osteoclasts express receptors for VEGF,

such as VEGFR-1 (Flt-1) and VEGFR-2 (Flk-1/KDR) [13; 14]. Thus, vessel formation may be potentially linked with osteoclastogenesis in our model.

In **Chapter 3** we determined that *in vitro* mineralisation decreased the expression of pro-angiogenic markers by chondrocytes and consequently vessel-forming capacity in the presence of hMSC-derived cartilage subjected to mineralisation. The negative effect of prolonged cartilage mineralisation on regional vascular network formation was further demonstrated by the direct co-culture system with hMSC-originated cartilage and vasculature in **Chapter 4**. While we did not specifically investigate the mechanisms underlying this effect, these may be associated with the induction of cell apoptosis due to mineralisation (**Chapter 3**). While a small portion of hypertrophic chondrocytes can undergo transdifferentiation into osteoblasts during endochondral ossification, apoptosis is considered to be their predominant ultimate fate [15]. *In vitro*, increased apoptosis will cause an overall lower number of cells producing pro-angiogenic factors. Furthermore, there is evidence that chondrocyte differentiation is associated with increased levels of oxidative phosphorylation and ROS production [16]. High levels of ROS can negatively impact endothelial cell function, leading to reduced proliferation and migration, which are essential for angiogenesis [17]. In **Chapter 4** we further observed that mineralisation can lead to reduced vessel and osteoclast formation during cartilage-vessels-osteoclasts co-culture. These are relevant aspects that need to be taken into consideration for further developing complex co-culture systems with mineralising cartilage. It is also possible that the structural properties of the mineralised matrix generated *in vitro* or the timing in the induction of mineralisation is not yet ideal and could be further optimised in future work.

Applying in vitro models of endochondral ossification to study bone metastasis

To explore potential applications of *in vitro* models of endochondral ossification, we focused on a research field for which improved experimental models represent a major need, i.e. bone metastasis. In **Chapter 5** we evaluated different experimental options to model aspects of the bone microenvironment and to support cancer cell growth, including *ex vivo* cultured human bone and *in vitro* mineralised pellets derived from hMSCs. These may offer different advantages and limitations in studies on bone metastasis. *Ex vivo* cultured bone provides the native bone microenvironment, including the natural cancellous structure and a diverse cellular composition [18]. This model could potentially replicate the complex interactions between cancer cells and multiple native bone cells including osteocytes, osteoblasts, osteoclasts, and bone marrow cells, making it ideal for studying tumour cell-bone cell interactions. It is however very challenging to guarantee the survival and functionality of all these cell types once the tissue is explanted from the patient. The thick calcified tissue and the presence of bone marrow can hinder nutrient diffusion, leading to cell death and matrix degradation over time [19]. Furthermore, it may lack reproducibility due to donor variability and bone of origin. Mineralised hMSC pellets are much more simplistic in structure and composition, but, as shown in this thesis, they can be manipulated to host multiple cell types to recreate processes that underlie bone formation.

In **Chapter 5** we showed that *ex vivo* bone and mineralised pellets could evoke different responses in cancer cells, likely due to these differences in composition and secretion of factors. While characterising these differences goes beyond the scope of this thesis, we showed that *in vitro* mineralised pellets stimulated the migration and

supported *in situ* proliferation of cancer cells that can metastasise to the bone. They may thus provide a suitable environment for studying aspects of cancer cell behaviour *in vitro*. Importantly, this could also provide the opportunity to utilise cells from patients, ultimately allowing personalised *in vitro* bone models that closely mimic the unique biological properties of individual patients. This is particularly important given the heterogeneity among patients, which can affect cell behaviour and treatment responses due to variations in disease characteristics and genetic background [20; 21]. The main current limitation of such model lies in the absence of a complete bone microenvironment. While we took relevant steps in adding vascular and remodelling components, further advancements will be necessary to move towards microenvironments that better resemble mature bone. Finally, the integration of a dynamic flow system, here exemplified by the B2B device, represents another necessary advancement in modelling cancer cell metastasis *in vitro*. Dynamic culture conditions can strongly alter cancer cell behaviour, including proliferation rates and drug responsiveness [22]. While our preliminary results demonstrated successful cell migration to bone and pellets after circulation in the device, future studies should explore longer-term co-cultures to assess *in situ* proliferation and interactions with bone cells. In this context, integrating more advanced *in vitro* models of endochondral ossification with vasculature into the device chambers will further enhance the physiological relevance. The B2B platform can thus provide a versatile platform for investigating microenvironmental interactions in metastasis and screening therapeutic strategies under dynamic, humanised conditions.

Future developments of the in vitro bone modelling setup

In this study, we made relevant steps towards achieving better complexity in *in vitro* models of bone formation. Nevertheless, there are still limitations that we will need to face in the future. First, our setup lacks extensive vessel invasion into the cartilage template. An important direction will be to improve the *in vitro* model to achieve effective vessel invasion in the cartilage. While we did not observe clear differences after the introduction of osteoclasts, more prolonged culture periods could be beneficial to allow increased degradation of cartilage tissue and vessel penetration. In addition, the pellets could be scaled down in size to reduce the penetration distance and allow vessels to grow between pellets. The introduction of dynamic flow, which was so far only applied to the metastatic cancer cell experiments, will further increase the relevance of such models. Fluid flow in the vessels could introduce shear stress on endothelial cells, which is crucial for their alignment, proliferation, and migration. Endothelial cells respond to shear stress by activating signalling pathways that promote angiogenesis, including the VEGF pathway [23]. The directional cues provided by flow may help guide vessels into the cartilage matrix more effectively or more quickly [24]. Mechanical forces due to fluid flow could also act on bone cells better mimicking the *in vivo* situation and influencing cell signalling, proliferation, differentiation, and extracellular matrix production [25]. Additionally, it will be relevant to introduce vessel hierarchy and/or vessel subtypes in these models. The transition from large vessels to microvessels could mimic the hierarchical structure of the vascular system found *in vivo*. In actively growing bone, different microvascular structures can be described as H or L type vessels [26]. The veins branch into smaller arteries that terminate in type H vessels, which are located near osteoprogenitor cells in the metaphyseal and endosteal regions. L-type vessels, which are sinusoidal

vessels that terminate in central veins, are found throughout the bone marrow region. During bone remodelling, the secretion of PDGF-BB recruits endothelial cells and osteoblast progenitor cells to the bone remodelling site, thereby enhancing the formation of H-type blood vessels and bone matrix, playing a role in coupling angiogenesis and osteogenesis [27]. So far, H type vessels have been manipulated *in vivo* [28], but there has been no research to recapitulate these specialised structures *in vitro*.

HUVECs are frequently used in the field of tissue engineering to study endothelial cell behaviour and function. However, they are often not the most relevant endothelial cell type for the tissue of interest. HUVECs are derived from the umbilical vein, and while they can mimic certain physiological responses of endothelial cells, they may not fully replicate the behaviour of specialised endothelial cells found in other vascular microenvironments. For instance, arterial endothelial cells (AECs) have distinct signalling pathways and mechanical properties compared to venous endothelial cells like HUVECs, and this can affect how they interact with surrounding tissues and respond to stimuli [29; 30]. In the further developments of *in vitro* models of endochondral ossification, it will be necessary to consider the use of a more relevant endothelial cell type that better relates to the bone marrow microenvironment. Bone marrow endothelial cells (BMECs) can be an option offering several advantages over HUVECs in the context of tissue engineering. BMECs are specifically adapted to the bone marrow microenvironment, which is crucial for supporting haematopoiesis and maintaining stem cell niches. This makes them more relevant for applications targeting bone tissue engineering, as they can better mimic the *in vivo* conditions found in the bone marrow [31]. BMECs can also secrete MMPs (especially MMP-9) which may be important for tissue invasion [32]. BMECs may thus provide advantages for specific *in vitro* modelling applications in bone tissue engineering and regenerative medicine.

In the work of this thesis, we generated mineralised cartilage which is different from mature bone. While *in vitro* culture with BGP can recapitulate mineralisation, it will be important to move towards *in vitro* generated matrices which can better replicate the complex ECM of native bone. The bone matrix is composed of collagen type I and hydroxyapatite crystals; it is a hierarchical structure with distinct layers and vascular channels that support nutrient delivery and waste removal, crucial for maintaining healthy bone tissue. Additionally, other cellular components i.e. osteoblasts and osteocytes are crucial for dynamic remodelling and adaptation to mechanical stress. By adding osteoclasts, we observed signs of digestion of the cartilage matrix, but with this setup newly formed mineralised matrix cannot be produced. This could be achieved via the addition of osteoblasts to the system. Osteoblasts produce osteoid, the unmineralised organic matrix, which is crucial for subsequent mineralisation and facilitates the deposition of calcium phosphate crystals, leading to the hardening of the matrix into bone.

CONCLUSIONS AND FUTURE DIRECTIONS

This thesis made significant achievements in developing and characterising new in vitro models of endochondral ossification, providing insights into the complex processes of bone formation. Our work has progressed from in vivo characterisation of hMSC-based endochondral ossification to the establishment of sophisticated in vitro models that incorporate key aspects of this process. We have demonstrated that short-term chondrogenic priming of hMSC pellets is sufficient to initiate comprehensive bone formation and validated the effectiveness of short priming strategies for in vitro modelling purposes. Next, a novel achievement of this work is the development of a complex in vitro co-culture model that successfully recapitulates cartilage mineralisation, vascularisation, and osteoclastogenesis, which had not been performed before in the field of in vitro bone models. This model has provided new insights into the interactions between these processes, particularly the inhibitory effect of mineralisation on both vascularisation and osteoclastogenesis. Our preliminary application of the in vitro model for bone metastasis research opens up new opportunities for studying cancer cell behaviour in a controlled bone-like microenvironment. In the future, vessel infiltration could be promoted to recapitulate this critical process, in addition to introducing further cell types and improving the properties of the ECM. Additionally, our setup could be further validated and adapted for a broader range of skeletal diseases, possibly by using patient-derived cells or manipulating relevant genes or factors. In conclusion, this thesis provides a solid foundation for advanced in vitro modelling of endochondral ossification. The developed models offer new tools for studying aspects of bone biology, disease mechanisms, and potential therapeutic interventions.

REFERENCES

[1] A. Pirosa, R. Gottardi, P.G. Alexander, and R.S. Tuan, Engineering in-vitro stem cell-based vascularized bone models for drug screening and predictive toxicology. Stem Cell Res Ther 9 (2018) 112.
[2] C.A. Knuth, J. Witte-Bouma, Y. Ridwan, E. Wolvius, and E. Farrell, Mesenchymal stem cell-mediated endochondral ossification utilising micropellets and brief chondrogenic priming. European Cells & Materials 34 (2017) 142-161.
[3] M. Qiu, C. Li, Z. Cai, C. Li, K. Yang, N. Tulufu, B. Chen, L. Cheng, C. Zhuang, Z. Liu, J. Qi, W. Cui, and L. Deng, 3D Biomimetic Calcified Cartilaginous Callus that Induces Type H Vessels Formation and Osteoclastogenesis. Advanced Science 10 (2023) 2207089.
[4] S. Inglis, K.H. Schneider, J.M. Kanczler, H. Redl, and R.O.C. Oreffo, Harnessing Human Decellularized Blood Vessel Matrices and Cellular Construct Implants to Promote Bone Healing in an Ex Vivo Organotypic Bone Defect Model. Advanced Healthcare Materials 8 (2019) 1800088.
[5] G. Giavaresi, P. Torricelli, P.M. Fornasari, R. Giardino, R. Barbucci, and G. Leone, Blood vessel formation after soft-tissue implantation of hyaluronan-based hydrogel supplemented with copper ions. Biomaterials 26 (2005) 3001-3008.
[6] W. Yang, S.K. Both, G.J.V.M. van Osch, Y. Wang, J.A. Jansen, and F. Yang, Effects of in vitro chondrogenic priming time of bone-marrow-derived mesenchymal stromal cells on in vivo endochondral bone formation. Acta Biomaterialia 13 (2015) 254-265.
[7] K. Olstad, S. Ekman, and C.S. Carlson, An Update on the Pathogenesis of Osteochondrosis. Veterinary Pathology 52 (2015) 785-802.
[8] T. Deguchi, M.H. Alanne, E. Fazeli, K.M. Fagerlund, P. Pennanen, P. Lehenkari, P.E. Hänninen, J. Peltonen, and T. Näreoja, In vitro model of bone to facilitate measurement of adhesion forces and super-resolution imaging of osteoclasts. Scientific Reports 6 (2016) 22585.
[9] R. Owen, and G.C. Reilly, In vitro Models of Bone Remodelling and Associated Disorders. Front Bioeng Biotechnol 6 (2018) 134.
[10] B. Tosun, L.I. Wolff, A. Houben, S. Nutt, and C. Hartmann, Osteoclasts and Macrophages—Their Role in Bone Marrow Cavity Formation During Mouse Embryonic Development. Journal of Bone and Mineral Research 37 (2022) 1761-1774.
[11] Y. Yahara, T. Nguyen, K. Ishikawa, K. Kamei, and B.A. Alman, The origins and roles of osteoclasts in bone development, homeostasis and repair. Development 149 (2022).
[12] A. Garmendia Urdalleta, Witte-Bouma, J., Kops, N., Lolli, A., Farrell, E., Osteoclast incorporation in an *in vitro* 3D model of endochondral ossification. *Tissue Engineering part A* (Online ahead of print).
[13] D. Ribatti, and A. d'Amati, Bone angiocrine factors. Front Cell Dev Biol 11 (2023) 1244372.
[14] Y.-Q. Yang, Y.-Y. Tan, R. Wong, A. Wenden, L.-K. Zhang, and A.B.M. Rabie, The role of vascular endothelial growth factor in ossification. International Journal of Oral Science 4 (2012) 64-68.
[15] S.A. Hallett, W. Ono, and N. Ono, The hypertrophic chondrocyte: To be or not to be. Histol Histopathol 36 (2021) 1021-1036.

[16] J.M. Hollander, L. Li, M. Rawal, S.K. Wang, Y. Shu, M. Zhang, H.C. Nielsen, C.J. Rosen, and L. Zeng, A critical bioenergetic switch is regulated by IGF2 during murine cartilage development. Communications Biology 5 (2022) 1230.
[17] Y.-W. Kim, and T.V. Byzova, Oxidative stress in angiogenesis and vascular disease. Blood 123 (2014) 625-631.
[18] R. Laranga, S. Duchi, T. Ibrahim, A.N. Guerrieri, D.M. Donati, and E. Lucarelli, Trends in Bone Metastasis Modeling. Cancers (Basel) 12 (2020).
[19] M. Stoddart, P. Furlong, A. Simpson, C. Davies, and R. Richards, A comparison of non-radioactive methods for assessing viability in ex vivo cultured cancellous bone. Eur Cell Mater 12 (2006) 16-25.
[20] M.M. Morgan, B.P. Johnson, M.K. Livingston, L.A. Schuler, E.T. Alarid, K.E. Sung, and D.J. Beebe, Personalized in vitro cancer models to predict therapeutic response: Challenges and a framework for improvement. Pharmacol Ther 165 (2016) 79-92.
[21] Q. Wang, F. Guo, Y. Jin, and Y. Ma, Applications of human organoids in the personalized treatment for digestive diseases. Signal Transduction and Targeted Therapy 7 (2022) 336.
[22] T. Azimi, M. Loizidou, and M.V. Dwek, Cancer cells grown in 3D under fluid flow exhibit an aggressive phenotype and reduced responsiveness to the anti-cancer treatment doxorubicin. Scientific Reports 10 (2020) 12020.
[23] P. Campinho, A. Vilfan, and J. Vermot, Blood Flow Forces in Shaping the Vascular System: A Focus on Endothelial Cell Behavior. Front Physiol 11 (2020) 552.
[24] A. Martier, Z. Chen, H. Schaps, M.J. Mondrinos, and J.S. Fang, Capturing physiological hemodynamic flow and mechanosensitive cell signaling in vessel-on-a-chip platforms. Frontiers in Physiology 15 (2024).
[25] H. Bahmaee, R. Owen, L. Boyle, C.M. Perrault, A.A. Garcia-Granada, G.C. Reilly, and F. Claeyssens, Design and Evaluation of an Osteogenesis-on-a-Chip Microfluidic Device Incorporating 3D Cell Culture. Front Bioeng Biotechnol 8 (2020) 557111.
[26] S.K. Ramasamy, Structure and Functions of Blood Vessels and Vascular Niches in Bone. Stem Cells International 2017 (2017) 5046953.
[27] Y. Peng, S. Wu, Y. Li, and J.L. Crane, Type H blood vessels in bone modeling and remodeling. Theranostics 10 (2020) 426-436.
[28] Z. Liu, H. Liu, S. Liu, B. Li, Y. Liu, and E. Luo, SIRT1 activation promotes bone repair by enhancing the coupling of type H vessel formation and osteogenesis. Cell Prolif 57 (2024) e13596.
[29] J. Qiu, and K.K. Hirschi, Endothelial Cell Development and Its Application to Regenerative Medicine. Circulation Research 125 (2019) 489-501.
[30] C.D. Devillard, and C.A. Marquette, Vascular Tissue Engineering: Challenges and Requirements for an Ideal Large Scale Blood Vessel. Frontiers in Bioengineering and Biotechnology 9 (2021).
[31] T. Bessy, T. Itkin, and D. Passaro, Bioengineering the Bone Marrow Vascular Niche. Frontiers in Cell and Developmental Biology 9 (2021).
[32] I. Vande Broek, K. Asosingh, V. Allegaert, X. Leleu, T. Facon, K. Vanderkerken, B. Van Camp, and I. Van Riet, Bone marrow endothelial cells increase the invasiveness of human multiple myeloma cells through upregulation of MMP-9: evidence for a role of hepatocyte growth factor. Leukemia 18 (2004) 976-982.

CHAPTER 7

SUMMARY

SUMMARY

Using animal models to study bone biology has yielded many exciting findings including the discovery of the bone morphogenetic proteins. However, they have strong limitations related to differences with the human organism and ethical concerns. On the other hand, constructing relevant *in vitro* models of bone formation for the study of diseases and drug discovery remains a challenge, mainly due to the complexity of the bone formation process. The work of this thesis aimed to develop new *in vitro* models that accurately mimic endochondral ossification, the natural process through which most bones are formed. During endochondral ossification, a template of cartilage tissue is gradually mineralised, vascularised and remodelled into bone. The research addressed two primary challenges: first, we used a tissue engineering approach to understand the cellular mechanisms through which cartilage transforms into bone during endochondral ossification; next, we aimed to recreate the early stages of this process *in vitro*, by generating bone-forming constructs comprising of mineralising cartilage, vasculature and remodelling cells.

Chapter 1 introduced the state-of-the-art on the experimental modelling of bone formation and provided the rationale for constructing new bone models by mimicking endochondral ossification *in vitro* through tissue engineering. The chapter outlined the process of endochondral ossification and the most relevant cell types involved. The limitations of using animal models to study bone formation were pointed out, and the current challenges of available *in vitro* models of bone formation were emphasised.

To perform a detailed study of the cellular dynamics of endochondral ossification, we used a tissue engineering model where pellets of human marrow stromal cells (hMSCs) are chondrogenically-primed with TGF-β to generate cartilage and implanted subcutaneously in mice. After implantation, the cartilage is remodelled into mature bone. This is a well-established strategy, but the dynamics of the remodelling process and the impact of the duration of the *in vitro* chondrogenic priming have not been comprehensively described. Before developing an *in vitro* model of the process, it was necessary to fill this knowledge gap. In **Chapter 2** we characterised in detail the effect of the duration of chondrogenic priming *in vitro* on bone formation and the dynamics of endochondral ossification after pellet implantation *in vivo*. The study found that the duration of chondrogenic priming does not affect the process of endochondral ossification, while prolonged priming leads to increased bone volume. We characterised the sequence of events that cause a cartilage template to remodel into mature bone and the transcriptome associated with the bone formation ability of chondrogenically-primed cells. This provided a suitable starting point to develop *in vitro* models of bone formation with multiple phases and cell types.

Since we observed that after implantation the cartilaginous constructs undergo rapid mineralisation and vascularisation, we next investigated how to recapitulate these processes in the *in vitro* setting. Given that the relationship between mineralisation and angiogenesis is not extensively studied in the tissue engineering setting, we performed a series of analysis *in vitro*. In **Chapter 3,** we introduced *in vitro* mineralisation by adding β-glycerophosphate to chondrogenically-primed hMSC pellets and studied their interaction with vessel-forming cells. We found that the endothelial cell behaviour, specifically the process of cell migration, proliferation, and tube formation, was negatively regulated with the ongoing mineralisation. This improved our understanding of the relationship between mineralisation and

angiogenesis and informed us on how to proceed with establishing complex *in vitro* models of endochondral ossification that include vascularisation.

Next, we stepped forward by developing direct co-culture models to recapitulate vascularisation and remodelling during endochondral ossification. The studies performed in **Chapter 2** had shown that hMSC pellets chondrogenically primed for a short time *in vitro* can instruct angiogenesis and osteoclastogenesis. In **Chapter 4**, we first established separate co-cultures of chondrogenic pellets undergoing mineralisation with osteoclasts or with vessel networks, and eventually combined them into a single model. In this way, the integration of chondrogenesis, mineralisation, vascular network formation, and osteoclastogenesis into a complex 3D co-culture system was successfully achieved, providing a new platform for research on bone biology and bone disease modelling.

Chapter 5 focused on applying the *in vitro* hMSC pellet model to study a bone-related disease for which relevant *in vitro* models are severely lacking, i.e. bone metastasis. We performed *in vitro* co-culture experiments with hMSC pellets and breast cancer or melanoma cell lines, with the aim to replicate the migration of metastatic cancer cells towards bone-forming constructs. We showed that hMSC pellets could stimulate the migration and proliferation of cancer cells, and both cancer cell lines could grow in contact with the pellets. Finally, we employed a fluid-flow system to recapitulate the migration of cancer cells from circulation to the bone. Further developments of this platform may provide novel tools to study the influence of the bone microenvironment on cancer cell behaviour, and new insights into how the metastatic processes may be influenced by local tissue interactions.

In **Chapter 6**, the results of this thesis are comprehensively discussed and placed in a general context. Overall, this thesis emphasises the significance of endochondral ossification in the context of tissue engineering strategies to model bone formation or regeneration. We made significant progress in establishing *in vitro* models with multiple cellular elements, mimicking the processes of chondrogenesis, mineralisation, angiogenesis and osteoclastogenesis. These advanced co-culture systems are promising tools to mimic and study the interplay between chondrocytes, osteoclasts and endothelial cells during bone formation, paving the way for future research into bone diseases and potential therapeutic strategies. Future iterations of the model including additional cell types or processes such as vascular infiltration will further expand the range of applications, aiding a better understanding of bone biology and treatment of skeletal disorders.

APPENDICES

NEDERLANDSE SAMENVATTING

Het gebruik van diermodellen om botbiologie te bestuderen heeft veel resultaten opgeleverd, waaronder de ontdekking van de eiwitten die de botvorming regelen. Diermodellen hebben echter beperkingen die veroorzaakt worden door verschillen in fysiologie tussen mens en de gebruikte dieren. Bovendien zijn er ethische redenen om het gebruik van dieren voor wetenschappelijk onderzoek te beperken. Aan de andere kant blijft het construeren van relevante proefdiervrije laboratorium modellen (zogenaamde *in vitro* modellen) van botvorming voor het bestuderen van ziekten en het ontdekken van medicijnen een uitdaging. Dat komt voornamelijk omdat we het botvormingsproces, en de rol van de cellen die daarbij betrokken zijn, nog niet goed genoeg begrijpen. Het doel van dit proefschrift was om nieuwe *in vitro* modellen te ontwikkelen die endochondrale botvorming, het proces waarmee de meeste botten in ons lichaam worden gevormd, nauwkeurig nabootsen. Tijdens endochondrale botvorming wordt een sjabloon van kraakbeenweefsel geleidelijk gemineraliseerd, gevasculariseerd en omgevormd tot bot. Het onderzoek richtte zich op twee belangrijke uitdagingen: ten eerste gebruikten we een tissue engineering-benadering om de cellulaire mechanismen te begrijpen waarmee kraakbeen tijdens endochondrale botvorming in bot verandert; Ten tweede wilden we de vroege stadia van dit proces *in vitro* nabootsen door botvormende constructen te genereren die bestaan uit mineraliserend kraakbeen, bloedvaten en cellen die het kraakbeen kunnen helpen remodelleren.

Hoofdstuk 1 introduceerde de huidige kennis van de experimentele modellen voor botvorming en gaf de rationale voor het ontwikkelen van nieuwe botmodellen door endochondrale botvorming *in vitro* na te bootsen door middel van tissue engineering. Het hoofdstuk schetste het proces van endochondrale botvorming en de meest relevante celtypen die hierbij betrokken zijn. Er werd gewezen op de beperkingen en uitdagingen van het gebruik van diermodellen en van de huidige beschikbare *in vitro* modellen om botvorming te bestuderen.

Om een gedetailleerde studie uit te voeren van de cellulaire dynamiek van endochondrale botvorming, gebruikten we een tissue engineering model waarbij menselijke stromale cellen (hMSC's) uit het beenmerg met TGF-β aangezet worden om kraakbeen te vormen (zgn chondrogene priming) en vervolgens geïmplanteerd worden onder de huid in muizen. Na de implantatie wordt het kraakbeen omgevormd tot bot. Dit is een beproefde strategie, maar de dynamiek van het remodelleringsproces en de impact van de duur van de *in vitro* chondrogene priming zijn niet uitgebreid onderzocht. Voordat we een *in vitro* model van het botvormingsproces ontwikkelden, was het noodzakelijk om deze leemte in de kennis op te vullen. In **Hoofdstuk 2** karakteriseerden we in detail het effect van de duur van chondrogene priming *in vitro* op botvorming en de dynamiek van endochondrale botvorming na implantatie van de chondrogeen geprimede constructen *in vivo*. Uit het onderzoek bleek dat de duur van chondrogene priming geen invloed heeft op het proces van endochondrale botvorming, terwijl langdurige priming leidt tot een groter volume aan bot. We karakteriseerden de opeenvolging van gebeurtenissen die ervoor zorgen dat een kraakbenig sjabloon remodelleert tot volwassen bot en het transcriptoom dat geassocieerd wordt met het botvormend-vermogen van chondrogeen-geprimede cellen. Dit vormde het uitgangspunt voor de ontwikkeling van *in vitro* modellen van botvorming met meerdere fasen en celtypen.

Aangezien we zagen dat de kraakbenige constructen na implantatie een snelle mineralisatie en vascularisatie ondergaan, onderzochten we vervolgens hoe we deze processen konden nabootsen in een *in vitro* setting. Aangezien de relatie tussen mineralisatie en de vorming van nieuwe bloedvaten (angiogenese) in de tissue engineering setting niet uitgebreid bestudeerd is, voerden we een reeks analyses uit. In **Hoofdstuk 3** introduceerden we *in vitro* mineralisatie door β-glycerofosfaat toe te voegen aan chondrogeen-geprimede hMSC en bestudeerden we hun interactie met vaatvormende endotheelcellen. We ontdekten dat het gedrag van endotheelcellen, met name het proces van celmigratie, celdeling en buisvorming, negatief werd gereguleerd door de voortschrijdende mineralisatie. Dit verbeterde ons begrip van de relatie tussen mineralisatie en angiogenese en informeerde ons over hoe verder te gaan met het opzetten van complexe *in vitro* modellen van endochondrale botvorming die ook vascularisatie omvatten.

Vervolgens ontwikkelden we *in vitro* modellen met een directe co-kweek om vascularisatie én remodellering tijdens endochondrale botvorming na te bootsen. De *in vivo* studies uitgevoerd in **Hoofdstuk 2** hadden aangetoond dat hMSC die voor korte tijd *in vitro* chondrogeen geprimed worden, de angiogenese en de vorming van osteoclasten (cellen die gemineraliseerd weefsel afkunnen breken) kunnen instrueren. In **Hoofdstuk 4** hebben we eerst afzonderlijke co-kweken opgezet van constructen van chondrogeen-geprimde cellen die mineralisatie ondergaan met osteoclasten of met vasculaire netwerken, en deze uiteindelijk gecombineerd in één model. Op deze manier werd de integratie van chondrogenese, mineralisatie, vorming van vasculaire netwerken en osteoclastogenese in een complex 3D co-kweeksysteem met succes bereikt. Dit biedt een nieuw platform voor onderzoek naar botbiologie en het modelleren van botziekten *in vitro*.

Hoofdstuk 5 richtte zich op het toepassen van het *in vitro* model met getissue-engineerde constructen van chondrogeen-geprimde hMSC om een botgerelateerde ziekte te bestuderen waarvoor relevante *in vitro* modellen ontbreken, namelijk botmetastase. We voerden *in vitro* co-kweekexperimenten uit van deze getissue-engineerde constructen met borstkanker- of melanoomcellijnen, met als doel de migratie van uitgezaaide kankercellen naar botvormende weefsel na te bootsen. We toonden aan dat de constructen de migratie en proliferatie van kankercellen konden stimuleren en dat beide kankercellijnen konden groeien in contact met de constructen. Tot slot maakten we gebruik van een fluid-flow systeem om de migratie van kankercellen vanuit de circulatie naar het botweefsel na te bootsen. Verdere ontwikkeling van dit platform kan nieuwe hulpmiddelen opleveren voor het bestuderen van de invloed van de botmicro-omgeving op het gedrag van kankercellen en nieuwe inzichten in hoe metastase beïnvloed kan worden door interacties van kankercellen en botweefsel.

In **Hoofdstuk 6** worden de resultaten van dit proefschrift uitgebreid besproken en in een algemene context geplaatst. Dit proefschrift benadrukt het belang van endochondrale botvorming als tissue engineering strategie om botvorming of botregeneratie te modelleren. We hebben aanzienlijke vooruitgang geboekt bij het opzetten van *in vitro* modellen waarin meerdere cellulaire elementen samenkomen die de processen van chondrogenese, mineralisatie, angiogenese en osteoclastvorming nabootsen. Deze geavanceerde co-kweeksystemen zijn veelbelovende hulpmiddelen om de wisselwerking tussen chondrocyten, osteoclasten en endotheelcellen tijdens botvorming na te bootsen en te bestuderen, wat de weg vrijmaakt voor toekomstig

onderzoek naar botziekten en potentiële therapeutische strategieën. Toekomstige verbeteringen en uitbreidingen van het model met extra celtypen of processen zoals vasculaire infiltratie zullen de toepassingsmogelijkheden verder uitbreiden en bijdragen aan een beter begrip van botbiologie en de behandeling van skeletaandoeningen.

总　结

利用动物模型研究骨骼生物学已取得许多令人振奋的成果，其中包括骨形态发生蛋白的发现。然而，动物模型存在显著局限性，这既涉及与人体的差异，也面临伦理方面的问题。另一方面，由于骨形成过程的复杂性，构建用于疾病研究和药物研发的相关体外骨形成模型仍然是一项挑战。本论文旨在开发新的体外模型，以精确模拟软骨内骨化这一长骨形成的自然过程。在软骨内骨化过程中，软骨组织模板会逐渐矿化、血管化，并重塑为骨骼。本研究主要应对两项挑战：第一，我们采用组织工程方法，深入了解软骨在软骨内骨化过程中转化为骨骼的细胞机制；第二，我们试图在体外重现这一过程的早期阶段，通过生成包含矿化软骨、血管和重塑细胞的骨形成构建体来实现。

第 1 章介绍了骨形成实验建模的前沿进展，并阐述了通过组织工程在体外模拟软骨内骨化构建新骨模型的理论依据。该章概述了软骨内骨化的过程以及相关的主要细胞类型，指出了使用动物模型研究骨形成的局限性，并强调了现有体外骨形成模型目前面临的挑战。

为了详细研究软骨内骨化的细胞动力学，我们采用一种组织工程模型，利用转化生长因子-β（TGF-β）对人骨髓基质细胞（hMSCs）颗粒进行软骨诱导，以生成软骨，然后将其皮下植入小鼠体内。植入后，软骨会历经重塑成为成熟的骨骼。这是一种成熟的实验策略，但重塑过程的动力学以及体外软骨诱导启动时间的影响尚未得到全面的解释。在开发该过程的体外模型之前，有必要填补这一理论空白。在**第 2 章**中，我们详细研究了体外软骨诱导启动时间对体内植入颗粒后骨形成和软骨内骨化动力学的影响。研究发现，软骨诱导启动时间并不影响软骨内骨化过程，但延长启动时间会增加骨质体积。我们通过分析与软骨诱导细胞的骨形成能力相关的转录组，描述了软骨模板重塑为成熟骨骼的一系列事件。这为开发包含多个阶段和多种细胞类型的体外骨形成模型提供了合适的起点。

由于我们观察到短时间诱导的软骨构建体在植入后会迅速矿化和血管化，因此接下来我们研究如何在体外重现这些过程。鉴于在组织工程领域，矿化与血管生成之间的关系尚未得到广泛研究，我们进行了一系列体外分析。在**第 3 章**中，我们通过向软骨诱导的 hMSC 颗粒中添加 β-甘油磷酸酯来诱导体外矿化，并研究其与血管形成细胞的相互作用。我们发现，随着矿化的进行，内皮细胞的行为，特别是细胞迁移、增殖和管腔形成过程受到负调控。这增进了我们对矿化与血管生成之间关系的理解，并为我们建立包括血管化在内的复杂体外软骨内骨化模型提供了指导。

随后，我们进一步开发直接共培养模型，以重现软骨内骨化过程中的血管化和重塑过程。**第 2 章**的研究表明，体外短时间软骨诱导的 hMSC 颗粒能够诱导血管生成和破骨细胞生成。在**第 4 章**中，我们首先分别建立了矿化软骨诱导颗粒与破骨细胞或血管网络的共培养体系，最终将它们整合为一个模型。通过这种方式，成功将软骨生成、矿化、血管网络形成和破骨细胞生成整合到一个复杂的三维共培养系统中，为骨骼生物学研究和骨疾病建模提供了一个新平台。

第 5 章着重将体外 hMSC 颗粒模型应用于骨转移研究。这一领域尚缺乏骨相关疾病相关的体外模型。我们进行了 hMSC 颗粒与乳腺癌或黑色素瘤细胞系的体外共培

养实验，旨在模拟转移性癌细胞向骨形成构建体的迁移过程。结果显示，hMSC 颗粒能够刺激癌细胞的迁移和增殖，并且两种癌细胞系都能与颗粒接触生长。最后，我们利用流体循环系统模拟癌细胞从循环系统向骨骼的迁移。该平台的进一步开发可能为研究骨微环境对癌细胞行为的影响提供新工具，并为了解局部组织相互作用如何影响转移过程提供新的视角。

在**第 6 章**中，我们全面讨论了本论文的研究结果，并将其置于更广泛的背景下进行分析。总体而言，本论文强调了软骨内骨化在组织工程模拟骨形成或再生策略中的重要意义。我们在建立包含多种细胞成分的体外模型方面取得了显著进展。这些模型能够模拟软骨生成、矿化、血管生成和破骨细胞生成过程。此类先进的共培养系统有望成为模拟和研究骨形成过程中软骨细胞、破骨细胞和内皮细胞之间相互作用的有力工具，为未来骨疾病的研究和潜在治疗策略的开发奠定基础。未来我们将对该模型的进一步优化，如纳入其他细胞类型或复现更多生物过程（如血管浸润）。我们将进一步拓展其应用范围，这将有助于更深入地理解骨骼生物学并为骨骼疾病的治疗提供帮助。

ACKNOWLEDGEMENTS

During these years, I was fully committed to my PhD programme. I felt as if I was chasing an incredible dream: to study abroad, to take care of myself independently, and to fulfil all the tasks in the lab. I am deeply grateful to the many people who have helped me in various ways during this amazing journey.

I would like to thank **Prof. Dr. Eric Farrell**. While you were supervising me, I heard many of your great ideas about the research topics. When I started my PhD, it was hard to get used to the environment at once. I had to be very careful to follow your speech and thoughts. You are really a person who thinks fast, talks fast, and works fast. I sincerely appreciate your patience in explaining your ideas to me many times so that I can follow up. I also appreciate your talkative networking. To me, connecting with so many people and making joint programs function seems like magic. It is also interesting to learn how much you enjoy tea. I hope I can get more opportunities to introduce you to Chinese tea!

Prof. Dr. Gerjo van Osch, I still remember our first virtual interview. Your insightful questions about my research reminded me of the directions that I had never thought of, and helped me to reassess and pinpoint the areas of my studies that I had missed. It might be my life challenge to follow your critical thinking. Your advice has consistently motivated me to aim for the final goal. I sincerely appreciate your guidance and the significant influence you have had on my PhD path.

Dr. Andrea Lolli, I have to show gratitude to you. You have been the person I turned to most often to discuss my studies. When I first stepped into the laboratory, a newcomer there, you patiently mentored me, showing me the ropes and helping me get familiar with the environment. You patiently checked my research plans, offering practical insights and suggestions that have significantly improved the quality and direction of my experiments. Moreover, your care in revising my manuscripts cannot be overstated. You have reviewed each version many times, paying attention to every detail, from the overall structure to the smallest typing error. I feel truly fortunate to have you as my supervisor. Thank you for all that you have done.

I would also like to express my gratitude to the **committee members,** for accepting the offer and spending the time to read and assess my dissertation.

Amaia, you have been an incredible collaborator on this academic journey, especially when we worked on our common paper. We faced the challenges together, but fortunately, we got our model working. Your insights and hard work were fundamental in helping us achieve great results. I am so grateful for the time we spent brainstorming, conducting research, and refining our ideas. Thank you for being such a good teammate.

M**arta,** although it is a pity that we did not have a longer period to collaborate on the same topic, I truly appreciate the time we spent working together. You are an incredibly hard-working PhD student. You always took the time to deeply consider the details of our studies, and your ideas have been so inspiring. I know it is not easy to juggle work across different institutions simultaneously, but you have managed it with

such expertise and hard work. Thank you for your contributions, and I hope we will have more opportunities to work together in the future.

I would like to express gratitude to the technicians in our lab. **Janneke**, your hard - work and dedication to the lab are truly impressive. Your experience in laboratory techniques has been critical for us, and you provided me with so much help during my research. Every bit of your effort has not gone unnoticed, and I am truly thankful for all that you have done for my projects. **Nicole**, thank you for your consistent support. Your attention to detail and commitment to maintaining the lab's operations have made a significant difference. **Wendy**, your passion for the lab is fantastic. Whether it is handling complex equipment or offering a helping hand, your positive attitude is always appreciated. Thank all of you again for making our lab a better place to conduct research!

Dr. Roberto Narcisi, thank you for patiently teaching me statistical analysis. The knowledge you've imparted has not only been useful at that time but will also be useful in my future research. I also appreciate your lectures on cell senescence. It was an outstanding course that provided a unique perspective.

Sandra, I wanted to express my heartfelt gratitude for your outstanding work as our department's secretary. Your handling of paperwork is truly remarkable. You managed my registrations, academic files, and administrative forms with great care, which eased our workload and enabled us to focus on working. Thank you for being so amazing!

I want to thank **Dr. Gert-Jan Kremers** and the Erasmus Optical Imaging Centre (OIC). You really introduced me to the imaging techniques and answered all my questions. That is really an important portion of my PhD work. Itis really satisfying to work with you!

I also have to mention **Dr. Andrea Banfi** and **Dr. Nunzia di Maggio** from the University Hospital of Basel. Your expertise in vascularisation and tissue engineering constitutes a necessary portion of my thesis. Your constant work and assistance have made me make great progress in my project. **Tristan** and **Adelin**, the collaboration with you two French guys was an happy one. I have also benefited a lot from your meticulous attitude towards scientific research. Thank you, **Lieke, Virginia** and **Niamh**, for your efforts. The outcomes of your experiment played a significant role in my research. I also like to thank **Prof. Marc Raaijmakers**, **Remco**, and **Eric** (M.J. Bindels) for helping me with my projects by sharing their experience. Thank you for helping me learn more about microfluidic and cancer-related research, **Dr. Mathieu Wijffels**, **prof. Michiel Verhofstad**, **Dr. Silvia Scaglione**, and **Dr. Astrid Parenti**.

A special thanks goes out to **Prof. Dr. Eppo Wolvius** leading the oral and maxillofacial surgery department; your help was crucial in guiding the project. I also learned a lot from the skeletal research conference, instructed by **Dr. Marjolein van Driel, Dr. Bram van der Eerden,** and **Dr. Jeroen van de Peppel.**

Jietao, you seemed calm but worked fast. You saved your time and got your PhD certificate much earlier than me. Congratulations! I also thank you for answering my questions about PhD issues. I hope you have an outstanding doctor career in

Hangzhou. We know thatis not easy at this time. **Yi He**, sincerely, I got to know you first and then surprisingly found out that you married **Jietao**. To be honest, it was really good to hear from you, a “PhD couple” who worked there in EMC. I also hope you will successfully get your PhD degree following your husband!

Andrea Schwab, Anna, Anne, Elias, Imke, Irene, Ivy, **Judith, Mauricio, Michele, Mike, Niamh, Pedro, Reimer, Tess, Tim,** I also want to express my sincere gratitude to you, my colleagues. Although our interactions may not have been as frequent or in-depth as with some others, you have all contributed significantly by participating in every meeting and activity in the lab. All of your projects and speeches, including editing iPSCs, imaging techniques, single cell sequencing, mechanical loading, cell “village”, the pillars for fibroblasts, and calcification, were quite inspiring for me. Your active attitudes also made the lab a pleasant and inviting place for me to work. **Judith** and **Imke**, I also appreciate the time we spent planning the Lab Day. Playing with these activities was quite amazing. **Enrique**, I thank you so much for showing the procedures of the bone ring model. In addition, **Callie** and **Yannick**, your theses papers are what I frequently turn to, providing me the fundamental knowledge on endochondral ossification.

Ziliang Ye and **Zhiqiang Liu,** you are the best roommates. We got to know each other since we are all from China and PhD students in Erasmus MC, looking for house rental at that time. When I departed from China, I still remember the time we started off for the longest flight in my life with **Zhiqiang**. We only lived together for a year, so it's a little unfortunate. Your Hunan culinary style is something I truly miss. I hope your relationship with your partner is going well and that you can publish your work. When I was not familiar with the surrounding, **Ziliang,** at the beginning of my life abroad, thank you so much for introducing me the setups and places nearby. I also appreciate your taking care of the house rental issue, acting like a big brother among us. I also seriously considered your suggestion for love affair and social networking, really inspiring for me.

I would like to express my gratitude to **my parents**. Their support has been the foundation for the completion of my PhD degree. They supported me in every way possible during these challenging years of study. Whether it was providing emotional comfort in times of stress, financial assistance to ensure that I could focus on my research without worry, or just patiently listening to me as I shared the ups and downs of my academic career, their love and support was always there. I am truly grateful to them and I know that I could not have achieved this goal without their constant companion and support.

LIST OF PUBLICATIONS

Lolli, A., **Ji, E.**, Witte-Bouma, J., Hoogenboezem, R. M., Bindels, E. M. J., Raaijmakers, M. H. G. P., van Osch, G. J. V. M., Niamh, F., & Farrell, E. “Making a long story short: tissue engineering bone with stromal cells subjected to brief chondrogenic priming”. Manuscript submitted.

Ji, E., Garmendia Urdalleta, A., Witte-Bouma, J., Kremers, G. J., Di Maggio, N., Banfi, A., Farrell, E., & Lolli, A. “Development of an advanced human in vitro model of endochondral ossification, comprising mineralised cartilage, osteoclasts and vascular components” Manuscript submitted.

Cecchi M., **Ji, E.**, Witte-Bouma, J., M.E. Wijffels M., H.J. Verhofstad M., Scaglione S., Parenti A., Lolli, A., & Farrell, E. “Metastasis to the bone: new in vitro models of bone formation to study migration and proliferation of metastatic cancer cells”. Manuscript in preparation.

Ji, E., Leijsten, L., Witte-Bouma, J., Rouchon, A., Di Maggio, N., Banfi, A., van Osch, G. J. V. M., Farrell, E., & Lolli, A. “In Vitro Mineralisation of Tissue-Engineered Cartilage Reduces Endothelial Cell Migration, Proliferation and Tube Formation”. Cells. 2023; 12(8), 1202.

Zhou, Y., Li, J., Xu, F., **Ji, E.**, Wang, C., & Pan, Z. “Long noncoding RNA H19 alleviates inflammation in osteoarthritis through interactions between TP53, IL-38, and IL-36 receptor”. Bone & joint research. 2022; 11(8), 594–607.

Ji, E., Wang, J., Wang, L., Pan, Z., & Gao, W. “Pharmacological Effects of Fasudil on Flap Survival in a Rodent Model”. The Journal of surgical research. 2020; 255, 575–582.

Wang, J., **Ji, E.**, Lin, C., Wang, L., Dai, L., & Gao, W. “Effects of bradykinin on the survival of multiterritory perforator flaps in rats”. World journal of surgical oncology. 2019; 17(1), 44.

PHD PORTFOLIO

Personal details	
Name	Encheng Ji
Department	Department of Oral and Maxillofacial Surgery, Erasmus MC, University, Medical Center Rotterdam, Rotterdam, The Netherlands
Research school	Erasmus MC Graduate school
PhD period	October 2020 – October 2024
Promotors	Prof. Gerjo J.V.M. van Osch, PhD, Dr. Andrea Lolli, PhD and Prof. Eric Farrell, PhD

		Workload (ECTS)
Courses		
Apr 2021	Erasmus MC - Course on Laboratory Animal Science	3.00
Mar 2021	Species-specific: small rodents	1.00
Apr 2022	Leica SP8 confocal microscope introduction course	0.20
Jul 2022	2022 PhD Training Course organized by the European Calcified Tissue Society	2.00
Feb 2022	Biomedical Writing for PhD candidates (LTC course)	1.50
Sep-2022	Scientific Integrity	0.30
(Inter)national Conferences		
Apr 2022	Netherlands society for Biomaterials and Tissue Engineering (NBTE) conference 2021	1.60
Jun 2022	Tissue Engineering and Regenerative Medicine International Society (TERMIS) European Chapter Meeting 2022	1.70
Dec 2022	Netherlands society for Biomaterials and Tissue Engineering (NBTE) conference 2022	1.00
Mar 2023	Tissue Engineering and Regenerative Medicine International Society (TERMIS) European Chapter Meeting 2023	1.70

Nov 2023	Netherlands society for Biomaterials and Tissue Engineering (NBTE) conference 2023	1.00
Department/consortium presentations and meetings		
Sep 2021	Galapagos meeting	0.50
May 2022	B2B M47 meeting	0.30
Jun 2022	Biomedical Sciences PhD day 2022	0.30
Jun 2022	Meeting of Oral and Maxillofacial Surgery department	0.30
2021 2022	Skeletal Tissues & Inflammation (CTR & Rheumatology	2.00
2020 2022	ACE bone & Joint meeting	1.00
Oct 2022	HypOA consortium meeting	0.50
2022-2023	Soup and Science Meeting	1.00
Aug-2023	ACE-SCORE-DAY	0.50
Jun-Dec 2023	Meeting Cell-cell and cell-matrix interactions in tissue repair mechanisms	1.50
2020-2024	Research meetings of connective tissue repair lab	2.00
2020-2024	Journal Club	1.00
Feb-Nov 2024	Skeleton research meetings	1.50
Student supervision		
2022-2023	Supervision of Bachelor and Master students	2.00
Miscellaneous		
Apr-2022	External collaboration in Maastricht University	1.00
	Total	30.40

CURRICULUM VITAE (ABOUT THE AUTHOR)

Encheng Ji was born on March 11th 1992 in Zhejiang, Wenzhou (China), and he is the only child in his family. During his senior high school education in Wenzhou sixth senior high school, he won the 2nd guitar contest championship in 2006. After his 3-year education at Zhejiang Wenzhou High School, he entered Wenzhou Medical University to study clinical medicine from 2011 to 2016. During this period, he had the chance to spend a short-term exchange at China Medical University (Taichung) for one month. Once he received his Bachelor's Degree in Clinical Medicine, he immediately turned to the orthopaedics field at the same university and he obtained a Master's Degree (research type) in Orthopaedics in 2019. During this time, Encheng devoted himself to the research on osteoarthritis and flap surgery. The main achievement was to demonstrate the effect of Fasudil on both chondrocytes and the perforator flap models. This work was performed in the Key Laboratory of Orthopaedics of Zhejiang Province, and Dr. Zheer Pan was his supervisor at that time. Following his Master's Degree, Encheng worked in Zhejiang Muke Biotechnology Co., Ltd. for half a year. This experience helped him get more insight into the biotechnology industry. In 2020 Encheng obtained the PhD position at Erasmus MC in Rotterdam (the Netherlands) under the supervision of Prof. Dr. Eric Farrell, Dr. Andrea Lolli and Prof. Dr. Gerjo J.V.M. van Osch. Due to the worldwide pandemic, Encheng had to face some initial challenges in travelling to the Netherlands and spending limited time in the laboratory, but he quickly adapted to the new situation and enthusiastically started his work. During his PhD period, his research mainly focused on the establishment of novel *in vitro* models of bone formation via endochondral ossification. The work was presented at several national and international conferences, including those of the Netherlands society for Biomaterials and Tissue Engineering (NBTE), Tissue Engineering and Regenerative Medicine International Society (TERMIS) and European Orthopaedic Research Society (EORS). Encheng is now enrolled by The First Affiliated Hospital of Wenzhou Medical University as an orthopaedic doctor.